Cis-Regulatory divergence and expression of ryanodine receptor paralogues in Medaka (*Oryzias latipes*)

Tahani Baakdhah

Supervisor: Dr. Jens Franck

A Thesis Submitted to the Faculty of Graduate Studies in Partial Fulfilment of the Requirements for the Masters of Science Degree.

Department of Biology

Masters of Science in BioScience, Technology and Public Policy Program

The University of Winnipeg
Winnipeg, Manitoba, Canada
December 2011

Copyright 2011 © Tahani Baakdhah

ABSTRACT

Ryanodine receptors (RyRs) are large homotetrameric proteins that in mammals are encoded by three genes: RyR1 in skeletal muscle; RyR2 in cardiac and smooth muscle; and RyR3 which is expressed in a diversity of cell types. RyR channels play a central role in the excitation-contraction (EC) coupling process by mediating Ca^{2+} release from the sarcoplasmic reticulum (SR). RyR1 paralogues are expressed in a fiber type-specific manner in fish skeletal muscles: RyR1a in slow-twitch skeletal muscle (red muscle) and RyR1b in fast-twitch skeletal muscle (white muscle). RyR1a and RyR1b are classic examples of spatial subfunctionalization, since they share an ancestral function, yet are expressed differentially in red and white muscle fibres respectively. Gene duplication and subsequent divergence in sequence, expression and interactions are considered to be one of the major driving forces in the evolution of diversity. After the upstream promoter regions, evolutionarily conserved introns are considered the second most important sites containing gene regulatory elements that control tissue-specific expression (gene enhancers or gene silencers). Using medaka (*Oryzias latipes*) as a model organism, I searched the noncoding sequences in medaka RyR1 and RyR3 genes to look for conserved noncoding elements for RyR co-orthologues and paralogues. The bioinformatic analyses revealed evidence of conservation of noncoding elements for RyR co-orthologues and divergence between RyR paralogues. I also analyzed the spatial and developmental expression of the RyR paralogues (RyR1a/RyR1b; RyR3a/RyR3b) in medaka. The expression analyses revealed conserved expression patterns for the RyR co-orthologues and divergent expression of the RyR paralogues.

ACKNOWLEDGMENTS

I would never have been able to finish my dissertation without the guidance of my committee members, help from friends, and support from my husband and my family. First and foremost I offer my sincerest gratitude to my supervisor, Dr. Jens Franck, for his continued guidance, caring, patience, and effort to provide me with an excellent atmosphere for research. I attribute a great part of my Master's degree to his unshakeble support and without him this thesis would not have been completed. One simply could not wish for a better and friendlier supervisor. I would also like to warmly thank Dr. Good for her critical guidance and input throughout the process of this research, as well as Dr. Civetta who was always willing to help and give his best scientific advice and suggestions.

I would also like to acknowledge Robyn Cole for her great work in the animal complex, especially the fish aquarium, where she was taking care of fish feeding and breeding as well as being a great help to me in handling the fish throughout the process of this research.

In my daily work I have been blessed with a friendly and cheerful group of fellow students. Many thanks to Fatimah Alsaffar for helping me in collecting tissues samples, feeding the fish and collecting medaka eggs. I am also indebted to my many colleagues who supported me including: Saivash Darbandi, Ian Kasloff, Rebecca Vanderhooft, Nada Sagga, and Maram Felemban.

I dedicate this dissertation to my husband, Wael Alnami. He always stood by me through the good and bad times. Thank you dear Wael, you made my dream come true. My kids Hashim Alnami and Ahmad Alnami were my inspiration; they filled my life with joy and happiness necessary to reach my goals.

I would also like to thank my parents, my father Waheeb Baakdhah, my mother Amal Abualjadayl, They were always encouraging me with their wishes and prayers.

Special thanks for the Saudi Arabian Cultural bureau for giving me this opportunity and for supporting my research.

Last but not least, my family and friends back home and the one above all of us, God, for answering my prayers and giving me the strength to plod on despite my constitution wanting to give up, thank you so much Allah for making all things possible.

TABLE OF CONTENTS

LIST OF TABLES

LIST OF FIGURES

LIST OF APPENDICES

ABBREVIATIONS AND NOMENCLATURE

aCNE: Ancient conserved noncoding elements

bp: Base pair

BLAST: Basic Local Alignment Search Tool

Ca^{2+}: Calcium cation

CaCl2: Calcium chloride

CaCl2.2H2O: Calcium Chloride Dihydrate

CART: Cocaine-amphetamine-regulated transcript

CCD: Central core disease

cDNA: Complementary DNA (reverse transcribed from RNA)

CICR: Calcium-induced calcium release

CLOX: Cut like homeobox

CNEs: Conserved noncoding elements

CREs: *Cis*-regulatory elements

CT value: The cycle number at the threshold level of log-based fluorescence

dCNE: Duplicated conserved noncoding elements

ddH2O: Doubled-distilled water (RNase-free water)

DEPC: Diethylpyrocarbonate

DHPR: Dihydropyridine receptor

DICR: Depolarization-induced calcium release

dNTP: Deoxyribonucleotide triphosphate

E: Efficiency

E.Coli: Eschreshia coli

E-C coupling: Excitation contraction coupling

EDTA: Ethylenediaminetetraacetic acid

Ef1α: Eukaryotic Elongation factor 1 alpha

EVI-1: Ecotropic virus integration site 1

FOX: Forkhead transcription factors

FSD: Fish specific genome duplication

G: Gram

GATA: Globin transcription factor 1

HCNEs: Highly conserved noncoding elements

HCNS: Highly conserved noncoding sequences

HEPES: 4-(2-hydroxyethyl)-1-piperazineethanesulfonic acid

HKG: Housekeeping genes

HNF-1: Hepatocyte nuclear factor 1

HNF-3: Hepatocyte nuclear factor 3

HNF-3α: Hepatocyte nuclear factor 3 alpha

HNF-4: Hepatocyte nuclear factor 4

HNF-6: Hepatocyte nuclear factor 6

Hpf: Hours post fertilization

ICRCs: Intracellular calcium release channels

IPC: Intron position conservation

IPTG: Isopropyl b-D-thiogalactopyranoside

Kbp: Kilobase pairs

KCl: Potassium chloride

M: Molar

Mbp: Million base pair

MEF2: Myocyte enhancer factor-2

µg: Microgram

Mg2+: Magnesium cation

MgCl2: Magnesium chloride

MH: Malignant hyperthermia

µl: Millilitre

mM: Milimolar

MO: Morpholino oligonucleotide

MS222: Tricaine methane sulphonate

mVISTA: Main VISTA

Mya: Million years ago

MYCMAX: Myelocytomatosis

MYOG: Myogenic factor 4

MYOD: Myogenic differentiation 1

NADH: Nicotinamide Adenine Dinucleotide

NaOH: Sodium hydroxide

ncDNA: Noncoding DNA

Ng: Nanogram

NKX6-1: NK6 homeobox 1.

NKX6-2: NK6 homeobox

NZCYM: NaCl, Zinc, Casamino acid, Yeast extract and Magnesium chloride (powder broth)

OCT: Octamer transcription factor

PBS: Phosphate Buffer Saline.

PCR: Polymerase chain reaction

qRT-PCR: Quantitative Real Time PCR

RNA Pol: RNA polymerase

Rnasin: Ribonuclease inhibitor

rRNA: Ribosomal RNA

rVISTA: Regulatory VISTA

RT: Reverse transcroptase

RyR: Ryanodine receptors

SDH: Succinate dehydrogenase

SEs: Standard errors

SGD: Single gene duplication

S.N.A.P.: Simple Nucleic Acid Purification

SSC: Saline Sodium Citrate buffer

STAT: Signal Transduction and transcription

TE: Tris Ethylenediaminetetraacetic acid (Tris EDTA)

TFs: Transcription factors

TFBSs: Transcription factors binding sites

UTR: Untranslated region

WGD: Whole genome duplication

X-Gal: 5-bromo-4-chloro-3-indolyl- beta-D-galactopyranoside

CHAPTER 1

LITERATURE REVIEW

1.1 Ryanodine Receptors (RyRs)

1.1.1 Structure

Cytoplasmic Ca^{2+} plays essential roles in cell excitability, neurotransmitter release, muscle contraction and other biological processes. The concentration of cytoplasmic Ca^{2+} can be increased either by Ca^{2+} entry across the plasma membrane or by Ca^{2+} release from intracellular stores (Nakashima et al., 1997). Intracellular Ca^{2+} release channels (ICRCs) form a superfamily of genes that include two subfamilies: the inositol triphosphate receptor (IP_3R) and the ryanodine receptor (RyR) genes, which encode the largest ion channels known today (Sorrentino et al., 2000). RyRs are large homotetrameric proteins with a total molecular mass of approximately 2.2 – 2.3 million Daltons (Sharma and Wagenknecht, 2004). In mammals, the three RyR isoforms (RyR1, RyR2, and RyR3) are encoded by three different genes (Fill and Copello, 2002). While mammals encode three RyR genes, fish have duplicated genes e.g. RyR1a and RyR1b that are expressed in a tissue-specific manner (Franck et al., 1998).

The RyR channel has two different domains: the cytoplasmic assembly, consisting of loosely-packed protein densities and the transmembrane assembly that protrudes from the center of the cytoplasmic assembly (Fig. 1) (Schatz et al., 1999). The size and the shape of the ryanodine binding protein complex is similar to that of the ‘’feet’’ structures, which appear to physically link the transverse (T) tubule and sarcoplasmic reticulum (SR) (Fill and Copello, 2002). The RyR1 channel has a four-

fold symmetry that likely reflects its formation by four RyR protein monomers (Radermacher et al., 1994).

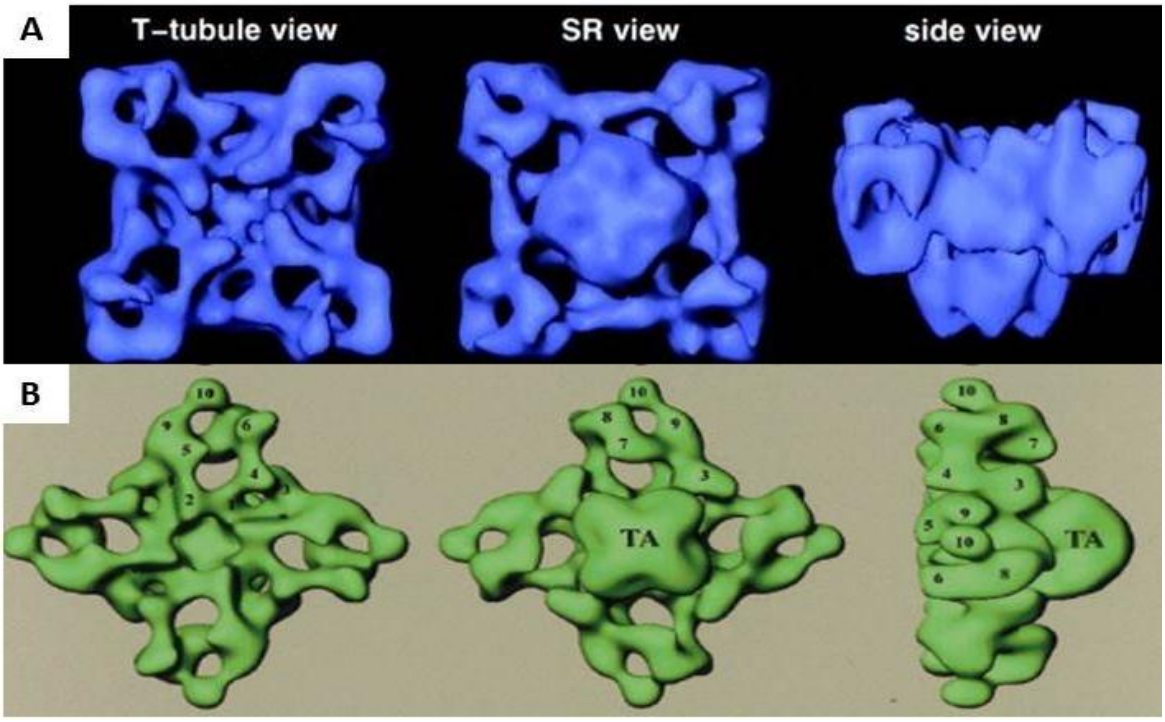

Figure 1: Ryanodine receptor structure RyR1 (blue) and RyR3 (green). (A) Solid body representations of the 3D reconstruction of RyR1 are seen from the T tubule–facing side (left), SR-facing side (middle), and from the side (right) with the cytoplasmic moiety of the receptor on top, and the transmembrane assembly at the bottom (Samso et al., 1999). (B) 3D reconstructions of RyR3 are shown in three different views. On the left: top views of the cytoplasmic surface, which interacts with the transverse-tubule in muscle. In the center: bottom views of the surface that would face the sarcoplasmic reticulum lumen. On the right: side views. TA, transmembrane assembly; SR, sarcoplasmic reticulum (Zheng Liu et al., 2001).

1.1.2 RyR Role in Excitation Contraction Coupling

Excitation contraction (EC) coupling is defined as the physiological process of converting an electrical stimulus (excitation) to a mechanical response (muscle contraction) (Sandow, 1952). RyRs are large intracellular channels that play an essential role in the EC coupling process (Protasi et al., 2000). Dihydropyridine receptors (DHPRs) are L-type Ca^{2+} channels, which act as voltage sensors in skeletal type EC coupling (Fig. 2) (Protasi et al., 2000). The primary role of the DHPR in vertebrate skeletal muscles is to act as a voltage sensor that directly modulates the activation gate of adjacent RyR1 channels (Fill and Copello, 2002). The skeletal DHPR in the T-tubules are arranged in clusters of four, known as tetrads. These tetrads are organized in distinct arrays. The RyR1 channels in the SR membrane are arranged in a corresponding fashion (Fill and Copello, 2002). Depolarization of the T-tubule membrane (i.e., excitation) induces conformational changes in the DHPR that ultimately leads to activation of the RyR channel in the SR membrane. The activation of RyR channels leads to massive Ca^{2+} release from the SR, which in turn initiates contraction (Fill and Copello, 2002). Two distinct skeletal muscle ryanodine receptor (RyR1s) are expressed in a fiber type-specific manner in fish skeletal muscles: RyR1-slow (RyR1a) from slow-twitch skeletal muscle and RyR1-fast (RyR1b) from fast-twitch skeletal muscle (Franck et al, 1998; Hirata et al; 2007; Darbandi and Franck, 2009). Interestingly, it has recently been discovered that zebrafish encodes two DHPR genes that are expressed differentially in superficial slow and deep fast musculature. Both subunits do not conduct Ca^{2+} but merely act as voltage sensors to trigger opening of the tissue-specific RyR isoforms. Non- Ca^{2+} conductivity of both DHPR isoforms is found to be a common trait of all higher teleosts (Schredelseker et al., 2010). Cardiac EC coupling processes require the presence of extracellular Ca^{2+}. In cardiac muscle, the DHPR receptor (L-type

Ca^{2+}channel) carries a small Ca^{2+} influx that activates the RyR2 channel (Fig. 2) (Fill and Copello, 2002).

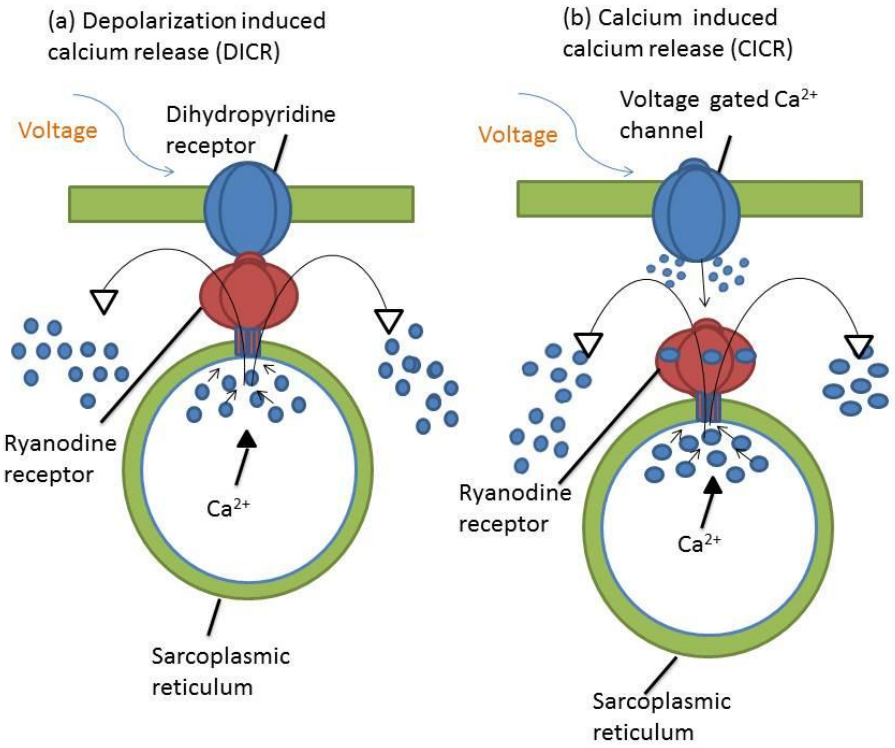

Figure 2: Regulation of excitation-contraction coupling. (a) A close contact of the transverse-tubule (TT) and sarcoplasmic reticulum (SR) membrane is essential for the coupling of extracellular Ca^{2+} entry and intracellular Ca^{2+} release. The dihydropyridine receptor (DHPR) located on the (TT) membrane functions as an L-type Ca^{2+} channel, as well as the voltage sensor of the plasma membrane. The ryanodine receptor (RyR) located on the SR membrane functions as the Ca^{2+} release channel. (b) In calcium-induced calcium release (CICR), the depolarization of the sarcolemma activates gates in the L-type channels in the membrane permitting extracellular calcium to enter. The extracellular calcium then acts as a ligand on the ryanodine receptor (RyR) resulting in release of calcium from the SR. In depolarization-induced calcium release (DICR), the depolarization of the sarcolemma affects a conformational change in the L-type calcium channel which mechanically opens the RyR of the sarcoplasmic reticulum. (Adapted from Lodish et al, 2000).

1.1.3 RyR Expression

Recently, it has become clear that all three RyR isoforms are widely expressed in both excitable and non-excitable cells (Ta and Pessah, 2006). RyR1 is expressed predominantly in skeletal muscle and at lower levels in cerebellar Purkinje cells, gastric smooth muscle and B lymphocytes, among others (Giannini et al, 1995). RyR2 was originally purified from cardiac muscle (it is the major isoform expressed there), but is also robustly expressed in neurons, and in visceral and arterial smooth muscle. RyR3 is the least understood of the RyR isoforms and seems to play an essential role during development, while in mature cells RyR3 is found in the diaphragm, epithelial cells, brain, and smooth muscle (Lanner et al., 2010). RyRs are expressed in variety of nonexcitable tissues, although the function of the RyRs expressed in nonexcitable cells is not fully established. They may contribute to the initiation of Ca^{2+} signals (pancreatic cells), or act as an agonist-specific (hepatocytes), or they may provide a subtle regulation of the magnitude and kinetics of hormone-evoked [Ca^{2+}] responses (Deborah et al., 1996).

Two skeletal muscle ryanodine receptor (RyR1s) are expressed in a fiber type-specific manner in fish skeletal muscles: RyR1-slow (RyR1a) in slow-twitch skeletal muscle and RyR1-fast (RyR1b) in fast-twitch skeletal muscle (Franck et al, 1998; Morrissette et. al., 2000). A recent study performed by Darbandi and Franck found that RyR1b and RyR3 are co-expressed at equivalent levels in certain zebrafish tissues (2009). In contrast, mammals express RyR3 at very low levels in skeletal muscle (Giannini et al, 1995). The co-expression of RyR1 and RyR3 genes in skeletal muscle has implications for EC coupling in fish skeletal muscle. Recently, Murayama

and Kurebayshi (2010) proposed a model whereby RyR3 serves as an uncoupled CICR channel in non-mammalian vertebrates. According to their model, calcium release from RyR1b in a fast-twitch muscle myocyte would activate the parajunctional RyR3 via the CICR mechanism to trigger further release of Ca^{2+} from the sarcoplasm (Fig. 3).

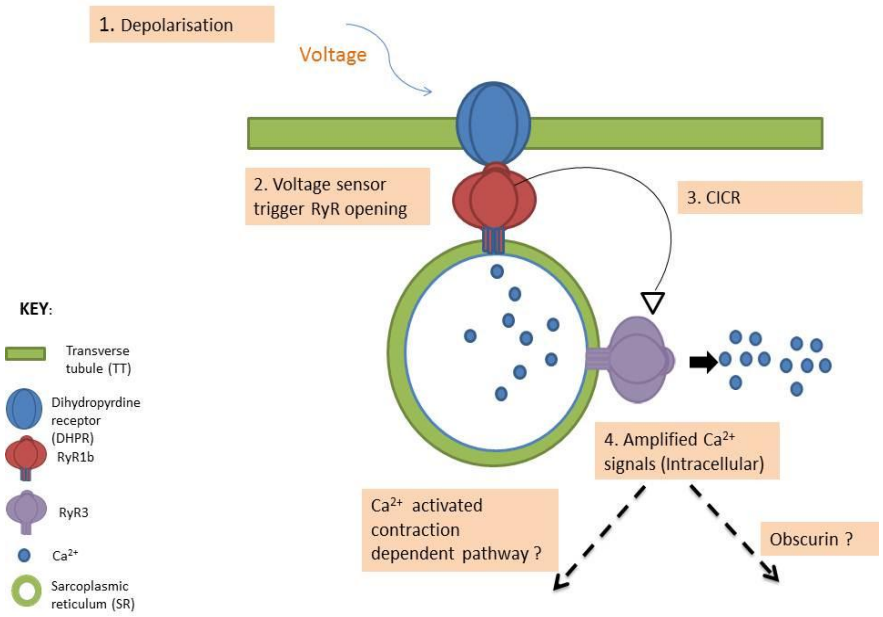

Figure 3: Proposed mechanism of action for RyR3 in zebrafish. In EC coupling, acetylcholine is released from the spinal cord motor neurons which binds to the acetylcholine receptor and causes action potential in the transverse-tubule (TT). (1.) Depolarisation is sensed by the DHPR, which acts as a voltage sensor and triggers (2.) the opening of the junctional RyR1b on the sarcoplasmic reticulum (SR) membrane. Ca^{2+} released through RyR1b subsequently activates neighbouring parajunctional RyR3 and triggers further release of Ca^{2+} via (3.) Calcium induced calcium release (CICR) mechanism. The resulting (4.) amplified Ca^{2+} signal is believed to contribute to the myofibril organisation directly through obscurin and spontaneous contraction indirectly through Ca^{2+} activated contraction-dependent pathway (Adapted from Murayama and Kurebayshi, 2010; Wu, 2011).

1.1.4 RyR Role in Disease

Two skeletal muscle diseases, malignant hyperthermia (MH) and central core disease (CCD) are linked to mutations in the RyR1 gene. The majority of RyR1 mutations are associated with the MH cluster in the cytoplasmic domain, whereas most mutations linked to CCD are in the pore-forming domain 3 (Hamilton, 2005). MH is a human autosomal dominant disease with variable penetrance, characterized by muscle rigidity, metabolic acidosis, rhabdomyolysis, and/or increase in body temperature in response to inhalation anesthetics and depolarizing muscle relaxants (Hamilton, 2005). The prevalence of the MH genotype in humans is 1 out of 20,000 anesthetized adults (Ta and Pessah, 2006). Central core disease (CCD) is a rare congenital myopathy, with high intra and interfamilial phenotype variability ranging from asymptomatic to severe symptoms. Patient symptoms include hypotonia, delayed motor milestones, proximal muscle weakness, and skeletal anomalies such as hip dislocation, scoliosis, and foot deformities (Kossugue et. al., 2006).

RyR3 mutations results in changes in hippocampal synaptic plasticity, without disturbing hippocampal morphology, basal synaptic transmission or presynaptic function (Balschun et. al., 1999). RyR3 knock-out mice show impairment of the performance in the contextual fear conditioning test, passive avoidance test, and Y-maze learning test (Kouzu et. al., 2000).

Fish models have contributed significantly to our understanding of vertebrate development and, more recently, human disease (Storer and Zon, 2010). Zebrafish have organs and cell types similar to mammals. Organogenesis occurs rapidly and the

entire organs are present in the larvae by 5 to 6 days post-fertilization (Robenstien, 2003). Thus, zebrafish have attracted many researchers in fields of neuroscience, hematopoiesis, cardiovascular research, toxicology and drug research, and developmental research. Many diseases have been studied using zebrafish as a model organism including: muscular dystrophy, Duchenne muscular dystrophy, limb-girdle muscular dystrophy, neurodegenerative disease, Alzheimer's disease, Huntington disease, hemophilia, thrombosis, leukemia, inflammation, diabetes and dilated cardiomyopathies (Robenstien, 2003; Guyon et al., 2003; Cheng et al., 2006). The disease model can be generated by either knocking down the gene or using a chemical that can induce a disease state (Robenstien, 2003). Medaka have also been utilized as a disease model. Medaka possesses several biological advantages over zebrafish (Table 2) which makes it a perfect organism for a disease model. Recently, medaka has been used as a model organism in the study of certain human diseases (e.g. oncology, endocrine, muscle dystrophy, and polycystic kidney disease), toxicological research, molecular genetics, organogenesis and developmental research (Kinoshita et al., 2009; Wittbrodt et al., 2002; Takeda et al., 2011).

1.2 Evolution of Duplicated Genes

1.2.1 Overview

Gene duplications are considered an essential driving force in the evolution of genetic diversity. Gene duplicates represent 8–20% of the genes in eukaryotic genomes, and the gene duplication rate is estimated between 0.2% and 2% per gene per million years (Moore and Purugganan, 2003). Duplicate genes are important for acquiring new gene functions but to date, little is known about the early stages of the evolution of duplicated gene pairs (Moore and Purugganan, 2003). Two evolutionary forces drive the fixation and early evolution of duplicate loci: positive selection and neutral genetic drift (Moore and Purugganan, 2003). Theoretical studies suggest that the importance of these two evolutionary forces differs depending on the ultimate functional fate of the duplicate gene pair (Lynch et al., 2001). The fish-specific genome duplication (FSGD) hypothesis predicts that fish have more genes than other vertebrates that do not share this genome duplication (Ohno, 1970; Van De Peer et al., 2001). The first round of genome duplication may have occurred shortly before the Cambrian explosion (about 590 million years ago) and the second genome duplication probably took place a surprisingly long time afterwards up to 150 million years later (Wang and Gu, 1999). According to this estimation, the majority of genes persisted without being lost for the 150 million years in between these two genome duplication events and most genes appear to have survived since the second genome-duplication in the Devonian more than 440 million years ago (Meyer and Schart, 1999). Large scale or whole genome duplications is evidenced by the conservation of gene order or

gene synteny surrounding duplicate genes. The RyR2 and RyR3 genes have conserved synteny and are believed to be the result of the second round (2R) of genome duplication (Franck et al., in preparation; Fig. 4). The RyR2a/RyR2b and RyR3a/RyR3b paralogues found in fish are also believed to the result of the FSGD as they have conserved synteny (Franck et al., in preparation). The RyR1a and RyR1b paralogues, however, do not show conserved synteny and are therefore believed to have resulted from a local gene duplication event. Medaka has two paralogous copies of RyR1 (RyR1a and RyR1b) as do fugu and zebrafish. The RyR1 gene duplication likely occurred early in the evolution of teleost fish as the paralogues are encoded in the genome of bichir, a basal ray-finned fish (Fig. 4) (Darbandi and Franck, 2009; Darbandi, 2010).

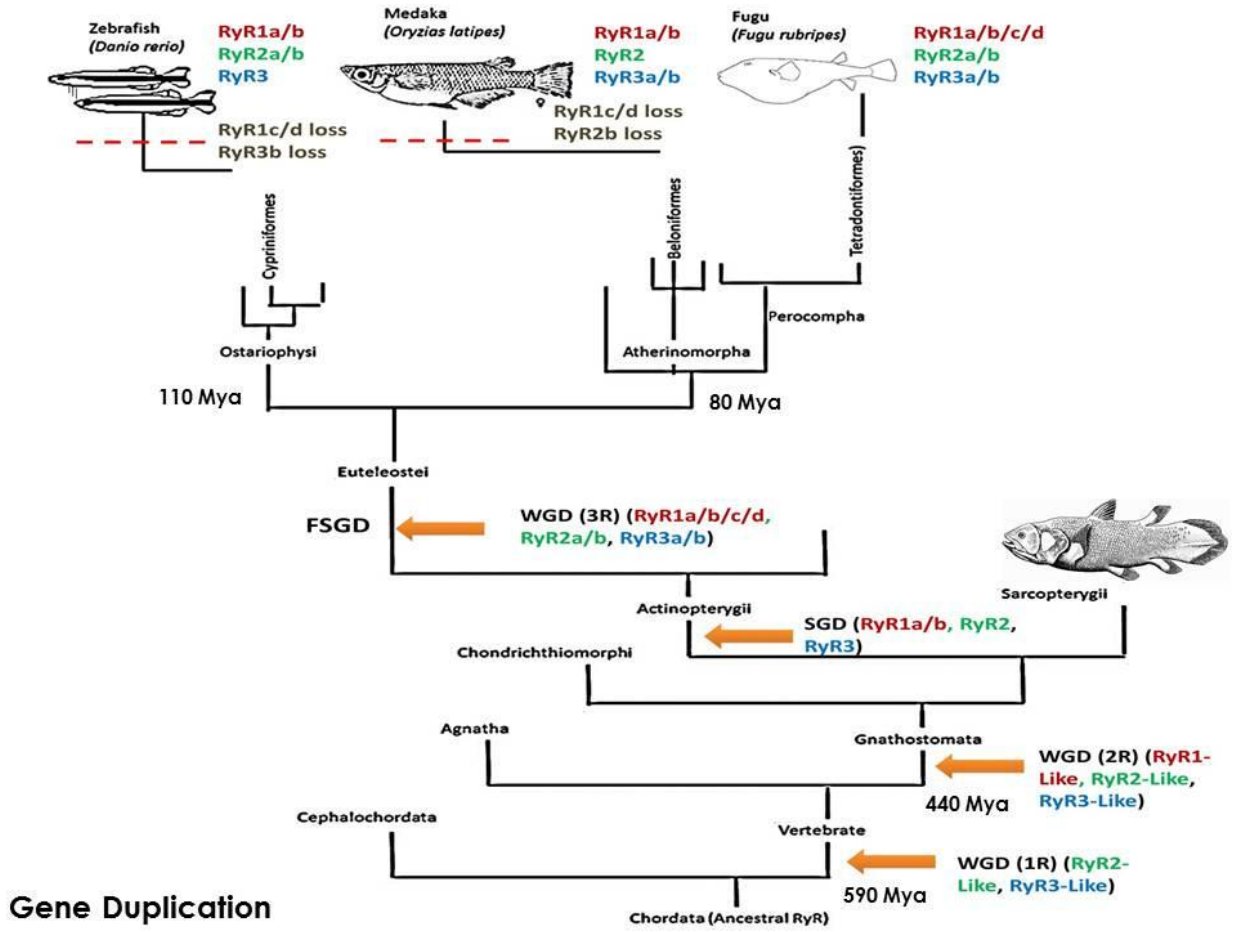

Figure 4: Evolution of the Ryanodine receptor gene family (Adapted from Darbandi, 2010). Medaka has two paralogues copies of RyR1 (RyR1a and RyR1b) as in fugu and zebrafish. The RyR1 gene duplication may be the result of a local or single gene duplication event that occurred at the base of the ray-finned lineage and multiple copies of RyR2 and RyR3 are results of Fish-Specific Genome-Duplication events during the evolution of teleosts. WGD, whole genome duplication; SGD, single gene duplication; FSGD, fish specific genome duplication.

1.2.2 Evolutionary Fate of Duplicate Genes

Gene duplication can lead to several functional relationships between duplicate gene copies, including: loss of gene function by pseudogene formation; redundancy (Nowak et al., 1997); diversification of gene function by means of neofunctionalization; or partitioning of ancestral gene function by the process of subfunctionalization (Lynch et al., 2001). Both pseudogenes and completely redundant unlinked genes are fixed by neutral genetic drift (Walsh, 1995). Gene preservation by neofunctionalization or functional divergence, however, appears to be driven by selective advantage of the duplicate locus (Walsh, 1995). The fixation mechanism of duplicated loci depends on several factors, including the relative levels of adaptive, neutral and deleterious mutations acting on duplicate gene pairs, the selection coefficients on duplicate loci, and the effective population size (Lynch et al., 2001).

Lynch and Conery (2000) and Lynch (2002) estimate that the half-life of a duplicated gene is only of the order of 4.0 million years and the increase in the number of genes in genomes due to small-scale tandem duplications is counteracted by a short half-life and high rate of gene loss. The evolutionary rate can differ remarkably between gene paralogues; usually one of the paralogues evolves faster than the other one (Van de Peer et al. 2001). This phenomenon can lead to problems in phylogenetic reconstruction, and also lower the efficiency of degenerate PCR primers, and can therefore result in a biased amplification of only one copy (Hoegg et al., 2004).

1.2.3 Contributions of Gene Duplication to Genomic and Organismal Evolution

Gene duplication allows each daughter gene to adopt one ancestral function, and further changes under positive selection can refine the functions (Hughes, 1999). Both positive selection and relaxation of purifying selection are necessary in the functional divergence of duplicate genes (Zhang, 2003). Without gene duplication, the plasticity of a genome or species in adapting to changing environments would be limited, because no more than two variants (alleles) exist at any locus within a (diploid) individual (Zhang, 2003). Gene duplication has also contributed to the evolution of gene networks in such a way that advanced expression regulations can be established (Wagner, 1994). Gene duplication has promoted species divergence and the acquisition of species-specific features (Zhang, 2003).

1.3 Evolution of Conserved Noncoding Elements (CNEs)

1.3.1 Overview

Temporal and Spatial regulation of gene expression is important during vertebrate development (McEwen et al., 2006). This regulation is expected to be mediated by coordinated binding of transcription factors to specific noncoding DNA sequences, allowing the integration of multiple signals to regulate the expression of specific genes (McEwen et al., 2006). These sequences, known as *cis*-regulatory elements (CREs) are often located away from the transcription start site of the target gene sometimes in the introns of neighboring genes (Aparicio et al. 2002; Lettice et al. 2003). Conserved noncoding elements (CNEs) are usually detected around genes that regulate development and most of the discovered CNEs are found to act as tissue-

specific enhancers during embryonic development (Vavouri and Lehner, 2009). After the upstream promoter regions, evolutionarily conserved introns are considered the second most common important site containing gene regulatory elements that control tissue-specific expression (gene enhancers or gene silencers) (Jegga and Aronow, 2006). Regulatory elements are short DNA sequences that determine the timing, location, and level of gene expression (Liu et al. 2004). CNEs are only 5 to 20 bp in length, but are vital for understanding gene regulation (Liu et al. 2004). 3.5% of the human genome contains CNEs, which comprise the majority of the estimated 5% of the noncoding sequences that has been subject to purifying selection throughout mammalian evolution (Xie et al., 2006). 0.1% of mammalian CNEs are conserved in the genomes of fish, while none are recognized in invertebrates such as insects and worms (Xie et al., 2006). Recently, it has been shown that 3.5% of noncoding DNA sequence is substantially conserved across diverse mammals (Siepel et al., 2005), and that a smaller amount of noncoding sequence is also shared with more distant vertebrates including chicken and fish (Bejerano et al., 2004).

1.3.2 *Cis*-Regulatory Elements

Cis-regulation is a term used to describe the control of gene expression by elements on the same DNA molecule as the target gene, as opposed to trans-regulation, which describes control by other molecules (Watson et al., 2007). *Cis*-regulation includes processes such as alternative splicing and the control of transcription initiation through the binding of transcription factors to DNA (Watson et al., 2007). These noncoding elements contain binding sites for transcription factors that control the amount of transcription of the target genes

(Levine and Tjian, 2003). There are four functional classes of transcriptional *cis*-regulatory elements: promoters, enhancers, repressors, and insulators (Levine and Tjian, 2003). They are named for their effect on the target gene: enhancers activate transcription, repressors repress transcription, and insulators prevent other *cis*-regulatory elements from acting on the gene (Blackwood and Kadonaga, 1998). The promoter is the region immediately proximal to the transcription start site of a gene (Alberts et al., 2002). The proximal promoter region of a gene includes the region within a few hundred bases upstream of the transcription start site (Levine and Tjian, 2003). The function of the promoter is to directly initiate the transcription complex RNA Pol II to the start site (Alberts et al., 2002). The remaining three classes of *cis*-regulatory noncoding elements are grouped together and are collectively referred to as distal *cis*-regulatory elements, due to the highly variable distance from their target genes (Blackwood and Kadonaga, 1998). For example some *cis*-regulatory elements can be found millions of bases away from their target genes (Lettice et al., 2003). The three-dimensional spaces of the nucleus can contribute to the regulation of gene expression. A dynamic role for chromatin in transcriptional regulation is materializing: enhancer elements interact with promoters forming loops that often bridge considerable distances and genomic loci, even located on different chromosomes, undergo chromosomal associations this associations form an extensive 'transcriptional interactome' (Schoenfelder et al., 2010).

1.3.3 Transcription Factors (TFs)

There are three different eukaryotic RNA polymerases (RNA Pol), and each RNA polymerase is responsible for a different class of transcription: PolI transcribes ribosomal RNA (rRNA), PolII transcribes messenger RNA (mRNA), and PolIII transcribe transfer RNA (tRNA) and other small RNAs (Ait-si-ali et al., 2002). Any protein that is required for the initiation of transcription is defined as a transcription factor. Transcription factors act by recognizing and binding to *cis*-acting sites that are parts of promoters or enhancers (Ait-si-ali et al., 2002). Transcription factors have three major domains: the first one is the DNA-binding domain (recognition of particular DNA sequence), the second one is the trans-activating domain (activates or suppresses the transcription of the gene), and the third one which is the protein-protein interaction domain that allows the transcription factor's activity to be adjusted by other transcription factors (Gilbert, 2000). Functional diversification among paralogues is thought to be through alterations in their expression patterns (Singh and Hannenhalli, 2010). Transcription factor binding sites and nucleosome occupancy have an important role in explaining the mechanisms underlying expression divergence (Singh and Hannenhalli, 2010). Positive selection on gene expression patterns and protein sequence in duplicate genes seems to be of a higher magnitude compared to orthologues genes and is reflected by accelerated rates of both *cis*-regulatory element and protein evolution (Castillo-Davis et al., 2004).

1.3.4 Properties and Proposed Functionality of CNEs

CNEs have been identified for groups of vertebrates and invertebrates separately. Although no sequence identity has been discovered so far between CNEs in vertebrates and CNEs in invertebrates, they share characteristics such as:

• High levels of identity (higher than that of protein-coding genes in most cases), across a wide range of species (Bejerano et al., 2004).

• Clustering around genes: The density of CNEs is higher in gene-rich regions in humans (Bejerano et al., 2004, Sandelin et al., 2004, Woolfe et al., 2005) and nematodes (Vavouri et al., 2007), with several CNEs clustered around each gene.

• Association with developmental genes: Gene association is determined by looking for the transcription start site nearest to each CNE. CNE-associated genes seem to be enriched for regulators of development such as transcription factors and signalling genes (Sandelin et al., 2004, McEwen et al., 2006).

1.3.5 Evolution of Conserved Noncoding Elements in Duplicated Genes

Many CNEs discovered in vertebrate genomes are found to function as tissue-specific enhancers (Lee et al., 2011). Lee et al., (2011), reported that 78-83% of CNEs have diverged in teleost fishes and only 24% and 40% have been lost in chicken and mammalian lineages, respectively. In comparison with bony vertebrates, teleost fish CNEs have been evolving at a remarkably higher rate and 68% of CNEs were lost before the divergence of the teleosts. This rapid rate of CNEs evolution has had an effect on the expression pattern of their target genes (Lee et al., 2011). The fish-

specific whole-genome duplication (FSGD) has a role in the accelerated evolution and the loss of a large number of both copies of duplicated CNEs in teleost fishes (Lee et al., 2011). Recent comparative analyses showed that many conserved sequences are often located in noncoding regions (Lee et al., 2011). Most of the conserved noncoding elements (CNEs) are located near genes responsible for the regulation of transcription and development (Sandelin et al. 2004; Woolfe et al., 2005). Functional analyses of many CNEs have shown that they function as *cis*-regulatory elements (or enhancers) of tissue-specific expression during early stages of development (Woolfe et al., 2005). The FSGD in the ray-finned fish lineage has led to duplication of genes that are single-copy in mammals (Lee et al., 2011). Lee and colleagues (Lee et al., 2011) showed that a similar proportion of CNEs were lost in both single and duplicated genes. The loss percentage was (38–41%) in singleton and (39–42%) in duplicate genes in stickleback, medaka, and fugu. However, in zebrafish, duplicate genes have lost a higher percentage (34%) of CNEs than singleton genes (27%) suggesting a relaxed constraint on both copies of duplicated CNEs (Lee et al., 2011). In the Lee et al. study, the authors showed that 68% of CNEs had disappeared in the ray-finned fish lineage before the divergence of zebrafish and the three acanthopterygians (stickleback, medaka, and fugu). These fishes are closely related species and their subdivisions together include 95% of living teleosts (Nelson 2006). 68% of CNEs have disappeared in the common ancestor of these fishes which could be explained by the majority of the CNEs diverging before the diversification of teleost fishes (Lee et al., 2011). There is now evidence that the FSGD occurred in the ray-finned fish lineage before the diversification of teleost fishes (Hoegg et al. 2004;

Jaillon et al. 2004; Crow et al. 2006). The FSGD that occurred in the ancestor of teleost fishes is therefore believed to be a contributing factor in the diversification of teleost fishes (Hoegg et al. 2004; Meyer and Van de Peer 2005; Crow et al. 2006; Santini et al. 2009). The whole-genome duplication event allows relaxed constraint on one or both copies of duplicated genes resulting in loss of a large number of duplicated genes and an asymmetric rate of evolution of genes retained in duplicate (Lynch and Conery 2000; Semon and Wolfe 2007). Consistent with this prediction, analysis of the evolutionary rate of protein-coding genes has indicated that both singleton and duplicate genes in teleost fishes have been evolving at a faster rate than their orthologues in mammals (Jaillon et al. 2004; Steinke et al. 2006). The accelerated rate of nucleotide substitution in teleosts is triggered by the fish-specific genome duplication and led to rapid divergence of protein-coding sequences and CNEs (McEwen et al., 2006). The higher substitution rate in some CNEs could be due to positive selection acting on these CNEs (McEwen et al., 2006). Evolutionary changes have been observed in the duplicated conserved noncoding elements (CNEs) within a genome in both nucleotide sequence and length than orthologous CNEs between genomes (McEwen et al., 2006). This indicates that 50–150 Mya following the duplication of these *cis*-regulatory elements and their associated genes, there was an increased rate of change within both the protein coding (Hughes and Friedman 2004) and regulatory sequences reflecting a possible relaxation of evolutionary constraint in one of the gene copies (McEwen et al., 2006) (Fig. 5).

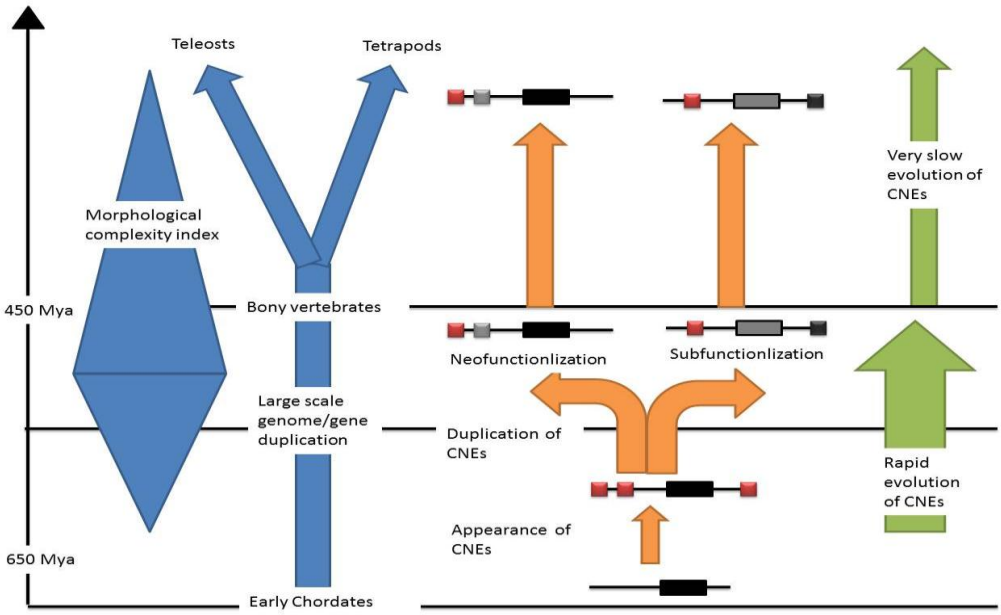

Figure 5: Evolution of CNEs in vertebrates. Modern bony vertebrates evolved from the chordate lineage between 650 and 450 Mya, during a period of rapid morphological change (represented here in blue). During this period an early ancestral vertebrate underwent one, or possibly two, whole genome duplications. The appearance of CNEs in vertebrate genomes (red boxes adjacent to gene loci, depicted as dark boxes) can be dated prior to these large-scale duplication events. This evolution must have occurred rapidly following duplication (orange arrows) over a relatively short evolutionary period (~50–150 Mya) In contrast, in the period since the teleost–tetrapod divergence (~450 Mya) (blue arrows), duplicated CNEs have had a remarkably slow mutation rate and have remained practically unchanged (green arrows) (Adapted from McEwen et al., 2006).

1.4 Comparative Genomics

Distinguishing between orthologues and paralogues is necessary to compare genome organization in different organisms. Orthologues are homologous genes in different species that encode a protein with the same function and which have evolved by direct vertical descent (Primrose and Twyman, 2003). Paralogues are homologous genes within an organism encoding proteins with related but non-identical functions.

Orthologues evolve simply by the gradual accumulation of mutations, whereas paralogues arise by gene duplication followed by mutation accumulation (Primrose and Twyman, 2003). Comparative genomics is the study of the similarities and differences between genome sequences of different species (Koonin, 2005). The structure of a protein determines its function (Hegyi and and Gerstein, 1999), and protein coding genes with shared ancestry but highly divergent sequences can have very similar structure and function (Wilson et al., 2000). Similar to protein-coding genes, noncoding sequences and their associated secondary structure information can help to define their homologies (Gardner et al., 2009; Meynert, 2010). Functional noncoding elements are more likely than non-functional DNA sequences to be under selective pressure to remain the same over time, as mutations might change or destroy their functionality (Miller et al., 2004). It is frequently assumed that noncoding elements with a high degree of sequence similarity between different genomes are likely to be homologous and functional (Miller et al., 2004).

1.5 Model Organism

1.5.1 Overview

Medaka (*Oryzias latipes*) is a small egg-laying freshwater teleost fish that is primarily endemic to Japan, Korea, Taiwan, and China (Wittbrodit et al., 2002). The adult fish are approximately 3 cm long, and the female lays a cluster of eggs (10-30 eggs) every day (Wittbrodit et al., 2002). The embryos develop externally and both the embryo and chorion are transparent. Medaka embryos hatch eight days after fertilization at 26 °C and grow to sexual maturity within 2 to 2.5 months (Takeda and

Shimada, 2010). Medaka is hardy and tolerates a wide range of temperatures (10- 40 °C); it is easy to breed and highly resistant to common fish disease (Wittbrodit et al., 2002). Male and females are easily distinguished by a clearly dimorphic dorsal fin. Because the eggs are connected to the female body by attachment filaments, reproductively active females can be easily identified and propagated (Witbrodit et al., 2002). Medaka is perfect for genetic studies because its genome is estimated to be 800 Mb, one quarter of the human genome and one half of the zebrafish genome and it is the first fish to prove that Mendelian laws are valid in vertebrates as early as 1913 (Wittbrodt et al., 2002).

1.5.2 Developmental Stages

The natural breeding season of *Oryzias latipes* extends from mid-April to late September in Japan. Oocyte maturation occurs at night (Iwamatsu, 1965 and Iwamatsu, 1974), and ovulation occurs at dawn (Egami, 1954 and Iwamatsu, 1978). Under regular daily photoperiod with more than 13 hours of artificial lighting (Yoshioka, 1963), ovulation occurs about 1 hour before the onset of the light period, and oviposition occurs for 1 hour before and after the onset of the light period throughout the year. Careful observation of the process of embryonic development by light microscopy identified 39 stages based on diagnostic features of the developing embryos (Iwamatsu, 2004) (Fig. 6). The principal diagnostic features are the number and size of blastomeres, form of the blastoderm, extent of epiboly, development of the central nervous system, number and form of somites, optic and otic development, development of the notochord, heart development, blood circulation, the size and

movement of the body, development of the tail, membranous fin (fin fold) development, and development of such viscera as the liver, gallbladder, gut tube, spleen and swim (air) bladder (Iwamatsu, 2004). After hatching, development of the larvae (fry) and young can be divided into six stages based on such diagnostic features as the fins, scales and secondary sexual characteristics (Iwamatsu, 2004). Table 1 describes the developmental process occurring in each stage.

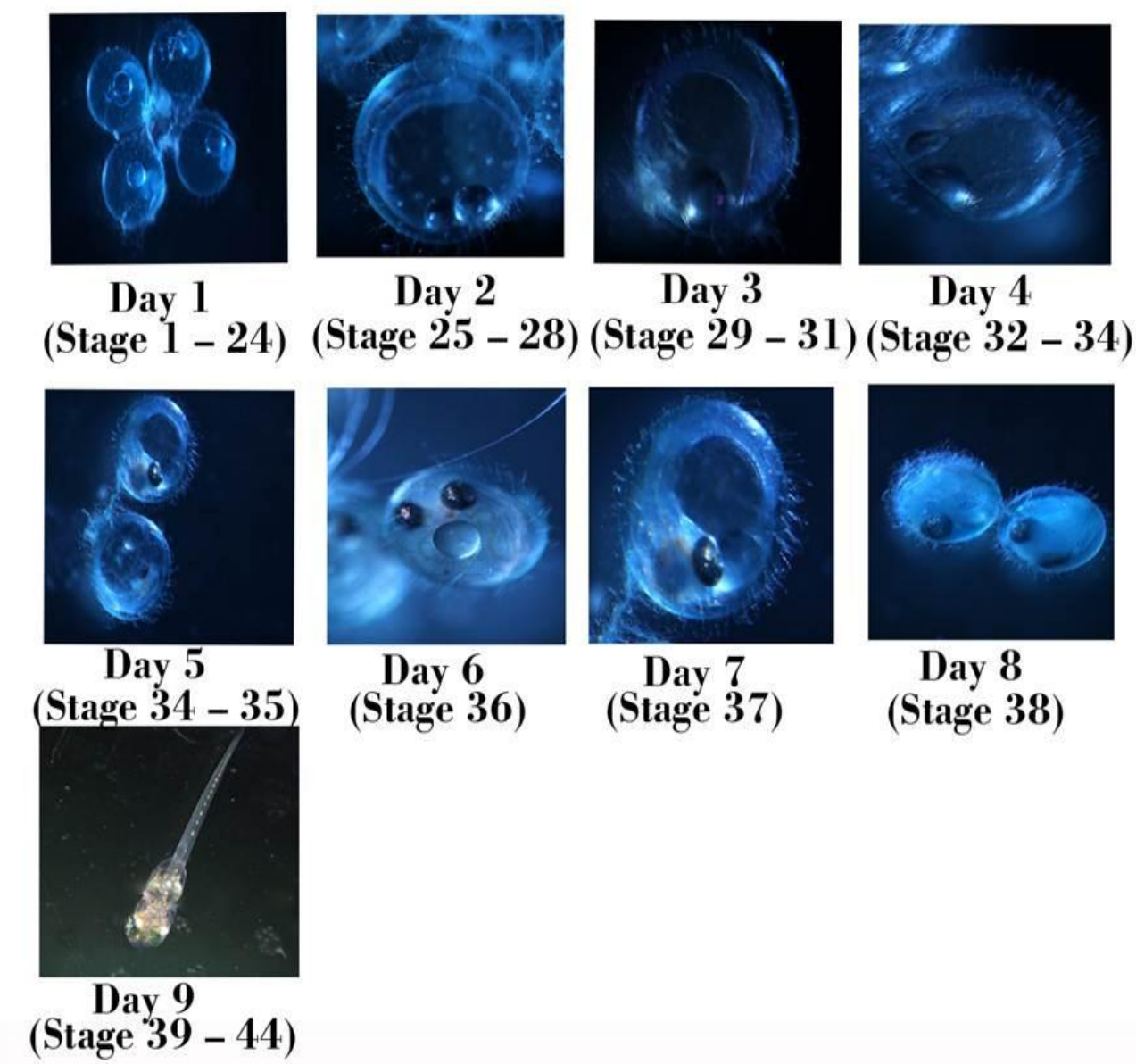

Figure 6: Medaka (*Oryzias latipes*) embryos developmental stages (Iwamatsu, 2004). Medaka embryos go through 45 developmental stages and they usually hatch within 9 days. Day1: stage1-stage 24, Day2: stage 25- stage 28, Day3: stage 29- stage 31, Day4: stage 32- stage 34, Day5: stage 35, Day6: stage 36, Day7: stage37, Day8: 38,and Day9: stage 39- stage 45 (Photographs by author).

Table 1: Developmental processes occurring during different developmental stages in Medaka (*Oryzias latipes)* embryos (Iwamatsu, 2004).

Days	Stage	Developmental processes
First 21 hours (stage 1 – stage 16)	Stage 1	Activated egg stage
	Stage 2	Blastodisc stage : formation of zygot nucleus appearance and division of chromosomes
	Stage 3 – stage 7	Blastomeres formation and cell cleavage (2 cell stag – 32 cell stage)
	Stage 8 – stage 9	Morula stage
	Stage 10 – stage 11	Blastula stage
	Stage 12 – stage 16	Gastrula stage
Day 1 (stage 17 – stage 24)	Stage 17 – stage 18	Neurula stage
	Stage 19 – stage 21	Somite stage: optic and auditory differentiation
	Stage 22 – stage 24	Somite stage: formation of tubular heart and start of heart beating
Day 2 (stage 25 – stage 28)	Stage 25	18 – 19 somite stage: 0nset of blood circulation
	Stage 26	22 somite stage: development of notochord and differentiation of eye.
	Stage 27	24 somite stage: appearance of pectoral fin bud. Formation of liver and gut.
	Stage 28	30 somaite stage: onset of retinal pigmentation
Day 3 (stage 29 – stage 31)	Stage 29	34 somite stage: internal ear formation, atrium and ventricle differentiation. Aorta formation
	Stage 30	35 somite stage: blood vessels development to supply gills, kidneys, brain,muscle and liver. Formation of swim bladder.
	Stage 31	Gill blood vessels formation stage. Formation of gallbladder

Table 1 Continued		
Day 4 (stage 32 – stage34)	Stage 32	Somite completion stage: formation of pronephros and air bladder.
	Stage 33	Stage at which notochord vacuolization is completed.
	Stage 34	Pectoral fin blood circulation stage.
Day 5 (stage 35)	Stage 35	Formation of visceral blood vesseles
Day 6 (stage 36)	Stage 36	Heart development stage.
Day 7 (stage 37)	Stage 37	Pericardial cavity formation stage.
Day 8 (stage 38)	Stage 38	Spleen development stages. Differentiation of caudal fin begins.
Day 9 (stage 39 – stage 45)	Stage 39	Hatching stage
	Stage 40	First fry stage
	Stage 41	Appearance of fin rays of dorsal and anal fins.
	Stage 42	Vascularization of the artery and the vein and extend to formation of shape of all fins.
	Stage 43	Appearance of ray nodes of dorsal and venteral fins.
	Stage 44	Formation of single dichotomous blanching at the distal end of fin ray of fins. Appearance of secondary sex characteristics such as urogenital protuberance and papillar processes on fin rays.
	Stage 45	Three rotations of the gut and formation of double dichotomus blanching of the distal end of fin rays of all fins.

1.5.3 Anatomy and Dissection

In the lateral view, the anterior portion of the abdominal cavity is occupied by three prominent organs: the heart, liver and kidney (Fig. 7D. I). The heart is surrounded by the pericardial cavity, which is separated from the abdominal cavity (Fig. 7D). The heart is positioned slightly to the right of the ventral midline. The liver is pink and stretches from the anterior one-third to one-fourth of the abdominal cavity (Fig. 7I). The reddish kidneys are located most dorsal in the abdominal cavity, just ventral to the spinal cord. Gonads are seen antroventral to the transparent air bladder (Fig. 7G). The oocytes in the ovary are discernible clearly from the right in females. The gut can be observed from both lateral and ventral sides (Fig. 7E, F).

In the dorsal view, the brain and spinal cord appears as a yellowish structure in the midline (Fig. 7A, C). In the gill, the fine comb-like structure of the branchial arches and their associated primary lamellae can be viewed through the operculum (Fig. 7H).

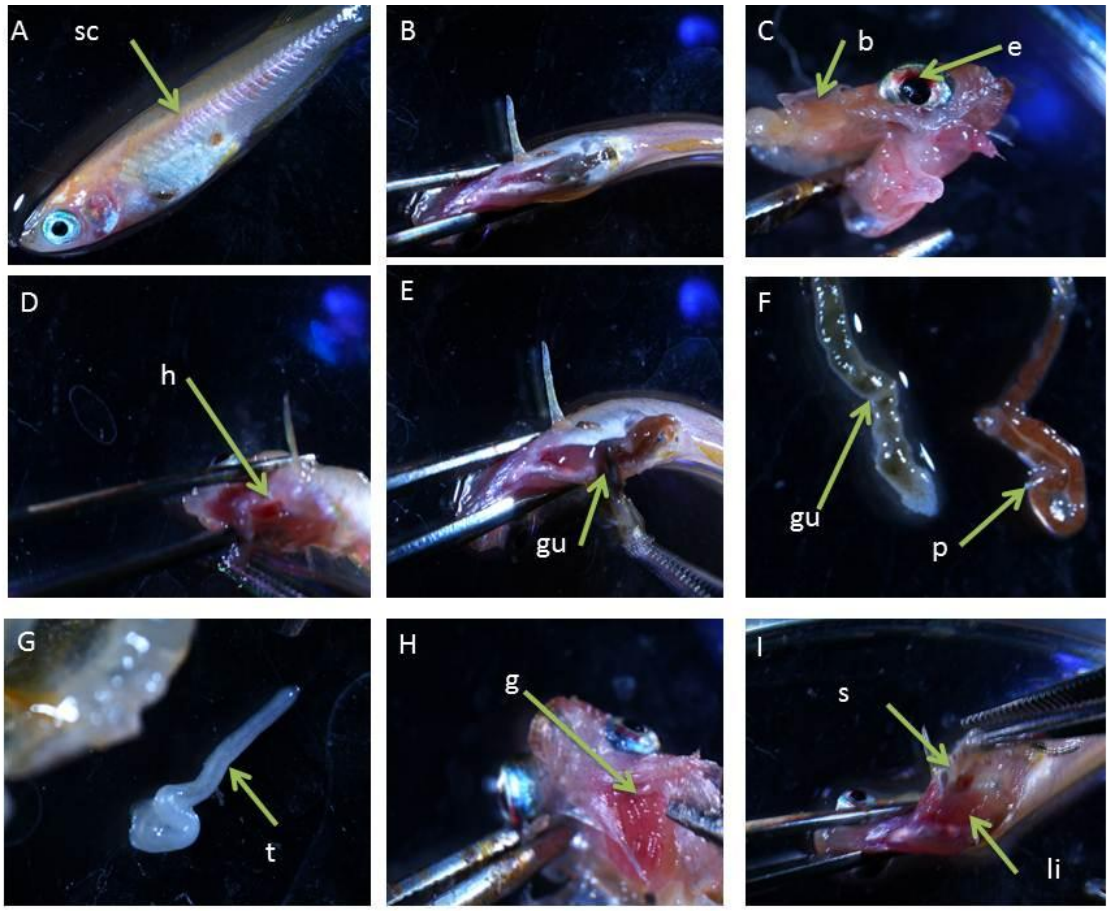

Figure 7: Dissected adult male medaka (*Oryzias latipes)* (A). Top view showing dissected medaka belly from anus to the chest (B). Dissected brain and eyes in ventral view (C). Top view showing dissected open chest with arrow pointing to the heart (D). Dissected belly showing gut (E). Surgically removed gut and pancreas (F). Dissected testis (G). Top view showing dissected gills (H). Opened abdomen showing liver and spleen (I). sc, spinal column; b, brain; e, eyes; h, heart; gu, gut; t, testis; g, gills; s, spleen; li, liver; p, pancreas (Photographs by author).

1.5.4 Advantage of Medaka as a Model Organism

There are three main fish model organisms commonly used, zebrafish (*Danio rerio*); medaka (*Oryzias latipes*); and fugu (*Takifugu rubripes*). Their major features and evolutionary relationship are compared in Table 2 and Fig. 8, respectively.

Recently, medaka has been used as a model organism in the study of certain human diseases (e.g. oncology, endocrine, and muscle dystrophy), toxicological research, molecular genetics, organogenesis and developmental research. The fact that medaka and zebrafish were separated from their common ancestor 110 Mya positions them as important models for comparative studies (Fig. 8). This evolutionary distance is reflected in many aspects of their biology, including early development and sex determination. Both fish models offer several advantages and both combine the power of genetics with experimental embryology and molecular biology (Wittbrodit et al., 2002). Early medaka development is rapid; whereas zebrafish larvae hatch after 2–3 days, medaka embryos are enclosed in a tough chorion that protects them in their natural habitat until they hatch as feeding young adults after 7 days. All zebrafish techniques including single-cell injections, transplantation and morpholino knockdown technology, also apply to medaka (Wittbrodit et al., 2002).

Medaka is the most genetically polymorphic vertebrate (3-4 % sequence divergence among regional populations). This large genetic polymorphism among regional populations is not found in other vertebrate models (Kinoshita et al., 2009).

The estimated genome size of medaka is about 800 million base pairs (Mbp) and that of zebrafish is 1700 Mbp (Kinoshita et al., 2009).

Table 2: Biological characteristics and availability of experimental tools in three teleost fish model organisms (Ishikawa, 2000).

Biological Characteristics	Zebrafish	Medaka	Fugu
Genome size	1700 Mb	800 Mb	400 Mb
Chromosome number of 2n	50	48	-
Sex determination	-	XY type	-
Life cycle	3 month	3 month	-
Outdoor breeding	no	yes	yes
Crossing in laboratories	yes	yes	No
Linkage map	yes	yes	no
The number of inbred strain	0	12	0
The number of mutant strains	2000	120	0
Transgenic fish	yes	yes	no

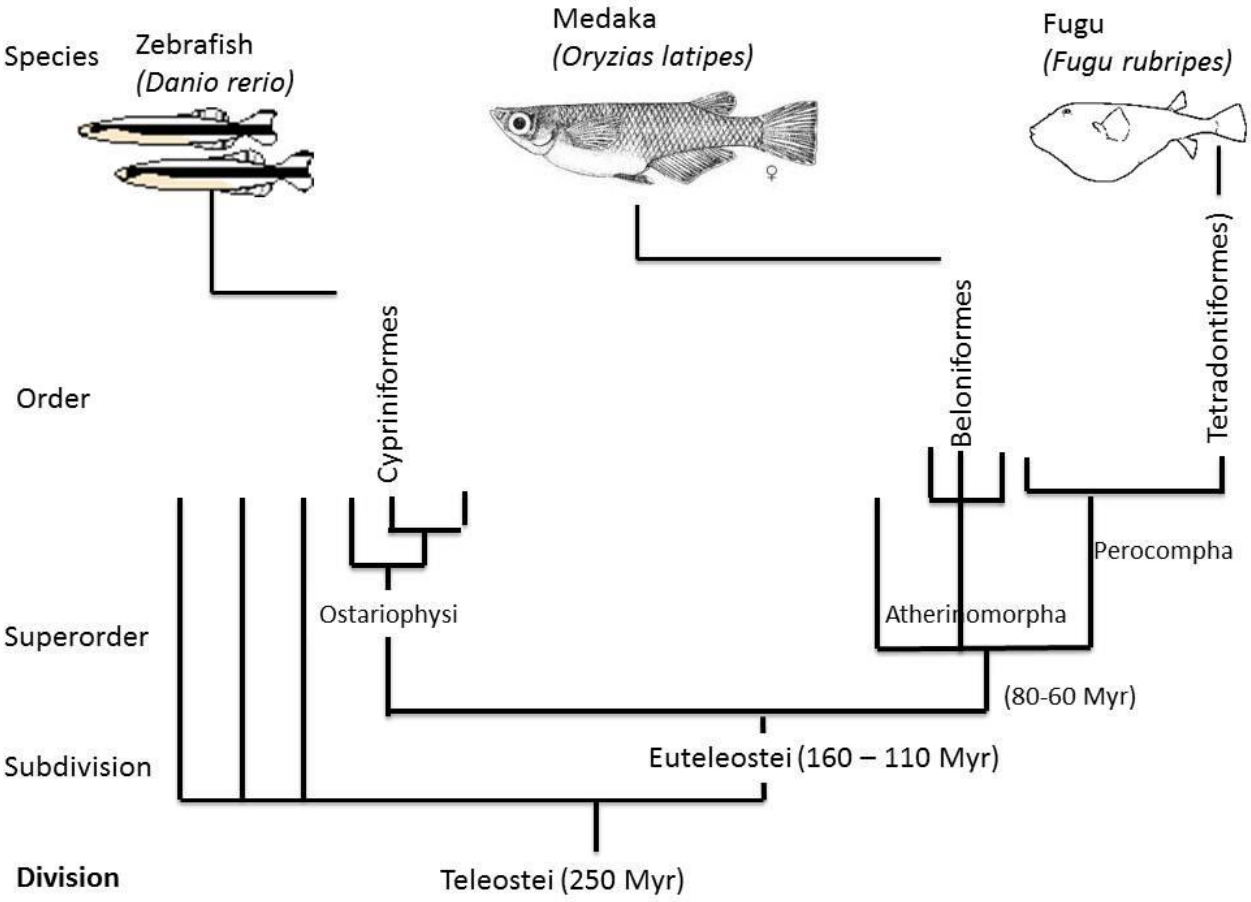

Figure 8: Evolutionary relationships among fish models. This evolutionary tree illustrates that the last common ancestor of medaka and zebrafish lived more than 110 million years ago (Mya). Notably, medaka is a much closer relative to fugu than it is to zebrafish, or than zebrafish is to fugu (Wittbrodit et al., 2002).

1.6 Objectives

The expression of RyR1 and RyR3 genes has been extensively studied in many model organisms including mouse and zebrafish but to date nothing is known about the expression of RyR1 and RyR3 genes in medaka. The first objective of my research is to search for evidence of divergence between regulatory elements in noncoding regions (introns) of the RyR paralogues that could be the basis for differential expression. The noncoding sequences (introns) are important after the upstream promoter region in controlling gene expression and harboring transcription factors binding sites. Previous multisequence alignments for RyR1 and RyR3 promoter sequences in zebrafish show no conservation with other co-orthologues including medaka (Kasloff, 2009; Vanderhooft, 2009). I decided to search the noncoding sequence of medaka RyR1 and RyR3 genes, looking for conserved noncoding regions with co-orthologues and within paralogues as well. This can be achieved using a multisequence alignment to compare medaka RyR1 and RyR3 co-orthologues including fugu, zebrafish, mouse, and human to determine whether any sequence conservation is present. Intron sequences obtained from the Ensembl (Stalker et al., 2004) database were first imported to the mVISTA (Loots and Ovcharenko, 2004) bioinformatics program to look for conserved noncoding regions. Conserved regions were assessed for transcription factors binding sites (TFBSs) using the rVISTA bioinformatics program.

The second objective of my research was to analyze the expression of the RyR paralogues (RyR1a/RyR1b; RyR3a/RyR3b) in developing medaka embryos to investigate whether temporal differences exist in their expression profile. Quantitative real time PCR (qRT-PCR) is utilized to measure the expression of the RyR paralogues both temporally (developmental stages) and spatially (dissected tissues). The overall objective of this part of the research was to look for evidence of divergence between paralogues and conservation with co-orthologues with respect to gene expression.

CHAPTER 2

MATERIALS AND METHODS

2.1 Conserved Noncoding Elements (CNEs) in RyR 1 and RyR3 genes

Intron sequences were located by database searching for RyR1 and RyR3 genes of medaka (*Oryzias latipes*), fugu (*Takifugu rubripes*) and zebrafish (*Danio rerio*). These sequences were analyzed together using a program called main VISTA (mVISTA) to identify areas of sequence conservation between introns. Regulatory VISTA (rVISTA) was utilized to search for transcription factor binding site hits in the sequences (Loots and Ovcharenko, 2004). The RyR1 and RyR3 introns were surveyed for a selection of 20 different TF sites. The identities of the RyR1 and RyR3 orthologues, located on the Ensembl genome browser, are listed in table 6 and table 7. Previous studies done in Dr. Franck's lab, show little conservation in the RyR3 promoter region of zebrafish in comparison with other vertebrates including humans. The noncoding intron regions are considered the second most important areas after the promoter to look for TFBSs. Regions with more than 70% conservation between medaka and fugu (RyR1a, RyR1b, RyR3a, and RyR3b) were submitted to the rVISTA program to search for transcription factor binding sites (TFBS) hits. The following list of TFBSs was used to search for conserved hits: FOX, MEF-2, MUSCLE, MYOD, MYOGENIN, STAT, CART-1, CLOX, EVI-1, GATA, HANDIE47, HNF-1, HNF-3, HNF-3α, HNF-4, HNF4-α, HNF-6, MYC, MYCMAX, MYOGNF-1, NKX6-1, NKX6-2, OCT, and TATA (Abbreviations and Nomenclature). These transcription factors were selected according to analysis with the matinspector software program (Genomatix) results (Cartharius et al., 2005). Matinspector software uses a wide library of matrix descriptions for TFBDs to locate matches in DNA sequences through assigning a quality rating to each match, this will facilitate for quality-based filtering

and selection of matches based on its grouping of transcription factor binding sites into matrix families based on functional similarity. Mismatches may be avoided by toggling the parameter “core similarity”, a term used to describe a TFBDs sequence identity to a precomputated, highly conserved four base pair sequence in the anchored center of a given matrix. A decrease in core similarity allows for a lower degree of specificity for the core region of a specific TF, while an increase in core similarity causes the program to overlook potential matches.

2.2 RNA Extraction

Homogenization of 100 mg of whole medaka fish tissue was performed in 1 mL of TRIzol reagent (Invitrogen Life Technologies). The tissues were homogenized with a motorized teflon pestle and glass mortar. Total RNA was precipitated from the supernatant with 95% ethanol, pelleted by centrifugation at maximum speed (14,000 ×g) and dried by speed-vacuum evaporation. The dried RNA pellet was resuspended in 50 µL of RNase free water, and quantified using a nanophotometer (UV_{260} was measured; Birds, 2005).

2.3 cDNA Synthesis

A 20 µL solution of 10 – 20 µg of total RNA was mixed with 0.05 µg/µL of Oligo dT 15 primer (to synthesize the first strand of cDNA) and heated to 95°C for five minutes and immediately chilled on ice. Next, 12 µL of 5X Oligo dT 15 buffer, 2 µL of 10 mM dNTPs, 24 µL double distilled H_2O (ddH_2O), 1 µL RNAsin and 1 µL of reverse transcriptase (SS II RT) were added and mixed. The solution was then incubated at room temperature for 15 minutes, followed by 30 minutes incubation at

37°C. 40 µL of 10X TE buffer was added to stop the reaction at room temperature (pH 8.0). The first strand cDNA was precipitated by adding 10 µL of 3M sodium acetate and 250 µL of 95% ethanol. The cDNA was precipitated at -20°C over night then pelleted by centrifugation at 14,000 ×g for 15 minutes, washed with 95% ethanol and centrifuged again at 3,000 – 4,000 ×g for 5 minutes. The pellet was dissolved in 100 µL of distilled, RNase and DNase free water (Invitrogen Life Technologies).

2.4 Identification of RyR1 and RyR3 Genes via Database Searching

A preliminary search was performed using Ensembl database website (http://www.ensembl.org). The RyR1a gene (ID ENSORLT00000008002) is located on chromosome 14, reverse strand. The total length of the predicted transcript is 14,880 bp with 110 exons with a predicted protein sequence of 4,959 amino acids. The RyR1b gene (ID ENSORLT00000001305) is located on chromosome 13, reverse strand. The predicted transcript length is 15,038 bp with 109 exons and the corresponding protein has 4,863 amino acids. The RyR3a gene (ID ENSORLT00000021133) is located on chromosome 22, reverse strand. The predicted transcript length is 13,497 bp with 100 exons with a predicted protein sequence of 4,498 amino acids. The RyR3b gene (ID ENSORLT00000022370) is located on chromosome 24, reverse strand. The predicted transcript length is 14,604 bp with 110 exons and the corresponding protein is 4,498 amino acids.

2.5 Primer Design

Primer pairs were designed for each gene by searching the terminal 1,000 bp of the predicted transcript using the Primer 3 program (Rozen *et al.*, 2000). The primers

amplified products of 906 bp for RyR1a, 520 bp for RyR1b, 523 bp for RyR3a, and 916 bp for RyR3b (Table 3).

2.6 Polymerase Chain Reaction (PCR)

Primers in Table 3 were used to amplify RyR messages from whole Medaka cDNA. 22.5 µL of master mix and 2 µL of template (equivalent of approximately 3 ng of cDNA template) were used for each PCR reaction. The master mix contained 2.5µL of 10X PCR buffer (Invitrogen Life Technologies), 0.75 µL of 50 mM MgCl2, 0.5 µL of 10 mM dNTPs, 1.5 µL of each primers, 0.2 µL recombinant Taq DNA Polymerase (0.5 U) and 15 µL of ddH_2O (RNase free water). The thermal conditions for PCR reaction are listed in table 4. PCR reaction products were then fractionated on a 1% low melting point agarose gel containing 0.5 µg/µL ethidium bromide and viewed on a Bio-Rad UV transilluminator (Universal Hood II), and purified with the S.N.A.P. Gel Purification Kit (Invitrogen Life Technologies) following the manufacturer's protocol.

Table 3: Primers used for PCR amplification of RyR1 and RYR3 in Medaka fish, *Oryzias latipes*

Target genes	**Accession number**	**Primer sequence**	**Product size (bp)**
RyR1a	ENSORLT00000008002	F: GCGTTTTCTGGCTCTGTTTC	906
		R: TCATCCTCGTCTTCGCTCTT	
RyR1b	ENSORLT00000001305	F: TGACCCACGGAAAGAAACCC	520
		R: ACGAGCTGTACCGCGTGGTC	
RyR3a	ENSORLT00000021133	F: CATCACCGACCAGCCGTCTG	523
		R: ACCTCTACACAGTGGTGGCC	
RyR3b	ENSORLT00000022371	F: AGGTGACGAGAACACGCTCT	916
		R: ATGAGGACGAGCCGGACATG	

*-The letter "F" in the primer name indicates a forward primer and an "R" indicates a reverse primer.

Table 4: Thermal conditions used for PCR reaction.		
Steps	**Temperature (° C)**	**Time**
1.Initial denaturation/enzyme activation	95	5 minutes
2. Denaturation	95	1 minute
3. Annealing	57	1 minute and 30 seconds
4. Extension	72	1 minute
5. Repeat step 2 to 4 for 35 more cycles		
6. Final extension	72	7 minutes

2.7 Cloning of PCR products

After purification, the PCR products were ligated with pGEM– T Easy vectors (Promega Biotech, Appendix 1). Ligation reactions were transformed into competent *Escherichia coli* JM109 cells (*E. coli* JM109; Promega Biotech). Transformed cells were plated on NZCYM growth media supplemented with 50 µg/mL ampicillin, 40 µg/mL X-gal and 0.1 mM IPTG (IPTG acted as an inducer of the *lac* operon in *E. coli* while X-gal was a visual indicator of β-galactosidase activity). The activity of IPTG in combination with X-gal allowed for screening of colonies. The plates then were incubated at 37°C overnight. Colonies with a functional *lac* operon appeared blue; while the recombinant colonies appeared white due to disruption of the β-galactosidase gene. Because the pGEM– T Easy vectors contain an ampicillin antibiotic resistance gene, the media was supplemented with ampicillin (50 µg/ml) to prevent the growth of non-transformed bacteria**.**

2.8 PCR Detection of Recombinants and Plasmid Purification

Bacterial colonies were randomly selected with a sterile pipette tip from each plate. The tip was then used to inoculate a PCR tube containing 15 µL of PCR master mix. The PCR master mix contain 1.5 µL 10X PCR buffer, 0.9 µL 50 mM MgCl2, 0.075 µL of 100 µM M13 forward primer, 0.075 µL of 100 µM M13 reverse primer, 11.925 µL ddH_2O, and 1.5 µL Taq DNA Polymerase, for approximately one minute at room temperature. PCR was performed using M13 forward (5´-GTTTTCCCAGTCACGAC-3´) and M13 reverse (5´ CAGGAAACAGCTATGAC-3´) primer pairs to amplify the cloned insert. The tip was subsequently used to inoculate a culture tube containing 3 ml of NZCYM media supplemented with 0.5 mg/ml ampicillin. The PCR program consisted of an initial denaturation step at 95°C for five minutes. The second step was at 95°C for one minute, followed by an annealing step of 57°C for thirty seconds and an extension step at 72°C for one minute. The second, third and fourth steps were cycled 35 times. The reaction products were fractionated on a 1.5% agarose gel containing 0.5 µg/µL ethidium bromides and viewed on a Bio-Rad UV transilluminator (Universal Hood II). Bacterial cultures corresponding to PCR products of expected size were grown overnight in NZCYM broth containing 50 µg/mL ampicillin.

2.9 Sequencing

Recombinant plasmids were sent to The Centre for Applied Genomics (The Hospital for Sick Children, University of Toronto) for sequencing. DNA sequences were aligned using the CLUSTALX (Thompson et al., 1994) and Genedoc software (Nicholas et al., 1997).

2.10 Medaka Embryo Collection

Medaka were kept in the animal complex in special breeding tanks on daily photoperiod of 16 hours light, 8 hours dark. Ovulation is expected to occur about 1 hour before the onset of the light period (Iwamatsu, 2004). Fish were fed with Brine shrimp (Artemia) along with dry food two times daily to increase the efficiency of breeding. Eggs were separated from the females using a small camel hair brush and pipettes for sorting and separating the eggs. The embryos were then transferred to a special culture dish where they were washed in 0.5% bleach to minimize the chance of bacterial growth. Embryos were incubated in culture medium of 10g/100ml of NaCl, 0.3g/100ml of KCl, 0.4g/100ml of $CaCl_2.H_2O$, 1.63g/100ml of $MgSO_4.7H_2O$ and 0.01g/100ml of Methylene blue to prevent fungal growth) (Shultz, 2009). The collected embryos were placed in the culture medium (1 ml/egg/plate). The medium was changed daily for each plate. The eggs develop to the hatching stage within 8 days at 26 °C (Iwamatsu, 2004). RNA was extracted from all developmental stages. Eggs were stored in RNA later reagent and RNA was extracted using TRIzol reagent. First strand cDNA was synthesized as per the protocol described previously. PCR reactions were performed using the same primers listed in Table 1.

2.11 Medaka Fish Dissection

Medaka were obtained from Trent University. Fish were sacrificed following a protocol approved by the University of Winnipeg Senate Animal Care Committee. Fish were euthanized immediately by immersion in 0.6 mg/ml MS222 (Tricaine Sulfate; 300 mg MS222 dissolved in 500 mL of ddH_2O; pH adjusted to 7.0 by adding 1 M NaOH). Tissues were dissected from the specimens using a dissecting microscope. White muscle (fast twitch), red muscle (slow twitch), cardiac muscle, brain, spinal cord, ovaries, testes and liver were carefully dissected. The dissected tissues were kept in RNA Later solution (Ambion) at -80°C for later usage. RNA was extracted using 1000 µL of TRIzol per 100 mg of tissue weight. TRIzol-digested tissues were extracted with 200 µL chloroform for each 1 ml of TRIzol and precipitated with 1000 µL 75% ethanol for each 1 ml TRIzol used, and 500 µL of isopropyl alcohol was used for the washing step. All the centrifugation steps were done at 4°C. Then cDNA synthesis and PCR amplification for all the above samples were done and fractionated on 1.5% agarose gel.

2.12 Quantitative Real Time PCR (qRT-PCR)

The expression level of the medaka RyR genes was measured relative to the average expression of 18S rRNA and beta-actin housekeeping genes. Primers used for quantification of housekeeping gene, RyR1 and RyR3 paralogues are listed in Tables 3 and 5 respectively. A 15 µL total reaction volume was used for each qRT-PCR reaction, consisting of 7.5 µL SYBR Green master mix, 1.5 µL each of forward and reverse primers at 10 µM concentration, 1 µL cDNA template and 3.5 µL ddH_2O. A single peak was indicative of a single PCR product in the reaction well. The results of

the qRT-PCR analysis were collected and analyzed using the CFX Monitor software (Bio-Rad). Efficiency of designed primers in binding and amplifying the target gene was determined by generating a standard curve from undiluted and 10^{-1}, 10^{-2}, 10^{-3} and 10^{-4} dilutions of cDNA template. Trials were run in triplicates (3 experimental sets) and the average concentration threshold (Ct) value was plotted against the log (dilution). The slope for RyR1 and RyR3 paralogues as well as for housekeeping genes was calculated to determine the efficiency (E) value ($E = 10^{-1}$/slope). The efficiency of the four target genes and housekeeping genes was very close to 2. The tissue with the highest Ct value was chosen as a calibrator. A relative fold expression of the four genes in each adult and developmental tissue was calculated using $2^{-\Delta\Delta}$CT method using the following equation:

$$\text{Relative expression} = 2^{-\Delta\Delta}CT$$

Where ΔCT target = Ct (target, calibrator) - Ct (target, test)

ΔCT Reference = Ct (Reference, calibrator) - Ct (Reference, test)

ΔΔCT = ΔCT Reference - ΔCT target

Standard deviation and standard error for reference and target genes where calculated using the following formula:

$$\sigma = \sqrt{\frac{\Sigma\ (x - \bar{x})^2}{n}} \qquad SE_m = \frac{s}{\sqrt{n}}$$

Where X is the individual sample mean, $\bar{X}$ is the average samples mean, S is the standard deviation and SE is the standard error.

Table 5: Primers used for amplification of housekeeping genes (18S and Actin) and qRT-PCR (Zhang and hu, 2007).

Target genes	GenBank Accession no.	Primer sequence	Product size (bp)
18S rRNA	AB105163	F: CGTTCAGCCACACGAGATTG	56
		R: CCGGACATCTAAGGGCATCA	
ß-actin	S74868	F: TCCACCTTCCAGCAGATGTG	76
		R: AGCATTTGCGGTGGACGAT	

CHAPTER 3

RESULTS

3.1 Bioinformatic Analyses of CNEs

3.1.1 mVISTA

A multisequence alignment of the co-orthologues RyR1a, RyR1b, RyR3a and RyR3b intron sequences from medaka, zebrafish, mouse, human and fugu was done using mVISTA. Fugu RyR1a, RyR1b, RyR3a and RyR3b sequences were used as a baseline for the co-orthologues from the other species. The number of introns for each gene is given in table 6 and table 7.

Table 6: RyR1a and RyR1b intron numbers.

	Ensembl ID	**Number of introns**
Medaka	RyR1a: ENSORLT00000008002	110
	RyR1b: ENSORLT00000001305	109
Zebrafish	RyR1a: ENSDART00000014749	105
	RyR1b: ENSDART00000036015	104
Fugu	RyR1a: ENSTRUT000000043571	107
	RyR1b: ENSTRUT00000039120	107
Mouse	RyR1: ENSMUST00000032813	106
Human	RyR1: ENST00000359596	106

Table 7: RyR3a and RyR3b intron numbers		
	Ensembl ID	**Number of introns**
Medaka	RyR3a: ENSORLT00000021133	99
	RyR3b: ENSORLT00000022371	109
Zebrafish	RyR3: ENSDART00000147464	97
Fugu	RyR3a: ENSTRUT00000036458	105
	RyR3b: ENSTRUT00000046340	107
Mouse	ENSMUST00000091818	103
Human	ENST00000415757	103

The mVISTA analysis identifies conserved regions with more than 70% sequence identity between the RyR1a orthologues (Fig. 9). Intron 73 in fugu RyR1a is conserved with intron 74 in medaka and intron 72 in zebrafish. The orthology of the introns is confirmed by alignment of the local protein sequences in the flanking exons (Fig. 10).

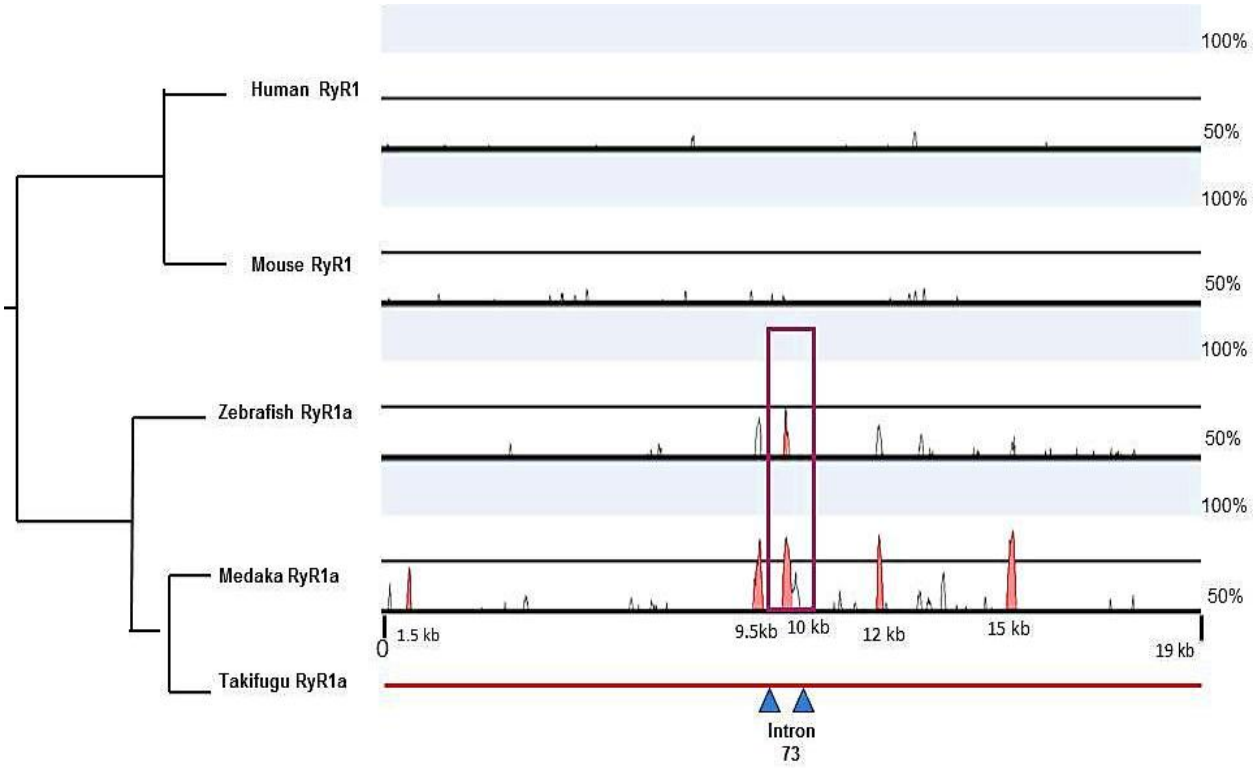

Figure 9: Analysis of conserved noncoding sequences (CNSs) in RyR1a orthologues. The takifugu RyR1a sequence is the baseline used for comparison. HCNS exceeding 70% between orthologues are shaded in red.

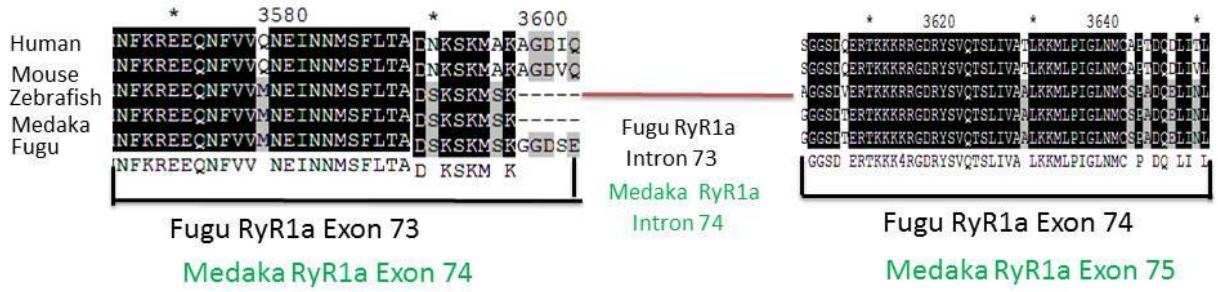

Figure 10: Local amino acid alignment for the RyR1 orthologues from human (RyR1), mouse (RyR1), zebrafish (RyR1a), medaka (RyR1a) and fugu (RyR1a). Fugu RyR1a intron number 73 is conserved with medaka RyR1a intron number 74.

Figure 11 illustrates the conserved regions identified using mVISTA with more than 70% conservation between RyR1b co-orthologues. Intron 72 in fugu RyR1b is found to be conserved with intron number 73 in medaka and intron 71 in zebrafish. The orthology of the introns is confirmed by alignment of the local protein sequences within the flanking exons (Fig. 12).

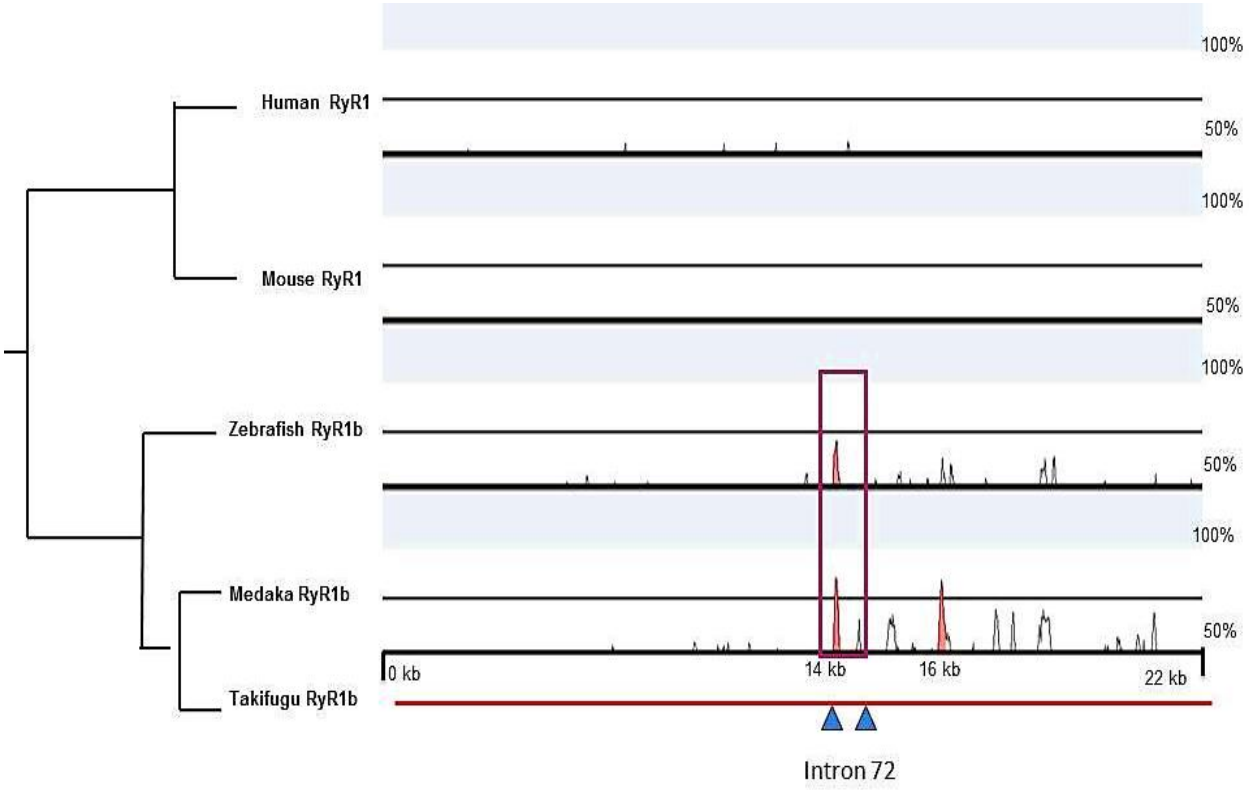

Figure 11: Analysis of conserved noncoding sequences (CNSs) in RyR1b co-orthologues. The takifugu RyR1b sequence is the baseline used for comparison. CNSs exceeding 70% between orthologues are shaded in red.

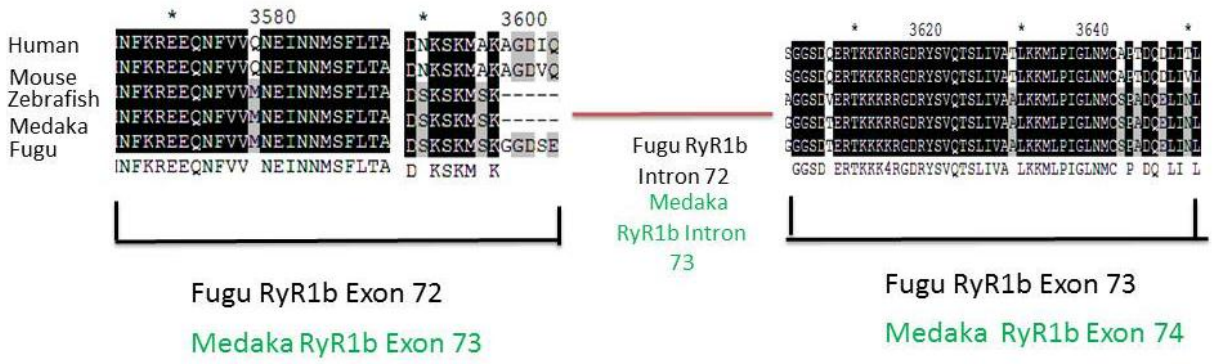

Figure 12: Local amino acids alignment for RyR1b co-orthologues. Fugu RyR1b intron 72 is conserved with medaka RyR1b intron 73.

Figure 13 illustrates the conserved intron regions found with more than 70% conservation between RyR3a co-orthologues. Intron 75 in fugu RyR3a is found to be conserved with intron 76 in medaka and intron 69 in zebrafish. The orthology of the introns is confirmed by alignment of the local protein sequences in the flanking exons (Fig. 14).

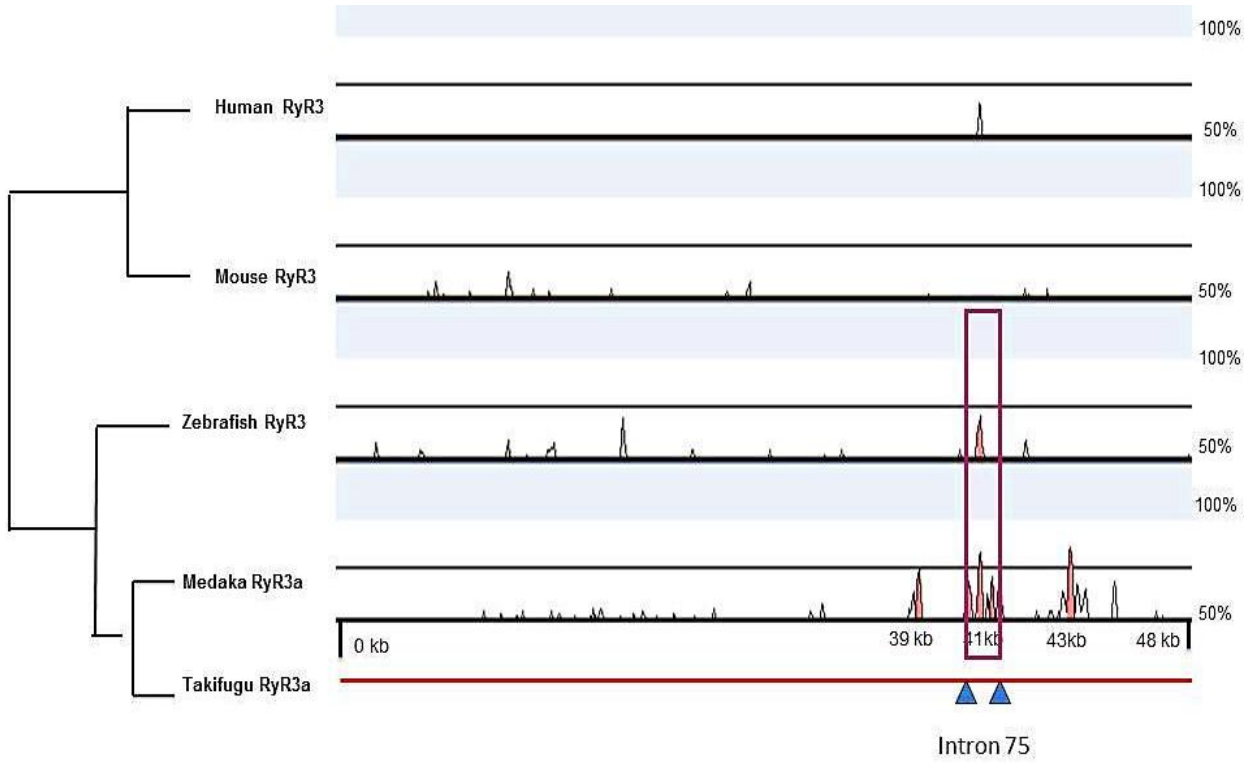

Figure 13: Analysis of conserved noncoding sequences (CNSs) in RyR3a co-orthologues. The takifugu RyR3a sequence is the baseline used for comparison. CNSs exceeding 70% between co-orthologues are shaded in red.

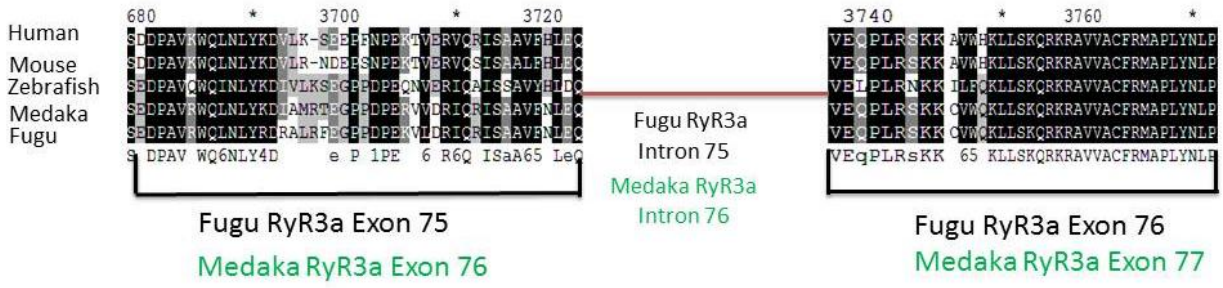

Figure 14: Local amino acids alignment for RyR3a co-orthologues. Fugu RyR3a intron 75 is conserved with medaka RyR3a intron 76.

Figure 15 illustrates the conserved region found with more than 70% conservation between RyR3b co-orthologues. Intron 78 in fugu RyR3b is conserved with intron 79 in medaka and intron 69 in zebrafish. To confirm the orthology of the introns a local protein sequence alignment was done to demonstrate the amino acid conservation in the flanking exons (Fig. 16).

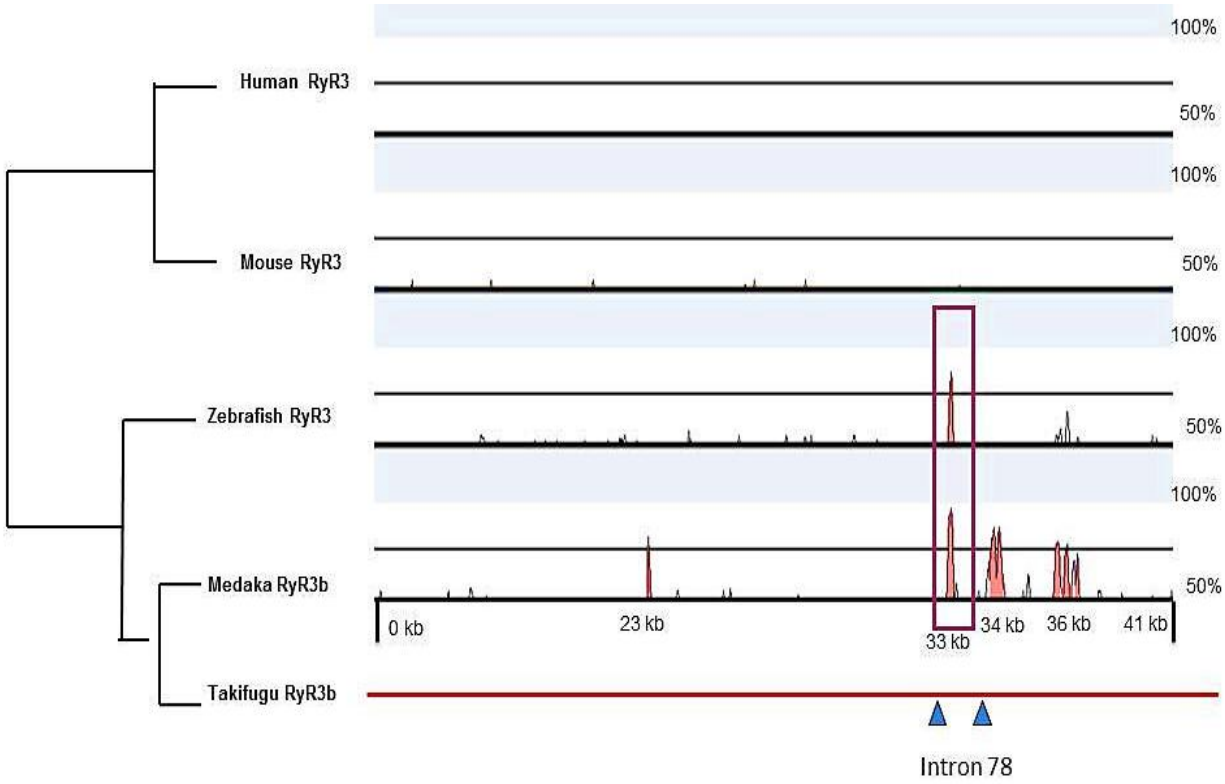

Figure 15: Analysis of conserved noncoding sequences (CNSs) in RyR3b co-orthologues. The takifugu RyR3b sequence is the baseline used for comparison. CNSs exceeding 70% between co-orthologues are shaded in red.

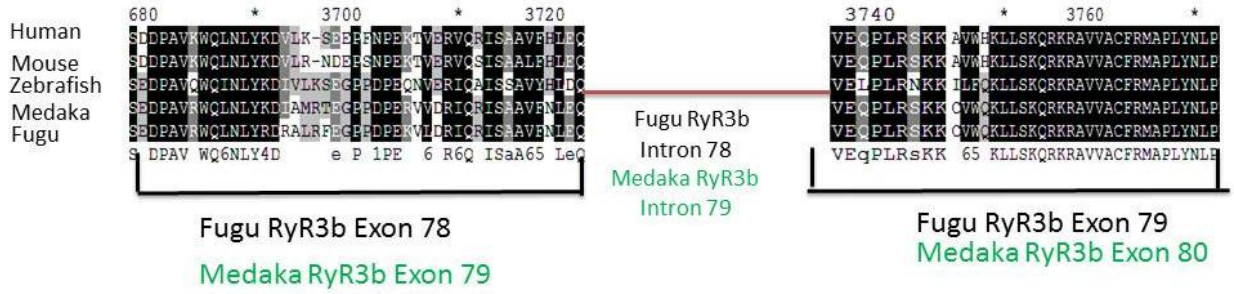

Figure 16: Amino acids alignment for RyR3b co-orthologues. Fugu RyR3b intron 78 is conserved with medaka RyR1a intron 79.

A pairwise sequence alignment using mVISTA between medaka RyR1a and RyR1b genes (Fig. 17) reveals divergence between the medaka RyR1 paralogues (RyR1a and RyR1b). Only one conserved region could be found between medaka RyR1a and RyR1b in contrast with 5 conserved regions found between medaka and fugu RyR1a (Fig. 9) and two conserved noncoding regions between medaka and fugu RyR1b (Fig. 11).

RyR3 paralogues (RyR3a and RyR3b) show evidence of divergence which is demonstrated in Fig. 18. A pairwise sequence alignment between medaka RyR3a and RyR3b noncoding (introns) sequences reveals one region of conservation between the sequences, whereas 6 regions of CNSs are found between medaka RyR3a and fugu RyR3a co-orthologues (Fig. 13) and 7 regions between medaka and RyR3b co-orthologues (Fig. 15).

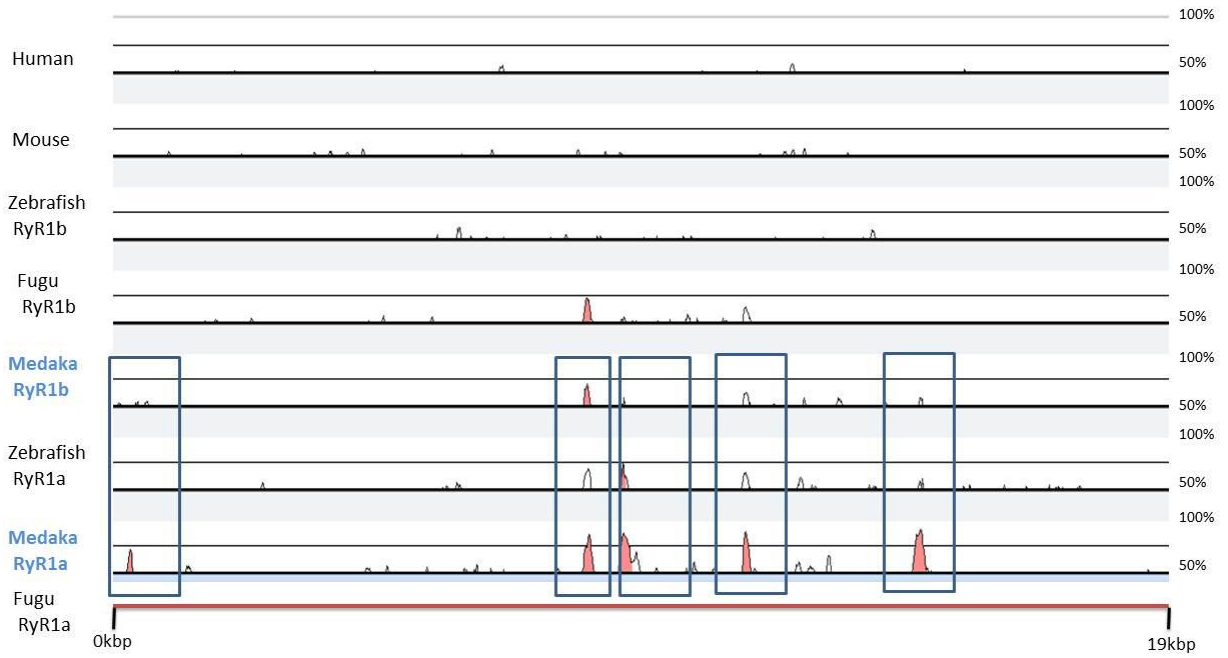

Figure 17: Evidence of divergence between Medaka RyR1a and RyR1b paralogues.

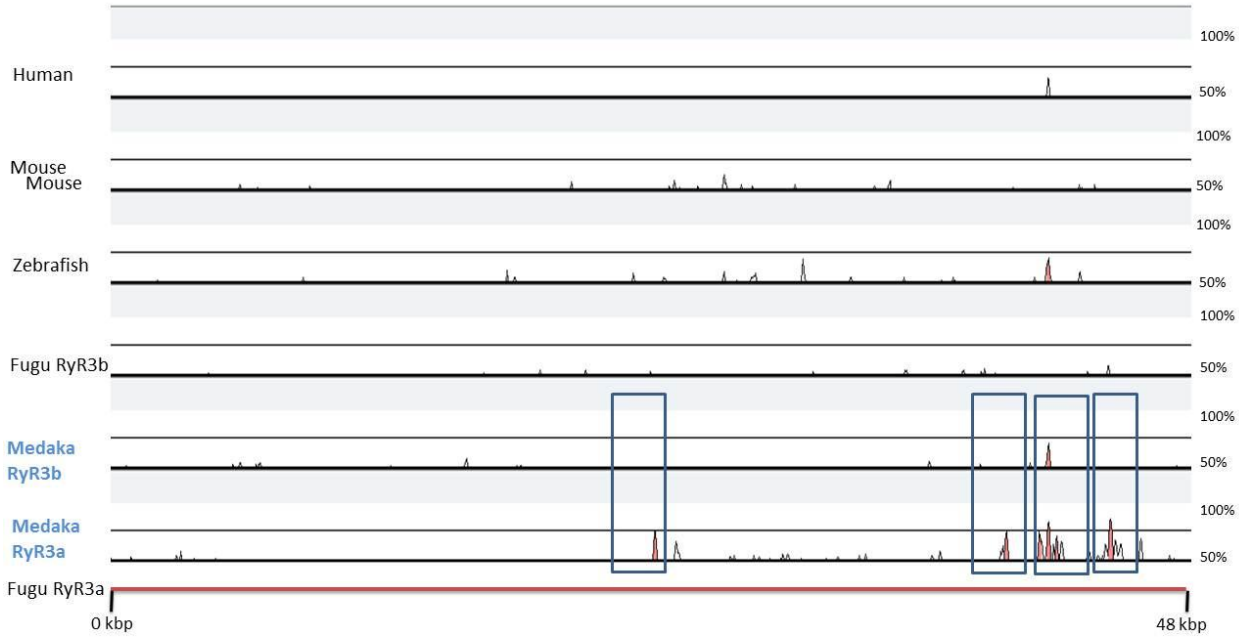

Figure 18: Evidence of divergence between Medaka RyR3a and RyR3b paralogues.

3.1.2 rVISTA Analysis: Search for Transcription Factor Binding Sites

I searched those sites with more than 70% conservation between fugu RyR1a and medaka RyR1a, fugu RyR1b and medaka RyR1b, fugu RyR3a and medaka RyR3a, and fugu RyR3b and medaka RyR3b using rVISTA to search for transcription factors binding sites (TFBs) conservation. Conserved TFBs for RyR1a, RyR1b, RyR3a and RyR3b are shown in Figs. 19, 20, 21 and 22 respectively. The following list of TFBSs was used for the search: FOX MEF-2, MUSCLE, MYOD, MYOGENIN, STAT, CART-1, CLOX, EVI-1, GATA, HANDIE47, HNF-1, HNF-3, HNF-3α, HNF-4, HNF4-α, HNF-6, MYC, MYCMAX, MYOGNF-1, NKX6-1, NKX6-2, OCT, and TATA. A list of the transcription factors along with their function are shown in table 10.

Using a threshold cutoff of 85% core similarity from MatInspector (Genomatix) results, these RyR1a, RyR1b RyR3a and RyR3b noncoding regions were surveyed for a selection of 20 different TF sites.

Table 8 lists the transcription factors that have been found in association with RyR1a and RyR1b. For RyR1a, clustering was observed for HNF4, HNF1, EVI1 followed by Muscle, HNF3 and HANDIE47. Other TFBSs including MEF2, NKX62, TATA, FOX, and GATA were not found. In contrast, RyR1b shows a higher level of HNF4 followed by EVI1 and Muscle. Little conservation has been found in HANDIE47, MOD, MYOGENIN and GATA. No conservation has been found between other TFBs including OCT, TATA, STAT, MEF2 and NKX62.

Legends for figures on following pages:

Figure 19: Transcription factors conserved between fugu RyR1a and medaka RyR1a genes. Clustering was observed of HNF4, HNF1, EVI1 followed by Muscle, HNF3 and HANDIE47. Other TFBSs including MEF2, NKX62, TATA, FOX, and GATA were not found.

Figure 20: Transcription factors conserved between fugu RyR1b and medaka RyR1b genes. RyR1b higher hits level of HNF4 followed by EVI1 and Muscle. Little conservation has been found in HANDIE47, MOD, MYOGENIN and GATA. No conservation has been found between other TFBs including OCT, TATA, STAT, MEF2 and NKX62.

Figure 21: Transcription factors conserved between fugu RyR3a and medaka RyR3a genes. Clustering was observed of HNF4, OCT. few clustering have been observed in FOX, Muscle, MYC MAX, STAT, TATA, NKX62 and HANDIE47. No conservation has been found in GATA and CART1 sites.

Figure 22: Transcription factors conserved between fugu RyR3b and medaka RyR3b genes. RyR3b shows clustering in HNF4, HNF1, and HNF3, EVI1 followed by few clusters in CART1, GATA, MYC MAX, STAT, TATA, NKX62 and HANDIE47.

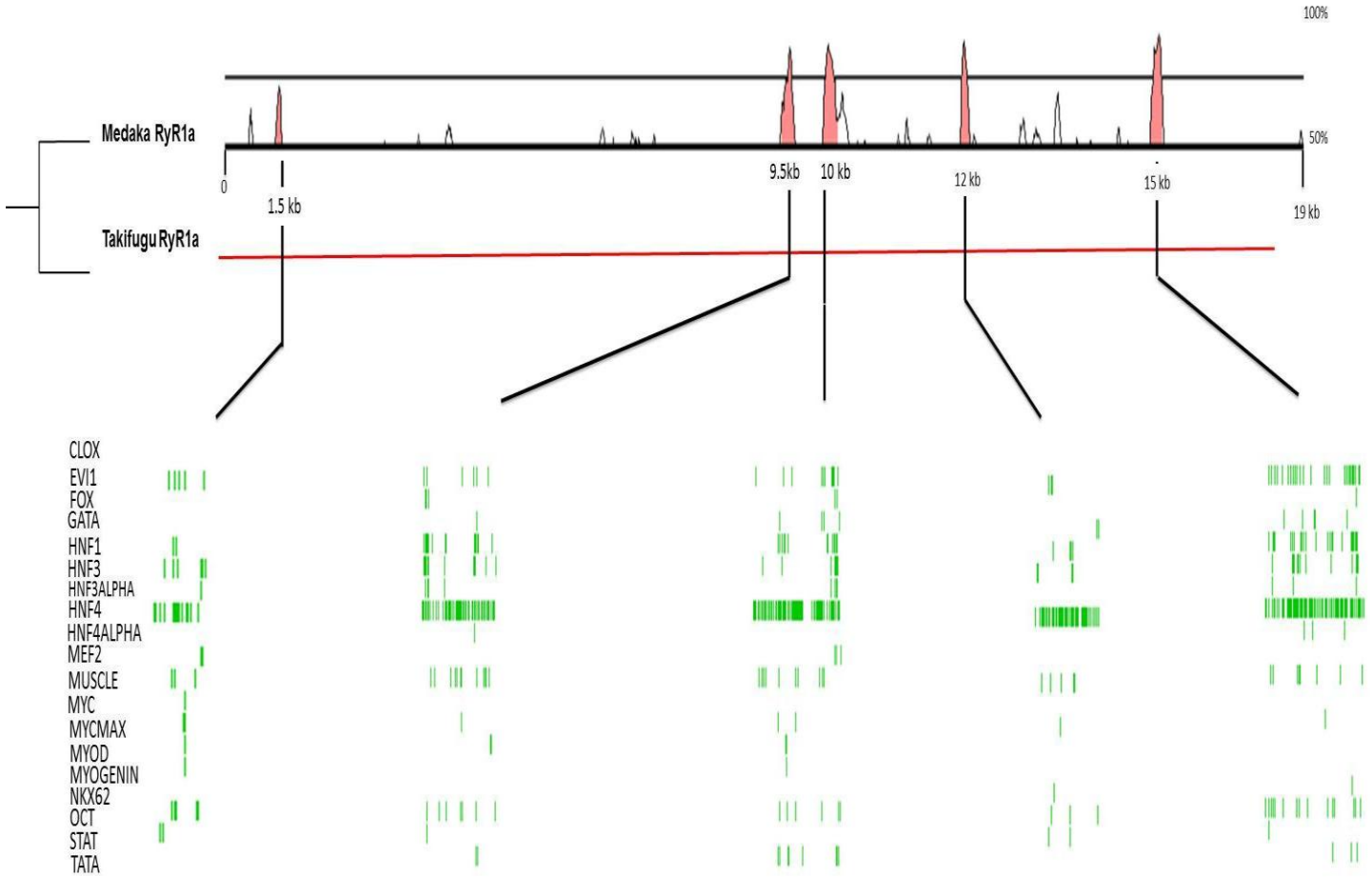

Figure 19: Transcription factors conserved between fugu RyR1a and medaka RyR1a genes.

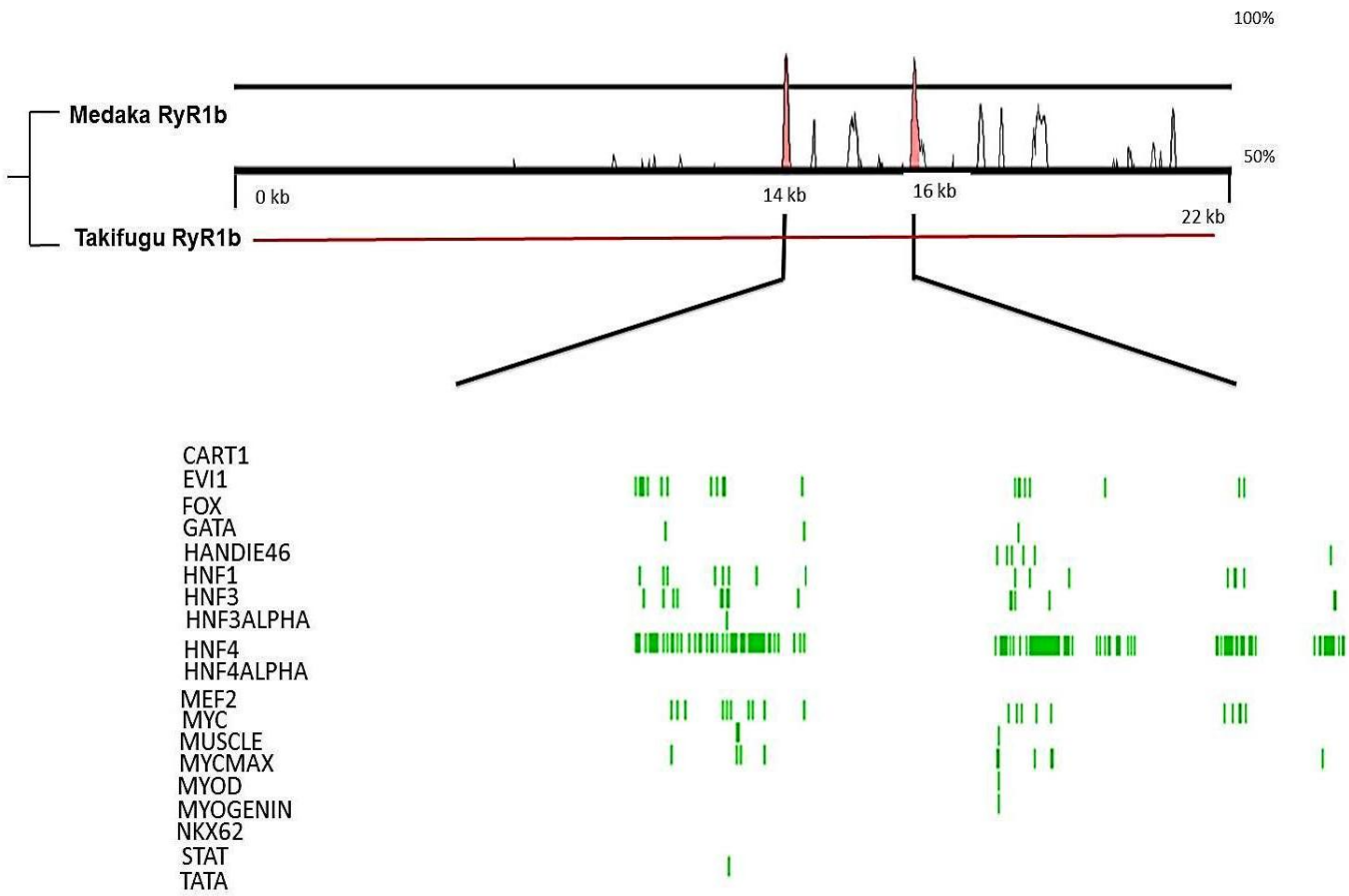

Figure 20: Transcription factors conserved between fugu RyR1b and medaka RyR1b genes.

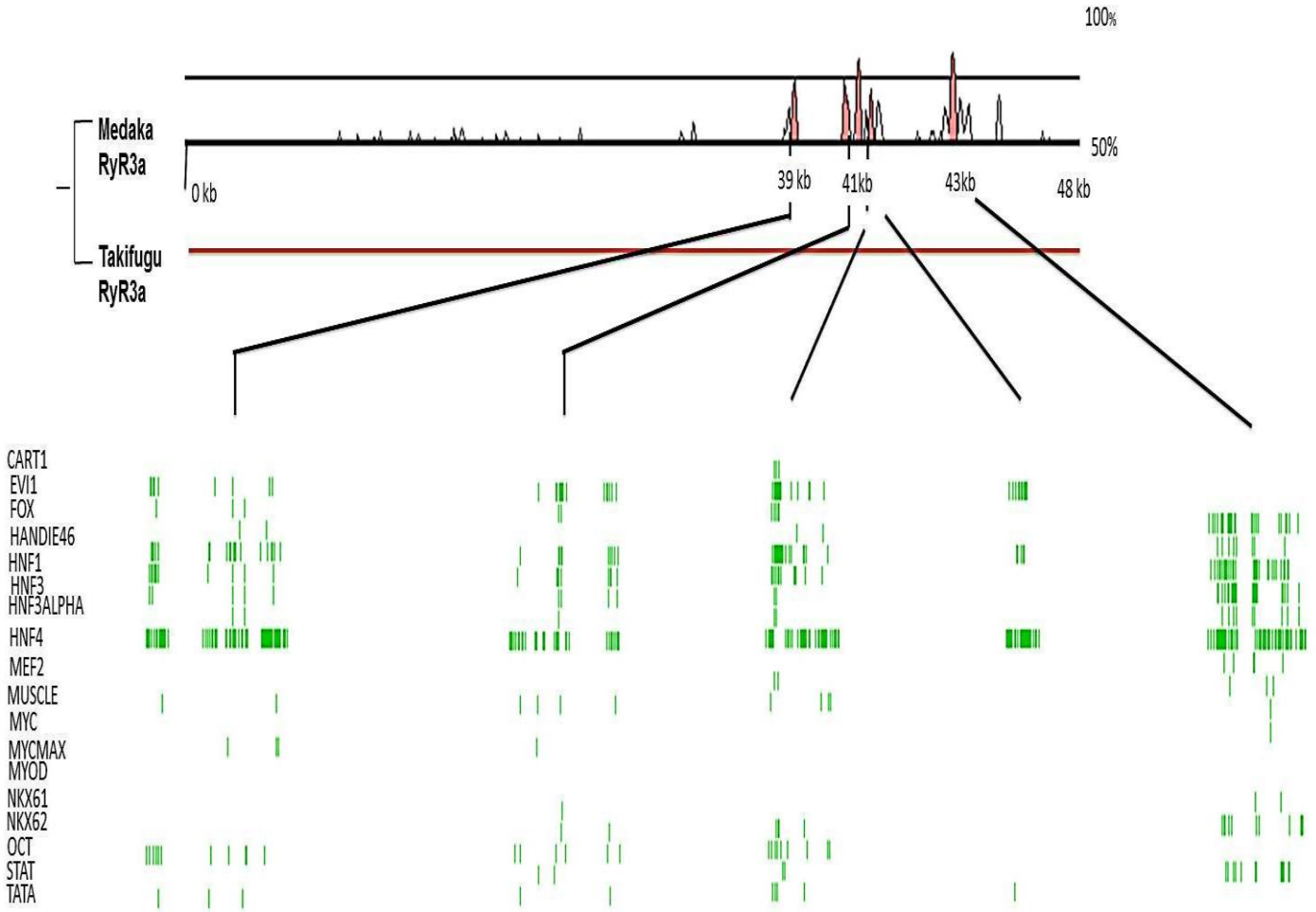

Figure 21: Transcription factors conserved between fugu RyR3a and medaka RyR3a genes.

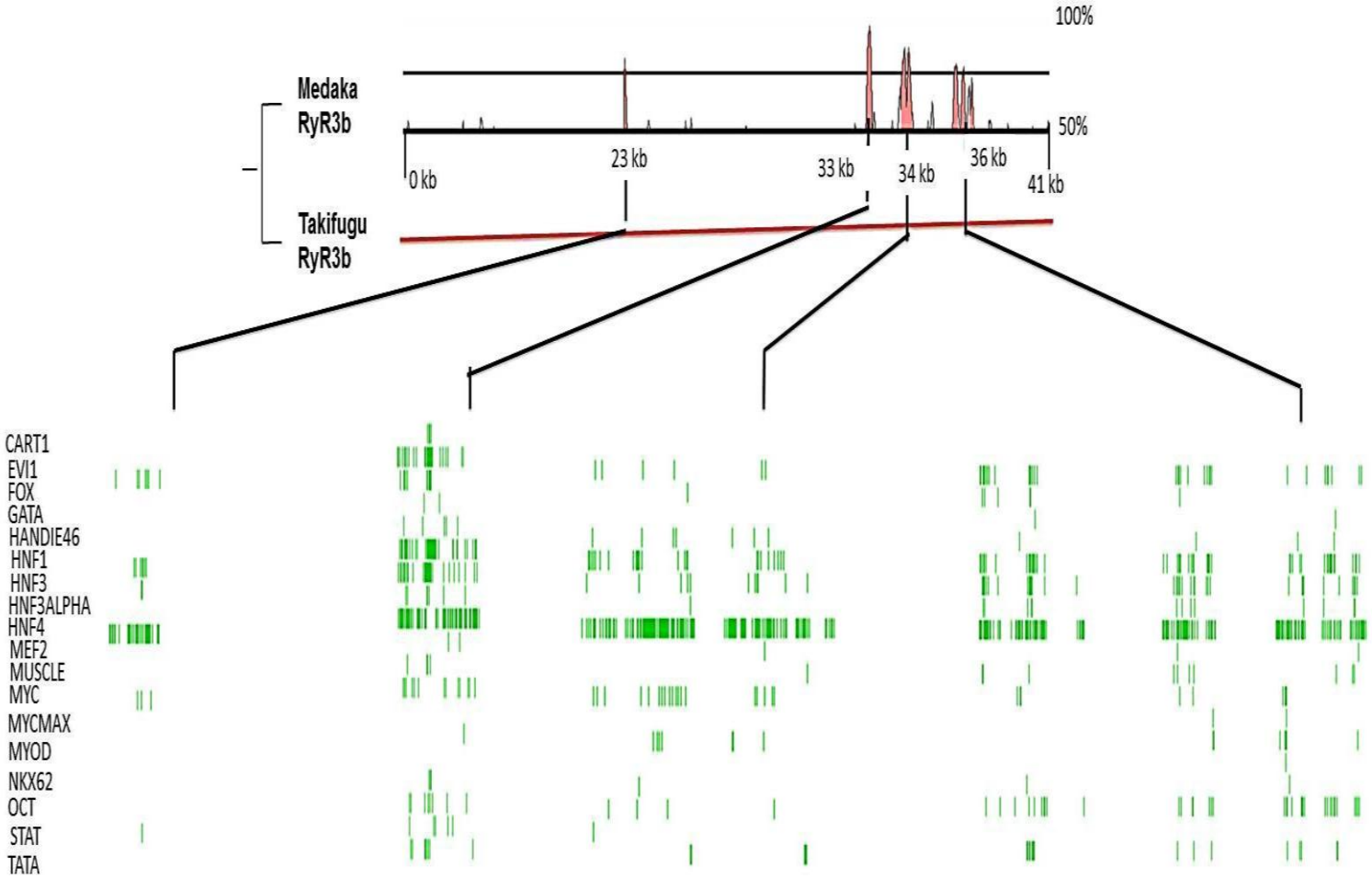

Figure 22: Transcription factors conserved between fugu RyR3band medaka RyR3b genes.

Table 8: Transcription factors binding site hits associated with RyR1a and RyR1b.		
Transcription factor	Number of Hits	
	RyR1a	RyR1b
EVI1	47	18
FOX	6	----
GATA	11	3
HNF1	57	11
HNF3	34	13
HNF3 ALPHA	11	1
HNF4	170	93
MUSCLE	34	15
MYC	1	2
MYOD	3	1
MYOGENIN	2	1
OCT	35	----
STAT	6	----
TATA	12	----
MEF2	5	----
NKX62	3	----
HAND1E47	-----	5

Conserved TFBSs for RyR3a and RyR3b are shown in Table 9. For RyR3a, clustering was observed for HNF4 and OCT TFs. Fewer hits were observed for FOX, Muscle, MYC MAX, STAT, TATA, NKX62 and HANDIE47. No conservation has been found in GATA and CART1 sites. RyR3b shows clustering in HNF4, HNF1, and HNF3, EVI1 followed by fewer hits for CART1, GATA, MYC MAX, STAT, TATA, NKX62 and HANDIE47.

Table 9: Transcription factors binding site hits associated with RyR3a and RyR3b.

Transcription factor	Number of Hits	
	RyR3a	RyR3b
CART1	----	3
EVI1	47	34
FOX	9	8
GATA	----	2
HNF1	32	65
HNF3	19	34
HNF3 ALPHA	9	7
HNF4	81	155
MUSCLE	8	34
MYC MAX	4	7
OCT	19	12
STAT	4	6
TATA	11	9
NKX62	5	3
HAND1E47	2	----

Table 10: Transcription factors binding sites found in association with RyR1a, RyR1b, RyR3a and RyR3b along with their functions.		
Gene	Transcription factors	Role
RyR1a	HNF1 HNF 3 HNF-3 alpha HNF-4	Development and metabolic homeostasis
	MYOD Myogenin MYC-Max	Myogenesis
RyR1b	HANDIE47	Cell proliferation and differentiation
RyR3a	EVI-1	Body patterning and neurodifferentiation.
	OCT-1	DNA repair
	HNF	Development and organogenesis
RyR3b	Myc	Cell growth

3.2 PCR Amplification of RyR1 and RyR3 Paralogues in Developmental Stages

RyR1a, RyR1b, RyR3a and RyR3b messages were amplified in different developmental stages using the primers listed in Table 1. Amplified bands showed the same size as those in dissected tissues (Fig. 23).

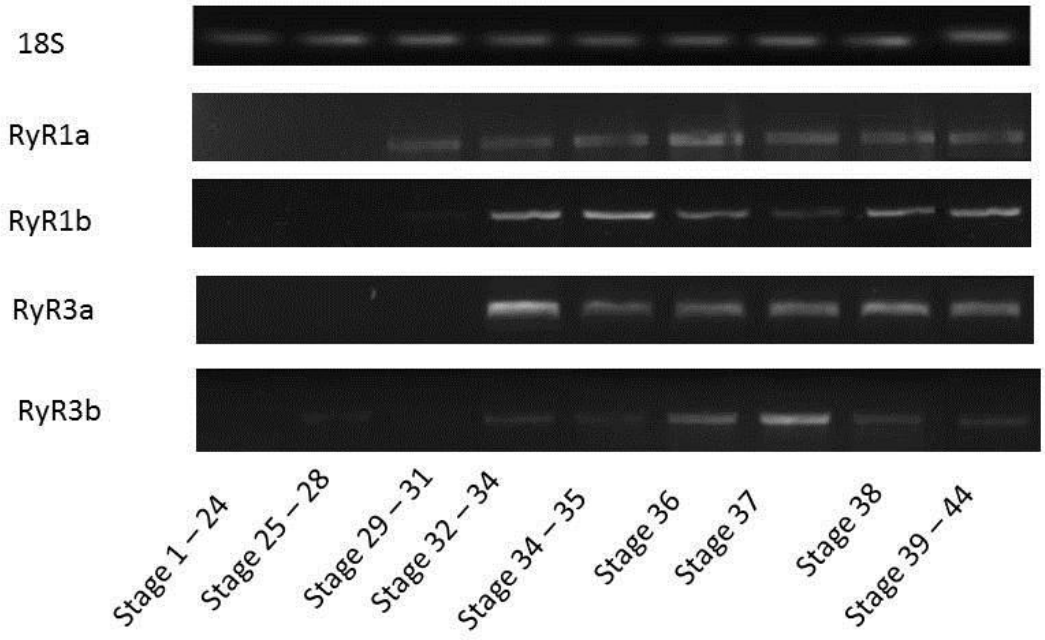

Figure 23: PCR amplification of developmental stages cDNA for RyR1a, RyR1b, and RyR3a and RyR3b genes. Row 1 represent 18S housekeeping gene amplification in all medaka developmental stages (product size 56 bp), row 2 shows RyR1a (906 bp , RyR1b in row 3 (520 bp), RyR3a in row 4 (523 bp), and RyR3b in row 5 (916 bp).

3.3 PCR Amplification of RyR1 and RyR3 Paralogues in Dissected Tissues

RyR1a, RyR1b, RyR3a and RyR3b genes were amplified in different dissected tissues including red muscle, white muscle, heart, brain, spinal column, ovaries, testes and biliary system (liver and gallbladder) using the primers listed in Table 1. Amplified bands were in the expected size of 906 bp for RyR1a, 520 bp for RyR1b, 523 bp for RyR3a, and 916 bp for RyR3b (Fig. 24).

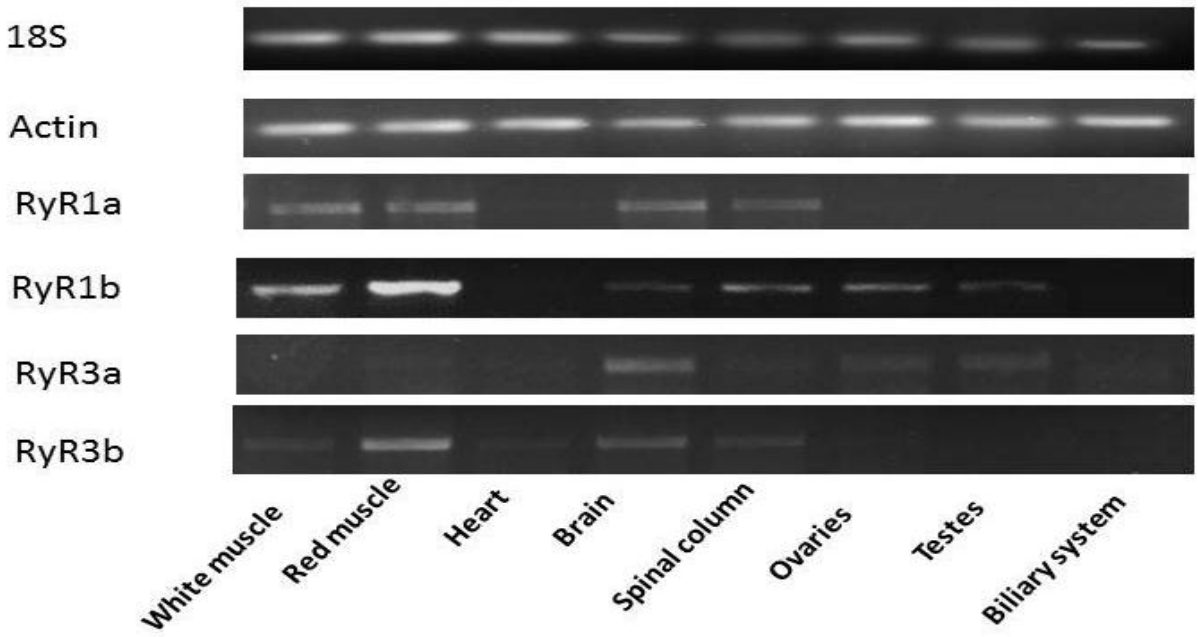

Figure 24: PCR amplification of dissected tissues cDNA for RyR1a, RyR1b, and RyR3a and RyR3b genes. Row 1 represent 18S housekeeping gene amplification in all medaka (product size 56 bp), row 2 beta- actin HKG (76 bp), row 3 shows RyR1a (906 bp , RyR1b in row 4 (520 bp), RyR3a in row 5 (523 bp), and RyR3b in row 6 (916 bp).

3.4 Sequencing and Alignment

Amplified PCR products of the four genes from whole medaka were sent for direct sequencing. The resulting sequences were aligned with other sequences obtained from the ensembl database using Genedoc software (Nicholas et al., 1997). The sequence alignments for RyR1a, RyR1b, RyR3a and RyR3b are shown in Appendix 2, 3, 4 and 5 respectively.

3.5 Temporal qRT-PCR analyses for RyR1 and RyR3 in Developing Medaka

The fold expression for RyR1 and RyR3 paralogues were estimated relative to the expression of the 18S rRNA housekeeping gene in developmental stages using $2^{-\Delta\Delta}$CT method. RyR1 paralogues average expressions with standard errors are shown in Fig. 25 and Table 11. RyR3 paralogues fold expressions are shown in Fig. 26.

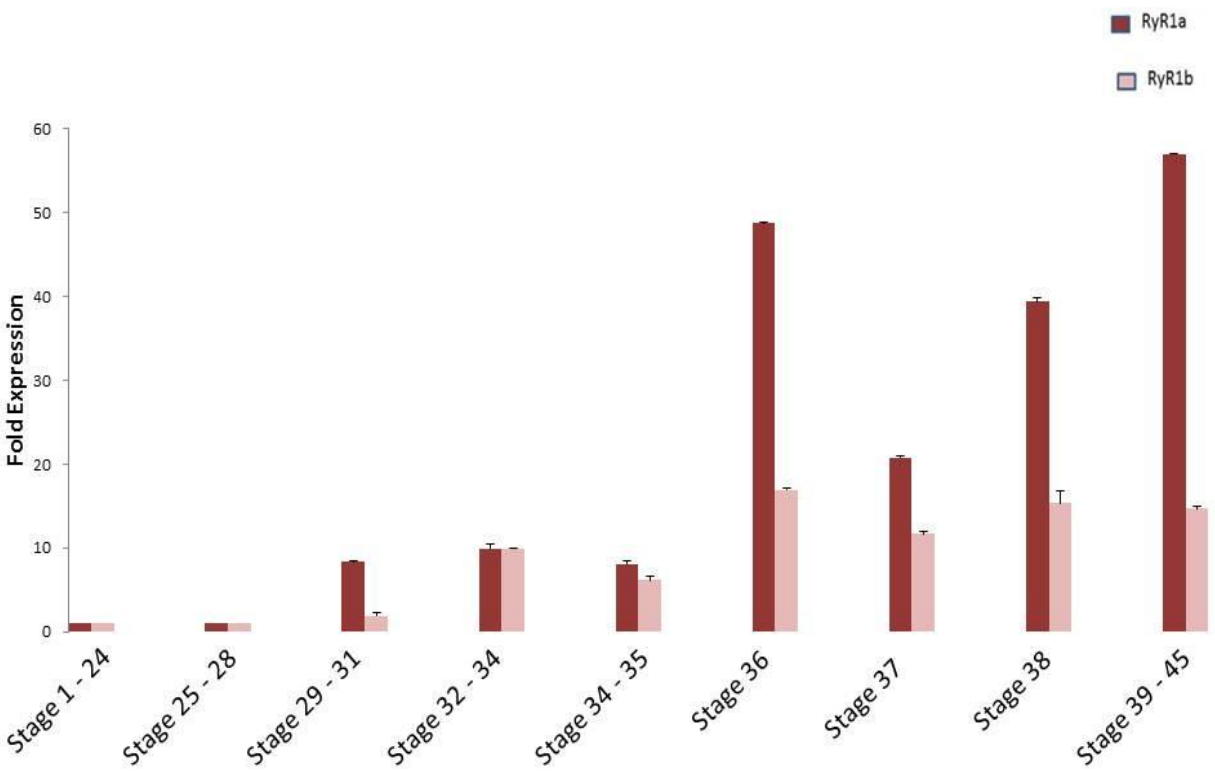

Figure 25: RyR1a and RyR1b developmental fold expression normalized to the expression of 18S housekeeping gene. Average fold expression for RyR1a (purple) and RyR1b (pink) are plotted with standard errors. Stage with highest Ct value was used as a calibrator (day 2). RyR1a/RyR1b ratio shows no significance according to the fold ratio criteria (fold ratio $\geq$ 4 and P-Value <0.01). Standard errors (SE) are small because there are no true replicates.

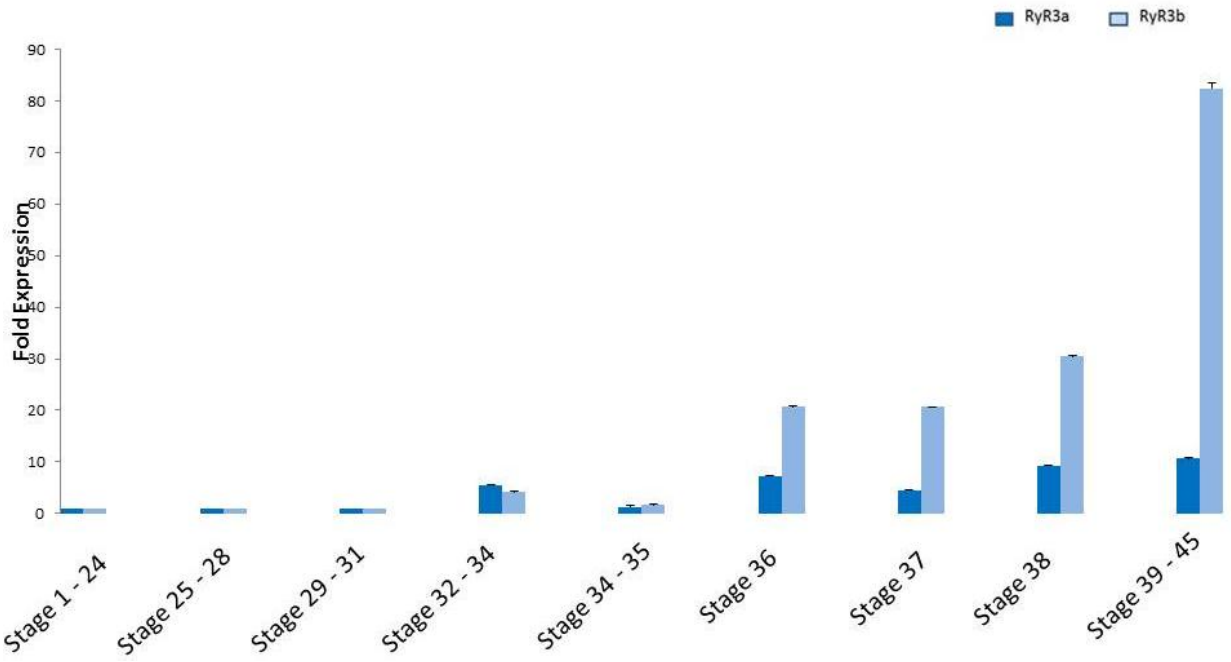

Figure 26: RyR3a and RyR3b fold expression normalized to the expression of 18S housekeeping genes. Average fold expression for RyR3a (dark blue) and RyR3b (light blue) are plotted with standard errors. Stages with highest Ct value were used as a calibrator (day 2 and day 3). No significance found for RyR3a/RyR3b ratio according to the fold ratio criteria (fold ratio $\geq$ 4 and P-Value <0.01). Standard errors (SE) are small because there are no true replicates.

Table 11: Average fold expression of RyR1 and RyR3 paralogues in different developmental stages relative to 18S housekeeping gene with standard errors.

	Gene	Relative expression to HKG (18S) ±SE
Day 3 (Stage 29 - 31)	RyR1a	8.316±0.122346
	RyR1b	1.929±0.28564
Day 4 (Stage 32 – 34)	RyR1a	9.893±0.53860
	RyR1b	9.948±0.07646
	RyR3a	5.502±0.186965
	RyR3b	4.122±0.16842
Day 5 (Stage 34 – 35)	RyR1a	8.061±0.3271
	RyR1b	6.207±0.4642
	RyR3a	1.327±0.264225
	RyR3b	1.611±0.24297
Day 6 (Stage 36)	RyR1a	48.765±0.136647
	RyR1b	16.908±0.30306
	RyR3a	7.295±0.15117
	RyR3b	20.658±0.14748
Day 7 (Stage 37)	RyR1a	20.742±0.23982
	RyR1b	11.717±0.18292
	RyR3a	4.597±0.0986
	RyR3b	20.686±0.03855

Table 11 continued		
Day 8 (Stage 38)	RyR1a	39.391±0.44491
	RyR1b	15.381±1.386
	RyR3a	9.2707±0.06514
	RyR3b	30.474±0.2473
Day 9 – Fry (Stage 39 – 45)	RyR1a	57.015±0.0289
	RyR1b	14.722±0.25334
	RyR3a	10.721±0.20865
	RyR3b	82.412±0.95953

3.6 Spatial qRT-PCR analyses for RyR1 and RyR3 in Selected Medaka Tissues

The level of expression for RyR1 and RyR3 paralogues was estimated relative to the average expression of two housekeeping genes: 18S and β–Actin in dissected tissues using the $2^{-\Delta\Delta}$CT method. RyR1 paralogues expressions with standard errors are shown in figure 27 and table 12 and RyR3 paralogues fold expression levels are illustrated in figure 28.

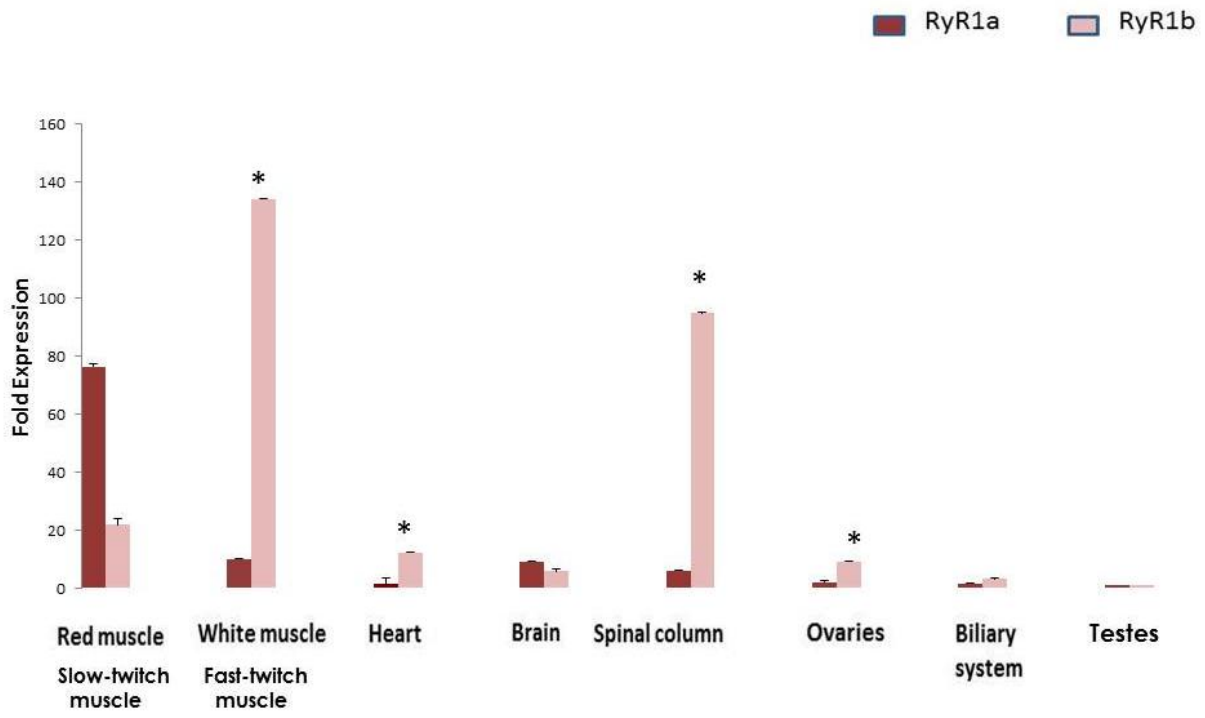

Figure 27: RyR1a and RyR1b tissues fold expression normalized to the average expression of 18S and β–Actin housekeeping genes. Average fold expression for RyR1a (purple) and RyR1b (pink) are plotted with standard errors. A tissue with the highest Ct value was used as a calibrator (testes). * indicates RyR1a/RyR1b significance according to the fold ratio criteria (fold ratio ≥ 4 and P-Value <0.01). Standard errors (SE) are small because there are no true replicates.

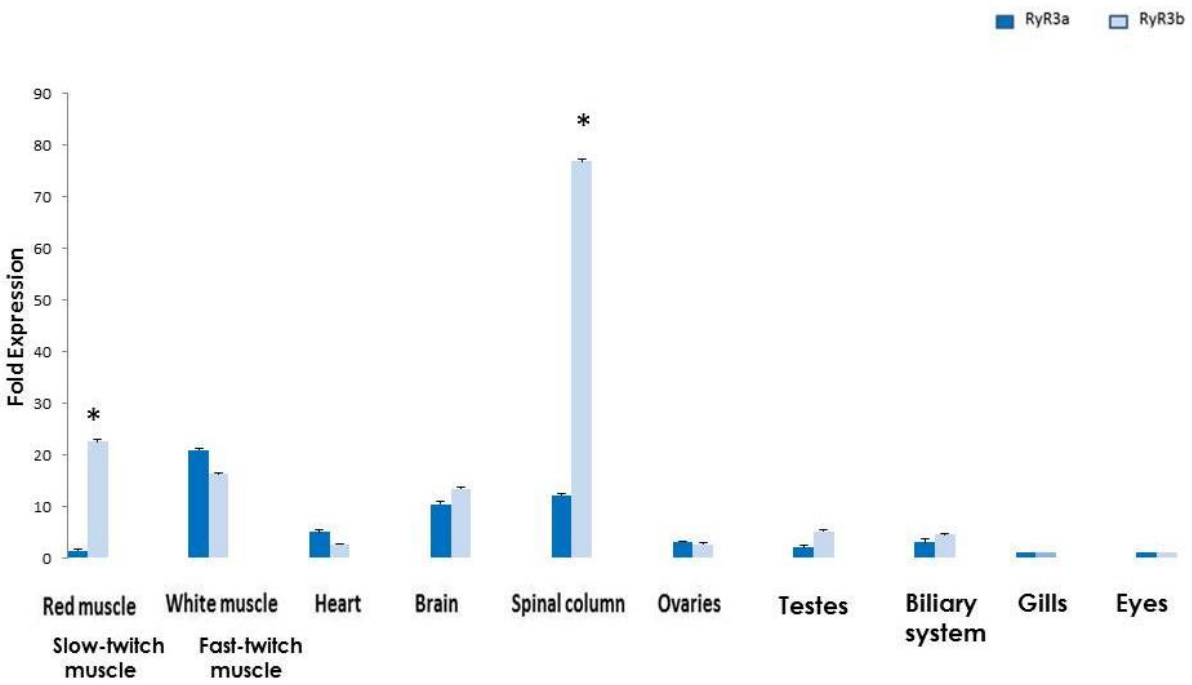

Figure 28: RyR3a and RyR3b tissues fold expression normalized to the average expression of 18S and β–Actin housekeeping genes. Average fold expression for RyR3a (dark blue) and RyR3b (light blue) are plotted with standard errors. Tissues with the highest Ct value were used as a calibrator (eyes and gills). * indicates RyR1a/RyR1b significance according to the fold ratio criteria (fold ratio ≥ 4 and P-Value <0.01). Standard errors (SE) are small because there are no true replicates.

Table 12: Average fold expression of RyR1 and RyR3 paralogues in dissected tissues relative to 18S and β–Actin housekeeping gene with standard errors.		
	Gene	Relative fold expression to HKG (18S and Actin) ±SE
Red muscle	RyR1a	76.409 ± 0.803
	RyR1b	21.812 ±0.2.29
	RyR3a	1.397 ±0.0.1855
	RyR3b	22.469 ±0.398
White muscle	RyR1a	9.967 ±0.0727
	RyR1b	134.141 ±0.383
	RyR3a	20.958 ±0.183
	RyR3b	16.205 ±0.2438
Brain	RyR1a	9.115 ±0.1364
	RyR1b	5.665 ±0.666
	RyR3a	10.389 ±0.5587
	RyR3b	13.346 ±0.277
Spinal column	RyR1a	5.888 ±0.1226
	RyR1b	94.885 ±0.26455
	RyR3a	12.096 ±0.3047
	RyR3b	76.909 ±0.1769
Heart	RyR1a	1.253 ±2.095
	RyR1b	12.277 ±0.2578
	RyR3a	5.0375 ±0.2855
	RyR3b	2.569 ±0.0285

Table 12 continued		
Ovaries	RyR1a	1.990 ±0.3923
	RyR1b	9.014 ±0.1412
	RyR3a	3.152 ±0.3910
	RyR3b	2.580 ±0.0794
Testes	RyR3a	1.945 ±0.25609
	RyR3b	5.156 ±0.4521
Biliary system (Liver-Gallbladder)	RyR1a	1.541 ±0.2794
	RyR1b	3.094 ±0.2109
	RyR3a	3.010 ±0.7352
	RyR3b	4.463 ±0.3268

3.7 Statistical Analyses

The significance of RyR1a/RyR1b fold expression ratio as well as RyR3a/RyR3b fold ratio was calculated using a two-tailed z test for developmental stages and different tissues. It has become increasingly common to require that differentially expressed genes satisfy a modest level of statistical significance ($P < 0.01$) then ranked significant genes by fold-change with a cut-off of 4 (McCarthy and Smyth, 2009).

CHAPTER 4

DISCUSSION

4.1 Conserved noncoding sequences (CNSs)

4.1.1 Evidence of Conserved Noncoding Regions Between RyR Orthologues

The RyR1a and RyR1b genes are believed to be the result of a local gene duplication event (Franck et al, in prep.) whereas the RyR3 gene is the result of the fish-specific genome duplication event during the evolution of teleosts (Fig. 4) (Meyer and Schartl, 1999). Previous studies have demonstrated that RyR1a and RyR1b paralogues are expressed in a tissue-specific manner (Franck et al, 1998; Darbandi and Franck, 2009). Darbandi and Franck (2009) also demonstrated that the RyR1a and RyR1b paralogues are expressed at different levels in adult zebrafish tissues. The objective of my research was to search for evidence of divergence between regulatory elements in the noncoding regions (introns) of the RyR paralogues that could be the basis for differential expression. I also analyzed the expression of the RyR paralogues in developing medaka to investigate whether temporal differences exist in their expression profile. Multisequence alignments between medaka and fugu co-orthologues introns revealed 5 conserved noncoding regions for RyR1a (Fig. 9), 2 regions for RyR1b (Fig. 11), 6 regions for RyR3a (Fig. 13), and 7 regions for RyR3b (Fig. 15). In contrast, only one conserved noncoding region is found between fugu and zebrafish for each of the four genes (RyR1a, RyR1b, RyR3a, and RyR3b. These observations indicate conservation between medaka and fugu RyR co-orthologues which is explained in Figure 8 by the close relation between medaka and fugu that diverged from zebrafish 110 Mya.

4.1.2 Evidence of Divergence Between RyR Paralogues.

The divergence of RyR noncoding regions is found between medaka paralogues, conservation is detected between co-orthologues of divergent species (e.g. medaka and fugu). Pairwise alignment between RyR1 paralogues (RyR1a vs RyR1b) and RyR3 paralogues (RyR3a vs RyR3b) reveal only one conserved region for both comparisons (Figs 17 and 18). Whereas, pairwise alignment between fugu and medaka reveals 5 conserved regions between RyR1a co-orthologues (Fig. 9), 2 regions in RyR1b (Fig. 11), 6 regions in RyR3a (Fig. 13), and 7 regions in RyR3b (Fig. 15). The lack of sequence similarity between the noncoding regions of paralogues and the higher degree of sequence conservation between noncoding sequences in co-orthologues suggests a rapid divergence of RyR noncoding regions followed by fixation of *cis*-acting regulatory elements (Ghanem et al., 2003).

4.2 *Cis*-regulatory Elements (CREs)

4.2.1 Evidence of Conserved Noncoding Elements Between RyR Orthologues

Highly conserved noncoding regions between Fugu and medaka RyR genes for TFBSs also revealed identical hits for transcription factors that regulate development and gene expression. Several studies have demonstrated that regulatory modules are under purifying selection and, therefore, are often conserved between related species (Loots and Ovcharenko, 2004).

4.2.2 Evidence of Divergence Between RyR Paralogues

Bioinformatic analyses to identify TFBSs hits show evidence of divergence in RyR1 and RyR3 paralogues. It seems likely that the whole-genome duplication allowed a relaxed constraint on the duplicated CNEs leading to the rapid divergence of their sequences. The fish-specific whole-genome duplication that occurred in the ancestor of teleost fishes is considered to be responsible for the diversification of teleost fishes (Hoegg et al. 2004; Meyer and Van de Peer 2005; Crow et al., 2006). It is therefore likely that the fish-specific genome duplication might have triggered an accelerated rate of nucleotide substitution in teleosts resulting in rapid divergence of protein coding sequences and CNEs.

4.3 Role of CNEs in Regulation of Temporal and Spatial Gene Expression

Regulation of gene expression in a spatial and temporal manner is crucial during vertebrate development. Such complex transcriptional regulation is thought to be mediated by the coordinated binding of transcription factors to discrete, typically noncoding DNA sequences, allowing the integration of multiple signals to regulate the expression of specific genes (McEwen et al., 2006).

It is widely accepted that gene duplication is a major source for the evolution of novel gene function, resulting ultimately in increased organismal complexity and speciation. Mutations in subsets of regulatory elements in either one of the duplicated paralogues may result in post duplication spatial and temporal partitioning of expression patterns (subfunctionalization) between them. As a result, both paralogues

can fulfill only a subset of complementary functions of the ancestral gene, and will thus be retained by selection and not be lost secondarily (Hadzhiev et al., 2007).

In the previous section I present evidence of conservation between noncoding sequences (intron) from orthologous RyR genes and divergence of noncoding sequences between RyR paralogues. In the next section I will discuss the expression of medaka RyR1 and RyR3 paralogues in developing and adult tissues in medaka.

4.4 Temporal Expression of RyR Paralogues

4.4.1 RyR1a and RyR1b

RyR1 paralogues expression is noticed as early as stage 22-24 (early somite stage) with very low expression and starting to increase from mid to late developmental stages. RyR1a average fold expression (Table 11 and fig. 25) is higher than RyR1b in the following stages: stage 34-35 (8.061), stage 36 (48.765), stage 37 (20.742), stage 38 (39.391) and stage (39-45) is (57.015). RyR1b, show similar pattern of fold expression with marked expression over RyR1a in a few stages (32-34) where fold expression is (9.948). Other stages show lower levels than RyR1a, 16.908 in stage 36, 11.717 in stage 37, 15.381 in stage 38 and 14.722 in stage 39-45. Using the fold ratio criteria I have calculated the RyR1a/b ratio in different developmental stages then I calculated z-score and p-value to test for significant differences. Ratios that meet fold criteria (fold ratio >2, P-value < 0.01) were considered significant.

4.4.2 RyR3a and RyR3b

RyR3a and RyR3b demonstrate expression patterns that range from mid to late stages (Table 11 and figure 26). The average fold expression for RyR3a is higher

RyR3b in stage (32-34) with fold increase of 5.502. The remaining stages show lower expression than RyR3b in stage (34-35) the fold expression is 1.3273, stage 36 fold expression is 7.295, stage 37 was 4.597, stage 38 9.2707 and stage (39-45) 10.7219. For RyR3b, the average fold expression was lower than RyR3a in stage (32-34) with fold expression of 4.1221. Otherwise, RyR3b has a high expression levels in other stages: 1.6119 in stage (34-35), 20.658 in stage 36, 20.686 in stage 37, 30.474 in stage 38 and 82.412 in stage 39-45.

4.5 Spatial Expression of RyR Paralogues

4.5.1 RyR1a and RyR1b

RyR1a is highly expressed over RyR1b in red muscle (slow-twitched muscle) (Fig. 27 and table 12) with fold expression of 76.409 and in the brain with 9.115 fold expression. RyR1b is highly expressed over RyR1a in white muscle (fast-twitched muscle) with fold expression of 134.141 followed by spinal column tissues with fold expression 94.885, heart 12.277, ovaries 9.014, and then biliary system tissues with fold expression of 3.094. This muscle expression in medaka is similar to that for zebrafish (Darbandi and Franck, 2009). However, Darbandi and Franck (2009) limited their analyses to only four selected tissues, namely red muscle, white muscle, cardiac and brain tissues. Using the fold ratio criteria I have calculated the RyR1a/b ratio in different adult tissues and calculated the z-score and p-value. Ratios that meet fold criteria (fold ratio >2, P-value < 0.01) are considered significant.

4.7.2 RyR3a and RyR3b

RyR3a is expressed more than RyR3b in white muscle (fold expression 20.958) followed by heart (fold expression 5.0375) and ovaries (fold expression 3.152) (Fig. 28 and table 12). RyR3b is highly expressed over RyR3a in red muscle (fold expression 22.469), then spinal column tissues (fold expression 76.909), brain (fold expression 13.346), testes (fold expression 5.156), and then biliary system tissues with fold expression of 4.463. The spinal column tissues shows high expression level of RyR1b (fold expression 94.885) and RyR3b (fold expression 76.909). Similarly, red muscle express RyR1a (fold expression 76.40) and RyR3b (fold expression 22.469) in high levels. White muscle highly express RyR1b (fold expression 134.141) and RyR3a (fold expression 20.958). Brain tissues express RyR3b (fold expression 13.346) and RyR1a (fold expression 9.115) in high levels. Heart show more expression of RyR1b (fold expression 12.277) and RyR3a (fold expression 5.0375). Ovaries have high expression of RyR1b (fold expression 9.014) and RyR3a (fold expression 3.152). Biliary tissues demonstrates increased levels of RyR3b (fold expression 4.463) and RyR1b (fold expression 3.094).

4.8 Role of RyR1 in Development and EC Coupling

Medaka encodes two copies of RyR1 as is the case for zebrafish and fugu. Wu (2011) recently published his PhD thesis online describing the expression of RyR genes in developing zebrafish. Wu's analysis is based solely on *in situ* hybridization to whole mount embryos and does not include qRT-PCR analysis. Wu shows that RyR1a first appears at 11 hpf (3- to 6-somite stage; early segmentation), prior to

RyR1b and that RyR1a is exclusively expressed in slow muscle and the slow muscle pioneers at 24 hpf (pharyngula period; late segmentation). This result is consistent with the report from Hirata and colleagues (2007). Wu's *in situ* study reveals that RyR1b is expressed in both the slow and fast muscle fibres of zebrafish embryos. My research of RyR expression in medaka agrees with the findings of both Wu (2011) and Hirata et al. (2007) for zebrafish. Developing medaka embryos, like zebrafish, show early expression of the RyR1a gene starting from stage 1 to 25 that increases until hatching (Figure 29 and 30) while RyR1b is expressed from stage 25 onward which is similar to zebrafish RyR1a and RyR1b temporal expression (Wu, 2011). Comparison between medaka and zebrafish developmental stages is described in figure 33. This early expression of RyR1a and RyR1b indicates their functional significance during the early stages of development. The relatively early expression of RyR1a in slow muscle may reflect the fact that the RyR1a receptor is required by these muscles prior to the fast skeletal muscle fibres. Embryonic development of fast and slow muscles in zebrafish originate from different cell lineages, and the latter is differentiated at early developmental stages from adaxial cells located on both sides of the notochord (Devoto et al., 1996; Daggett et al., 2007). Adaxial cells migrate radially from either sides of the notochord to the superficial part in the trunk, where slow muscle-specific proteins are expressed, and finally developed to slow muscle in a superficial region beneath the skin or remain as muscle pioneers in the horizontal myoseptum (Felsenfeld et al., 1991; Devoto et al., 1996; Ono et al., 2010). The red slow twitch muscle has important physiological functions in fish because they are used to power slow- and medium-speed movements while both slow fibers and the faster (white)

fibers are used during rapid movement (Jayne and Lauder., 1994). The conserved noncoding regions for the RyR1a and RyR1b described in section 4.2.1 have a predominance of binding sites for transcription factors involved in organogenesis (Table 8). Divergence of the RyR1a and RyR1b expression patterns, both temporal and spatial, could be related to the observed sequence divergence between noncoding regions in the genes.

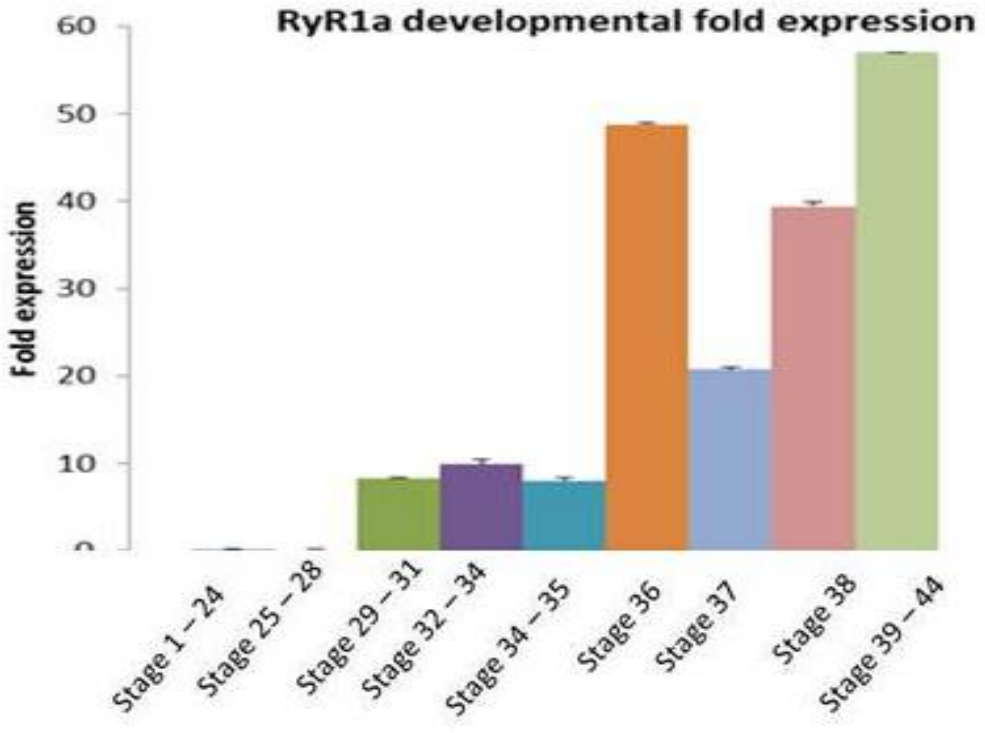

Figure 29: Developmental expression of RyR1a gene in medaka embryos normalized to the expression of 18S housekeeping genes. RyR1a shows early expression with low levels in qRT-PCR starting day 2. Day 2 has been used as a calibrator for calculation of the fold expression levels. Relative expression (RE) of RyR1a in day 1 and day 2 was meseaured using $2^{-\Delta\Delta}$CT method (RE in day1 = 0.000049, and in day 2 = 0.00001). Day 1: stage 1-stage 24, Day 2: stage 25- stage 28, Day 3: stage 29- stage 31, Day 4: stage 32- stage 34, Day 5: stage 35, Day 6: stage 36, Day 7: stage 37, Day 8: 38,and Day 9: stage 39- stage 45.

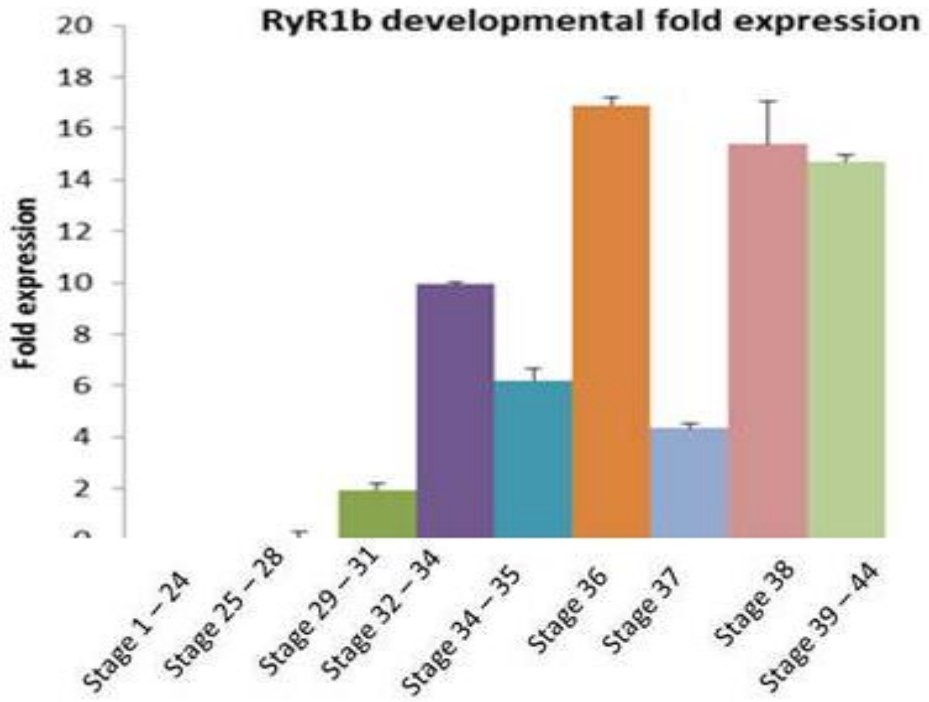

Figure 30: Developmental expression of RyR1b gene in medaka embryos normalized to the expression of 18S housekeeping genes. RyR1b shows early expression with low levels in qRT-PCR starting day 2. Day 2 has been used as a calibrator for calculation of the fold expression levels. Relative expression (RE) of RyR1b in day 2 was meseaured using $2^{-\Delta\Delta}$CT method (RE = 0.000073). Day 1: stage1-stage 24, Day 2: stage 25- stage 28, Day 3: stage 29- stage 31, Day 4: stage 32- stage 34, Day 5: stage 35, Day 6: stage 36, Day 7: stage37, Day 8: 38,and Day 9: stage 39- stage 45.

4.9 Role of RyR3 in Development and EC Coupling

RyR3 regulation and expression has been extensively studied using many model organisms including: zebrafish, mouse and human. Unlike medaka, all of the three models have one copy of the RyR3 gene. In a recent study done by Wu, 2011 using zebrafish shows that temporary RyR3 mRNA was observed to be maternally expressed quite strongly at 1-2 hpf (cleavage stage), then very weakly from 5.3 hpf

(gastrula stage) through to 18 hpf (mid-segmentation stage) and after which the level of expression became much stronger through to adulthood. In contrast, medaka encodes 2 copy of RyR3 which are first expressed in stage 25-31 (early to mid-somite stage) with low levels. RyR3a expression increases from stage 32 (late somite stage) and became much stronger through to adulthood. Similarly, RyR3b is expressed at low levels in early developmental stages and starts to increase significantly from stage 35 onward up to adulthood (Figs. 31 and 32).

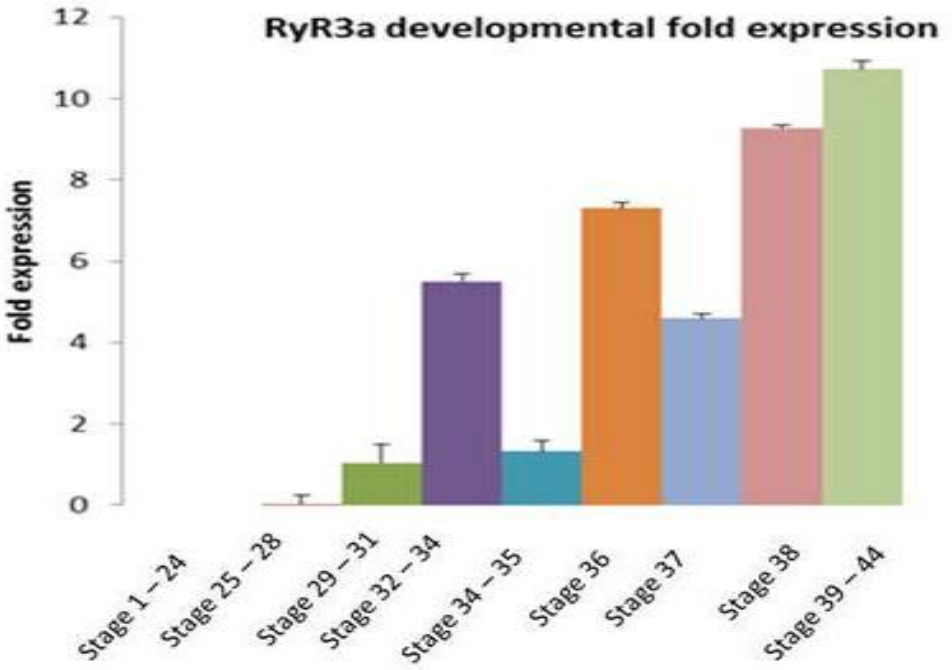

Figure 31: Developmental expression of RyR3a gene in medaka embryos normalized to the expression of 18S housekeeping genes. RyR3a shows early expression with low levels in qRT-PCR starting day 2. Day 2 has been used as a calibrator for calculation of the fold expression levels. Relative expression (RE) of RyR3a in day 2 was meseaured using $2^{-\Delta\Delta}$CT method (RE = 0.000073) Day 1: stage1-stage 24, Day 2: stage 25- stage 28, Day 3: stage 29- stage 31, Day 4: stage 32- stage 34, Day 5: stage 35, Day 6: stage 36, Day 7: stage37, Day 8: 38,and Day 9: stage 39- stage 45.

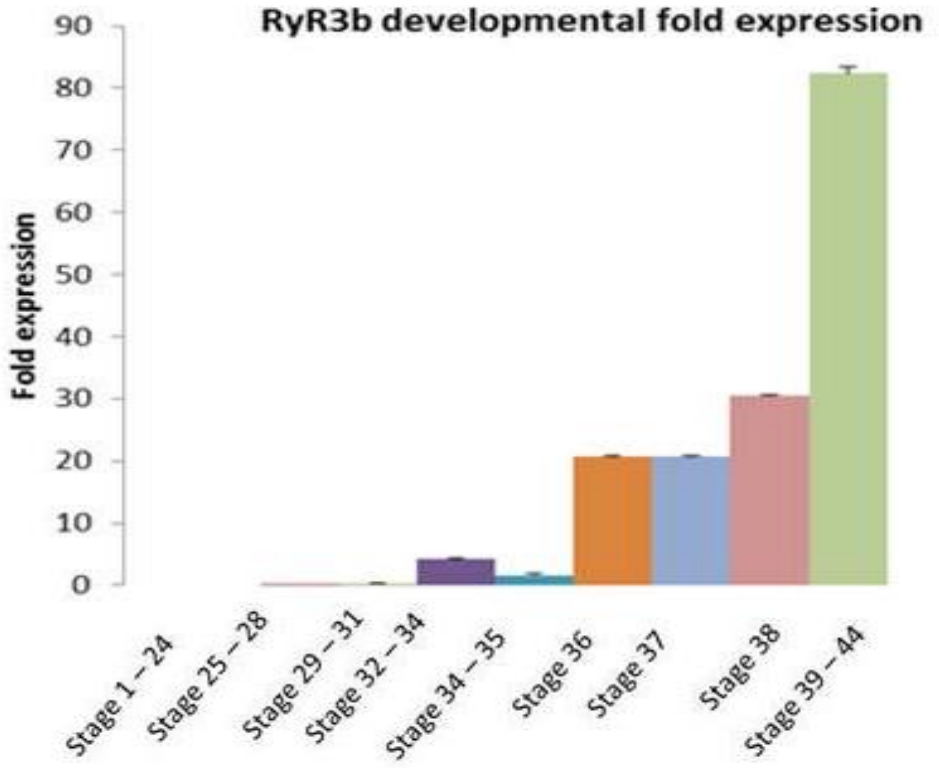

Figure 32: Developmental expression of RyR3b gene in medaka embryos normalized to the expression of 18S housekeeping genes. RyR3b shows early expression with low levels in qRT-PCR starting day 2. Day3 has been used as a calibrator for calculation of the fold expression levels. Relative expression (RE) of RyR3b in day 2 and day 3 was meseaured using $2^{-\Delta\Delta}$CT method (RE in day2 = 0.0002, and in day 3 = 0.00006). Day 1: stage1-stage 24, Day 2: stage 25- stage 28, Day 3: stage 29- stage 31, Day 4: stage 32- stage 34, Day 5: stage 35, Day 6: stage 36, Day 7: stage37, Day 8: 38,and Day 9: stage 39- stage 45.

Based on the temporal expression pattern reported above, it is evident that both RyR3a and RyR3b are expressed very early (18 somite stage in medaka), which could implicate functional significance during the early stages of medaka development. RyR3 gene knockdown in zebrafish embryos causes significant developmental

deformities from 10 hpf (late gastrula stage) onwards (Wu, 2011). Wu reports a significant difference in the spontaneous movement activity between the RyR3 morphants and the control injected embryos, indicative of disrupted neuromuscular development in the RyR3 knockdown embryos. Wu shows that RyR3 is solely expressed in the fast muscle fibres (red muscle) throughout the myotome at 24 hpf (late segmentation stage). Wu also observed that RyR3 knockdown results in defects like disorganised muscle fibres alignment, suggesting that RyR3 may have a role in myofibril organisation, which could be required for subsequent spontaneous movements in the developing embryos. My observation for RyR3a and RyR3b spatial expression in medaka shows that RyR3a is expressed more in fast muscle (white muscle) while RyR3b is expressed predominantly in slow muscle fibers (red muscle) (Fig. 28). Recently, RyR3 has found to function as an uncoupled CICR channel in non-mammalian vertebrates (Murayama and Kurebayshi, 2010). According to this finding, it is expected that the calcium release from RyR1b in fast-twitch muscle myocytes would activate the parajunctional RyR3 via a CICR mechanism to trigger further release of Ca^{2+} from the sarcoplasm (Fig. 3). RyR3b gene is also the predominant paralouge expressed in brain and spinal cord (neurological) tissues. Neurological development in medaka begins in stage 17, with the head (rudimentary brain) being recognizable anteriorly in the distinct embryonic body. Brain and nerve cord formation start in stage 18. The neurological development proceeds in stage 20 in which three parts of the brain (the fore-, the mid- and the hind-brain) are discernible. In stage 26, blood circulation to brain is established. The notochord is completely vacuolized to the end of the tail in stage 33 (Iwamatsu, 2004). Relating the anatomical

nervous system development to RyR3a and RyR3b expression, both genes start to be expressed in stage 25 with higher expression of RyR3b. At this stage, the hind and mid brain are well established and blood circulation to the brain is started. Later on in development, RyR3b is expressed in higher levels in the brain and spinal column tissues. Importantly, the RyR3a and RyR3b noncoding regions mentioned in section 4.2.1 show greater hits for regulatory elements responsible for cell differentiation (HNF) and neurodifferentiation (EVI1).

Figure 33 (on following page): Comparison between medaka and zebrafish developmental stages. Medaka and zebrafish progress through the same developmental stages including: cleavage, blastula, gastrula, segmentation, organogenesis, and hatching stages. Zebrafish does not have a distinct "neurula period" because the times of neurulation and segmentation overlap so extensively. Medaka embryos hatch within 9 days while zebrafish hatch after 72 hours. hpf, hour post fertilization; MED, medaka; zf, zebrafish.

MED.
ZF
Developmental stages
Developmental Process in medaka
Developmental Process in zebrafish
Stage 1- 9 (3 min – 5 hrs)
Stage 10 – 11 (6 – 8 hrs)
Stage 12 – 16 (10 – 21 hpf)
Stage 17 – 18 (24 hrs – 1 day and 2 hrs)
Stage 19 – 32 (1 day 3hrs – 4 days and 5hrs)
Stage 33 – 38 (4 days and 10 hrs – day 8)
Stage 39 – 45
0.7 – 2 hpf
2.5 – 5.25 hpf
5.25 – 10 hpf
11 – 24 hpf
24 48 hpf
48 – 72 hpf
cleavage period
Blastula stage
Gastrula stage
Neurula stage
Segmentation stage
Organogenesis
Hatching
2 cell stage - blastodermal cells (256-512 blastomeres)
blastoderm (about 1,000 cells)
blastoderm projection in yolk sac
blastomere migration
Blastoderm expand (Epibology) untill it cover ¾ of yolk sac
Head formation
Optic bud formation
2 – 35 somite stage
Formation of optic, otic bud, tubular heart, blood vessels, notochord vacuolization
Heart development , visceral blood supply, sleen, differentiation of caudal fin
Total length 3.8- 4.2 mm
Tail tip extend to the end of pectoral fin
2 – 64 cell embryo
256 cell stage to 50%-epiboly stage
Appearance of Tailbud
No neurula stage because the times of neurulation and segmentation overlap so extensively
1 – 26 somite stage
Formation of optic, otic bud, brain and hind brain neuromeres
Heart beat , Retinal pigmentation, tail pigmentation, and pectoral fin bud
Total length 3.1- 3.3 mm
elongated pectoral fin buds

CHAPTER 5

CONCLUSIONS

5.1 Project Summary

The differential spatial expression pattern for the duplicate RyR genes is a classic example of gene subfunctionialization in which duplicate genes partition the function of the ancestral gene. Gene duplication is integral to evolution, providing novel opportunities for organisms to diversify in function. A fundamental pathway of functional diversification among paralogues is via alterations in their expression patterns. Bioinformatic analyses of the RyR orthologues from zebrafish, medaka, and fugu (*Takifugu rubripes*) reveal evidence for *cis*-regulatory divergence of the duplicated genes. Additionally, conserved noncoding elements (CNEs) are found in the introns of orthologous RyR genes. Compared to orthologues, duplicate genes are unique in that they exhibit dramatically accelerated rates of both *cis*-regulatory and protein evolution. Ryanodine receptors have been extensively studied using other model organisms such as zebrafish, mouse and human. Medaka encodes 5 RyR genes (RyR1a, RyR1b, RyR2, RyR3a and RyR3b). This thesis shows evidence of diversity between RyR1a and RyR1b as well as between RyR3a and RyR3b in their CNSs. This divergence reflected on the differential expression, both temporally and spatially. Temporally, expression of the RyR1a gene starts from stage1 to 25, increasing until hatching, while RyR1b is expressed from stage 25 onward. Both RyR3a and RyR3b are expressed very early (18 somite stage in medaka). This early expression of RyR1a and RyR1b indicates their functional significance during the early stages of development. RyR1a and RyR3b were found to be highly expressed in red muscle (slow-twitch muscle) compared to RyR1b and RyR3a in white muscle (fast-twitch

muscle). Spinal column tissues show high expression levels of RyR1b and RyR3b genes over RyR1a and RyR3a.

5.2 Future Directions

5.2.1. Transgenesis

Future work will be done to amplify all the CNSs found in the four genes from genomic DNA of medaka fish and to determine if they function as enhancer sequences. My research, which is based on a combination of bioinformatics and expression analyses suggests a role in gene regulation. It is imperative, however, to confirm whether they are in fact enhancer sequences. This may be accomplished by ligation of these regions into the Tol2 transposase vector. The Tol2 vector can be used to inject both zebrafish and medaka embryos. The Tol2 element is a naturally occurring active transposable element found in vertebrate genomes. The Tol2 transposon system has been shown to be active from fish to mammals and is considered to be a useful gene transfer vector in vertebrates (Urasaki et al., 2006). This method takes advantage of the increased efficiency of genome integration that is afforded by this intact DNA transposon, activity that is mediated by the corresponding transposase protein (Fisher et al., 2006). This research would permit us to test whether the CNSs function as enhancers.

5.2.2. Morpholino Knockdown (RyR3a and RyR3b)

The divergent RyR3 paralogues, RyR3a and RyR3b, are expressed differentially both temporally and spatially in medaka. Further studies should be done to clarify their functional roles. This could be done by designing anti-sense

oligonucleotides (Morpholino oligonucleotides) to knockdown protein expression. Morpholino oligonucleotide (MO) knockdown is the most widely used anti-sense knockdown tool utilized in the zebrafish community (Bill et al., 2009). Morpholinos are designed to block translation of selected messenger RNAs (the sense strand) and are commonly called antisense oligos (Summerton and Weller, 1997). Two types of MO applications exist: splice blocking and translational blocking (Bill et. al., 2009). Splice blockers can be used to target specific transcripts by annealing and inhibiting specific splice sites (Bill et al., 2009). Translational blocking MOs bind to the mRNA sequence within the 5' untranslated region (UTR) near the translational start site hindering ribosome assembly (Bill et al., 2009).

The splice site blocking application may be the preferred technique for RyR genes for several practical reasons. Morpholino knockdown experiments involving translation blocks require one to perform a rescue experiment with synthetic mRNA transcripts for the gene of interest. The mRNA is injected into the embryo after knocking down the gene to determine if gene function can be regained. The rescue experiment therefore confirms that the gene of interest was specifically targeted. This might be impractical for the RyR gene since the message is extremely long, 16 kbp, and would be difficult to synthesize *in vitro* as well as ensure that it remains intact following injection into the embryo. With the splice site block, the effect of the MO can be confirmed by simply using primers to amplify the region around the splice site and determine if the intron was spliced out or not.

Knocking down the RyR3 paralogues (RyR3a and RyR3b) is important to determine the physiological process that control channels activity. The physiological

factors controlling the expression for RyR1 gene paralogues (RyR1a and RyR1b) and RyR3 have been studied using zebrafish and other vertebrate models. On the other hand, this information is lacking for medaka. Previous studies performed by Darbandi and Franck found that RyR1b and RyR3 are co-expressed at equivalent levels in certain zebrafish tissues (2009). In medaka fast and slow twitch muscle types there are two different pairings of the RyR1 and RyR3 isoforms. In white muscle RyR1b is co-expressed at equivalent levels with RyR3a whereas in red muscle the RyR1a and RyR3b genes are co-expressed at equivalent levels. Previous studies (Murayama and Kurebayshi, 2010; Wu, 2011) in zebrafish have suggested that the RyR3 channel is gated by the release of calcium from the mechanically gated RyR1 channel. In the case of fugu and medaka this model could still apply but the tissue-specific RyR3 paralogues, RyR3a and RyR3b, may have different sensitivities to calcium and other ligands (e.g. caffeine) and also may have different inactivation thresholds. In mammals, RyR1 is activated with low Ca^{2+} concentrations (nanomolar) while RyR3 needs micromolar Ca^{2+} concentration in order to be activated. This increase in Ca^{2+} concentration will cause deactivation of the RyR1 isoform channel located in the same triad. The RyR3 has low sensitivity to high Ca^{2+} concentration, which is important to maintain a sustained Ca^{2+} release after deactivation of RyR1; this would explain the RyR3 properties of RyR1 signal amplification through CICR (Sonnleitner et al., 1998). Moreover the slope conductance in zebrafish for both isoforms was higher than that of the mammalian RyR1 (this would help in maintaining high Ca^{2+} release from intracellular stores) and compared to mammals, zebrafish RyRs are found to be more resistant to inhibition with high Ca^{2+} concentrations. (Koulen et al., 2001). Similar to

mammals, non-mammalian vertebrates RyR3 gating kinetics differ from that of RyR1, where RyR3 exhibits longer open-time constants (Chen et al., 1997) and is also found to be more resistant to inhibition by Mg^{2+} than RyR1 (Morrissette et al., 2000**)**.

In summary, my research has revealed evidence for both conservation of noncoding sequences between RyR orthologues and divergence of noncoding sequences between RyR paralogues e.g. RyR1a vs RyR1b and RyR3a vs. RyR3b. Additionally, transcription factor binding motifs are conserved between RyR co-orthologues from medaka and fugu. The bioinformatic evidence for divergence between paralogues is reflected by the expression analyses where marked different expression is evident both spatially and temporally. The temporal and spatial expression patterns show paralogue-specific expression which is consistent for both medaka and zebrafish species.

REFERENCES

Ait-Si-Ali, S., Polesskaya, A. and A. Polesskaya. 2000. "CBP/p300 histone acetyl-transferase activity is important for the G1/S transition,"**.** *Oncogene***, 19 (20): 2430–2437.**

Alberts, B., Johnson, A., Lewis, J., Raff, M., Roberts, T., and P. Walter. 2002. *Mol. Biol. Cell (4th edn). NY Garland Publishing.*

Aparicio, S., Chapman, J., Stupka, E., Putnam, N., Chia, J.M., Dehal, P.,Christoffels, A., Rash, S., Hoon, S., and A. Smit. 2002. Whole-genome shotgun assembly and analysis of the genome of *Fugu rubripes*. *Science* **297:** 1301–1310.

Balschun, D., Wolfer, D., Bertocchini, F., Barone, V., Conti, A., Zuschratter, W., Missiaen, L., Lipp, H., Frey, J. and V. Sorrentino. 1999. Deletion of the ryanodine receptor type 3 (RyR3) impairs forms of synaptic plasticity and spatial learning. *The EMBO Journal*. **18**(19): 5264-5373.

Barta, E., Sebestyen, E., Palfy, T., Toth, G., C. Ortutay. 2005. DoOP: Databases of Orthologous Promoters, collections of clusters of orthologous upstream sequences from chordates and plants. *Nucleic Acids Research.* **33**: D86–90.

Bejerano, G., Pheasant, M., Makunin, I., Stephen, S., Kent, W., Mattick, J., and D. Haussler. 2004. Ultraconserved Elements in the Human Genome. *Science* **304,** 1321–1325.

Bertocchini, F., Ovitt, C. E., Conti, A., Barone, V., Scholer, H. R., Bottinelli, R., Reggiani, C., and V. Sorrentino. 1997. Requirement for the ryanodine receptor type 3 for efficient contraction in neonatal skeletal muscles. *EMBO J.* **16**: 6956–6963.

Bill, B.R., Petzold, A.M., Clark, K.J., Schimmenti, L.A., and S. C. Ekker. 2009. A primer for morpholino use in zebrafish. *Zebrafish.* **6**(1): 69-77.

Blackwood, E. M., and J. Kadonaga. 1998. Going the distance: a current view of enhancer action. *Science*. 3: 281(5373).

Cartharius, K., Frech, K., Grote, K., Klocke, B., Haltmeier, M., Klingenhoff, A., Frisch, M., Bayerlein, M. and T. Werner. 2005. MatInspector and beyond: promoter analysis based on transcription factor **binding sites.** *Bioinformatics*. **21**: 2933-42.

Castillo-Davis, C., Hartl, D. and G. Achaz, 2004. *Cis*-Regulatory and Protein Evolution in Orthologous and Duplicate Genes. *Genome***. 14:** 1530–1536.

Chen, S. R., Li, X., Ebisawa, K., and L. Zhang. 1997. Functional Characterization of the Recombinant Type 3 Ca21 Release Channel (Ryanodine Receptor) Expressed in HEK293 Cells. *The journal of biological chemistry*. **272** (26): 24234–24246.

Cheng , L., Guo, X.,Yang, X., Chong, M., Cheng, J., Li, G., Gui, Y., and D. Lu. 2006. d-sarcoglycan is necessary for early heart and muscle development in zebrafish. *Biochemical and Biophysical Research Communications*. **344**: 1290–1299.

Christoffel, s. A., Koh, E. G., Chia, J. M., Brenner ,S., Aparicio, S., and B. Venkatesh . 2004. Fugu genome analysis provides evidence for a whole-genome duplication early during the evolution of ray-finned fishes. *Mol Biol Evol.* **21**:1146-1151.

Conklin. M, W., Barone, V., Sorrentino, V., and R. Coronado. 1999. Contribution of ryanodine receptor type 3 to Ca2_ sparks in embryonic mouse skeletal muscle. *Biophys J.* **77**: 1394–1403.

Crow, K.D., Stadler, P.F., Lynch, V.J., Amemiya, C., and G. P. Wagner. 2006. The "Fish Specific" Hox Cluster Duplication is Coincident with the Origin of Teleosts. *Mol. Biol. Evol*. **23**(1):121-136

Daggett, D. F., Domingo, C. R., Currie, P. D., and S. L. Amacher. 2007. Control of morphogenetic cell movements in the early zebrafish myotome. *Dev Biol*. **309**: 169–179.

Darbandi, S. 2010. A Comparative Study of Ryanodine Receptors (RyRs) Gene Expression Levels in the Basal Ray-Finned Fish, Bichir (*Polypterus ornatipinnis*) and the Derived Euteleost Zebrafish (*Danio rerio*).

Darbandi, S. and J. P. C. Franck. 2009. A Comparative Study of Ryanodine Receptors (RyRs) Gene Expression Levels in Basal Ray-Finned Fishes, Bichir (*Polypterus ornatipinnis*) and the Derived Euteleosts Zebrafish (*Danio rerio*). *Comparative Biochem Physiol Part B* **154**: 443 – 448.

Deborah, L., Bennett, R., Cheek, J., Berridge, S., Parys, J., Missiaen, L. and M. D. Bootman. 1996. Expression and function of ryanodine receptor in nonexcitable cells. *The journal of biological chemistry.* **271** (11): 6356–6362.

Devoto, S. H., Melancon, E., Eisen, J. S., and M. Westerfield. 1996. Identification of separate slow and fast muscle precursor cells in vivo, prior to somite formation. *Development.* **122**:3371–3380.

Dong, D., Yuan, Z., and Z. Zhang. 2010. Evidences for increased expression variation of duplicate genes in budding yeast: from *cis*- to trans-regulation effects. *Nucleic Acids Research*. 1–11.

Egami,N. 1954 Effect of artificial photoperiodicity on time of oviposition in the fish, *Oryzias latipes*. *Annot. Zool. Japon.* **27**, pp. 57–62.

Felsenfeld, A. L., Curry, M., and C. B. Kimmel. 1991. The fub-1 mutation blocks initial myofibril formation in zebrafish muscle pioneer cells. *Dev Biol.* **148**:23–30.

Fill, M. and J. A. Copello. 2002. Ryanodine Receptor Calcium Release Channels. *Physiol Rev* **82:** 893-922.

Fisher, S., Grice, E. A., Vinton, R. M., Bessling, S. L., Urasaki, A., Kawakami, K., and A. S. McCallion. 2006. Evaluating the biological relevance of putative enhancers using Tol2 transposon-mediated transgenesis in zebrafish. *Nature Protocols* **1**: 1297 – 1305.

Fleischer, S., Ogunbunmi, E. M., Dixon, M. C. and E. A. Fleer. 1985. Localization of Ca2+ release channels with ryanodine in junctional terminal cisternae of sarcoplasmic reticulum of fast skeletal muscle. *Proc Natl Acad Sci U S A.* **82**(21): 7256-9.

Flucher, B., Conti, A., Takeshima, H. and V. Sorrentio. 1999. Type 3 and type 1 ryanodine receptors are localized in triads of the same mammalians skeletal muscle fibers. *The Journl of Cell Biology.* **146**(3): 621-629.

Force, A., Lynch, M., Pickett, F., Amores, A., Yan, Y., and J. Postlethwait. 1999. Preservation of Duplicate Genes by Complementary, Degenerative Mutations**.** *Genetics.* **151:** 1531–1545.

Forslund, K., Pekkari, I., and E. L. Sonnhammer. 2011. Domain architecture conservation in orthologs. *BMC Bioinformatics*. **12**:326

Franck, J. P., Morrissette, J., Keen, J. E., Londraville, R. L., Beamsley, M. and B. A. Block. 1998. Cloning and characterization of fiber type-specific ryanodine receptor isoforms in skeletal muscles of fish. *Am J Physiol* **275**: C401-415.

Franck, J.P.C., Reimer, K.R. and K. Hill. In preparation. Molecular evolution of the RyR gene family: A phylogenetic and comparative genomic analysis.

Frank, J. 1996. Three-Dimensional Electron Microscopy of Macromolecular Assemblies. *Academic Press*, New York.

Frazer, A., Patcher, L., Poliakov, A., Rubin, EM., and I Dubchak. 2004. VISTA: computational tools for comparative genomics. *Nucl. Acids Res*. **32**:W273-W279.

Friedman, R., and A. L. Hughes. 2004. Two Patterns of Genome Organization in Mammals: the Chromosomal Distribution of Duplicate Genes in Human and Mouse. *Mol. Biol. Evol*. **21**(6):1008–1013.

Gardner, P.P., Daub, J., Tate, J. G., Nawrocki, E. P., and D. L. Kolbe. 2009. Rfam: updates to the RNA families database. *Nucleic Acids Research* **37**: 136–140.

Ghanem, N., Jarinova, O., and A. Amores. 2003. Regulatory Roles of Conserved Intergenic Domains in Vertebrate *Dlx* Bigene Clusters. *Genome Res.* **13**: 533-543.

Giannini, G., Conti, A., Mammarella, S., Scrobogna, M. and V. Sorrentino. 1995. The Ryanodine Receptor/Calcium Channel Genes Are Widely and Differentially Expressed in Murine Brain and Peripheral Tissues. *The Journal of Cell Biology***.** **128**(5), 893-904.

Gilbert, S. F. 2000. *Differential Gene Transcription. Developmental Biology (6th edition).* Sunderland (MA). Sinauer Associates.

Guyon, J. R., Mosley, A. N., Zhou, Y., O'Brien, K. F., Sheng, X., Chiang,K., Davidson, A. J., Volinski, J. M., Zon, L. I. and L. M. Kunkel. 2003. The dystrophin associated protein complex in zebrafish. *Hum. Mol. Genet*. **12***:*601 -615.

Hadzhiev, Y., Lang, M., Ertzer, R., Meyer, A.,Strähle, U., and F. Müller. 2007. Functional diversification *of sonic hedgehog* paralog enhancers. identified by phylogenomic reconstruction. *Genome Biology*. **8:**R106.

Hamilton, S. L. 2005. Ryanodine receptors. *Cell Calcium*. **38**: 253-260.

Hardison RC. 2000. Conserved noncoding sequences are reliableguides to regulatory elements**.** *Trends Genet.* **16**:369-372.

He, Z., Eichel, K., l. Ruvinsky. 2011. Functional Conservation of *Cis*-Regulatory Elements of Heat-Shock Genes over Long Evolutionary Distances. PLoS one 6(7): e22677.

Hegyi, H., and M. Gerstein. 1999. The relationship between protein structure and function: A comprehensive survey with application to the yeast genome. *J Mol Biol*. **288**:147–164

Henricson, A., Forslund, K., and E. L. Sonnhammer. 2010. Orthology confers intron position conservation. *BMC Genomics.* 11:412.

Hirata, H., Watanabe, T., Hatakeyama, J., Sprague, S. M., Saint-Amant, L., Nagashima, A., Cui, W. W., Zhou, W. and J. Y. Kuwada. 2007. Zebrafish relatively relaxed mutants have a ryanodine receptor defect, show slow swimming and provide a model of multi-minicore disease. *Development*. **134**(15): 2771-81.

Hoegg, S., Brinkmann, H., Taylor, J. S., A. Meyer. 2004. Phylogenetic timing of the fish-specific genome duplication correlates with the diversification of teleost fish. *J Mol Evol.* **59**:190-203.

Hughes, A. L. 1994. The evolution of functionally novel protiens after gene duplication. *Proc Biol Sci*. **256**(1346):119-24.

Ishikawa, Y. 2000. Medakafish as a model system for vertebrate developmental genetics. *Bioessays.* **22**: 487-95

Iwamatsu, T. 1974. Iwamatsu, Studies on oocyte maturation of the medaka, *Oryzias latipes*. II. Effects of several steroids and calcium ions and the role of follicle cells on in vitro maturation. *Annot. Zool. Japon.*, **47**, pp. 30–42.

Iwamatsu, T. 1976. Iwamatsu, The medaka as a biological material. III. Observations of developmental process, *Bull. Aichi Univ. Edu.* Nat. Sci. **25**, pp. 67–89.

Iwamatsu, T. 1978. Iwamatsu, Studies on oocyte maturation of the medaka, *Oryzias latipes*. VI. Relationship between the circadian cycle of oocyte maturation and activity of the pituitary gland. *J. Exp. Zool.* **206**, pp. 355–363.

Iwamatsu, T. **2004.** Stages of normal development in the medaka Oryzias latipes. *Mech. Develop*. **121**: 605-618.

Jaillon, O., Aury, J. M., F. Brunet. 2004. Genome duplication in the teleost fish Tetraodon nigroviridis reveals the early vertebrate proto-karyotype. *Nature*.**431**:946-957

Jayne, B.C. and G.V. Lauder. 1994. How swimming fish use slow and fast muscle fibers: implications for models of vertebrate muscle recruitment. *J Comp Physiol A*. **175**:123-131.

Jegga, A. and B. J. Aronow. 2006. Evolutionarily Conserved Noncoding DNA. *Life Science*.

Kimmel, C. B., Ballard, W. W., Kimmel, S. R., Ullmann, B. and T.F.Schilling. 1995. Stages of embryonic development of the zebrafish. *Dev Dyn.* **203**(3): 253-310.

Kinoshita, M., Murata, K., Naruse, K. and M. Tanaka. 2009. Medaka: Biology, Management, and Experimental Protocols. Wiley-Blackwell.

Koonin, E. V. 2005. Paralogs and mutational robustness linked through transcriptional reprogramming. *BioEssays,* **27**: 865–868.

Koulen, P., Janowitz, T., Johenning, F. W., B.E. Ehrlich. 2001. Characterization of the Calcium-release Channel/Ryanodine Receptor from Zebrafish Skeletal Muscle. *J. Membrane Biol.* **183**: 155–163.

Kouzu, Y., Moriya, T., Takeshima, H., Yoshioka, T. and S. Shibata. 2000. Mutant mice lacking ryanodine receptor type 3 exhibit deficits of contextual fear conditioning and activation of calcium/calmodulin-dependent protein kinase II in the hippocampus. *Molecular Brain Research*. **76**(1): 142-150.

Kossugue, P., Paim, J., Navarro, M., Silva, H., Pavanello, P., Gurgel-giannetti, J., Zatz, M., and M. Vainzof. 2007. central core disease due to recessive mutations in *ryr1* gene: is it more common than described. *Muscle Nerve.* **35:** 670–674.

Kuzniar, A., van Ham, R. C. H., Pongor, S., and J. A. M. Leunissen. 2008. The quest for orthologs: finding the corresponding gene across genomes. *Trends Genet*. **24**(11):539-51.

Lang, M., Hadzhiev, Y., Siegel, N., Amemiya, C., Parada, C., Strähle, U., Becker, M., Müller, F. and A. Meyer. 2010. Conservation of shh *cis*-regulatory architecture of the coelacanth is consistent with its ancestral phylogenetic position. *EvoDevo*. 1:11.

Lanner, JT., Georgiou, DK., Joshi, AD. And SL. Hamilton. 2010. Ryanodine receptors: structure, expression, molecular details, and function in calcium release. *Cold Spring Harb Perspect Biol* 2010.

Laver, D. 2006. Regulation of ryanodine receptors from skeletal and cardiac muscle by components of the cytoplasm and SR lumen during rest and excitation. *Proceedings of the Australian Physiological Society.* **37**:31-38.

Laver, D. and B. Curtis. 1996. Response of ryanodine receptor channels to Ca^{2+} steps produced by rapid solution exchange. *Biophysical Journal.* 71: 732-741.

Lee, K., Sze Yen · Tan, Y., S. Brenner. 2011. Ancient vertebrate conserved noncoding elements have been evolving rapidly in teleost fishes. *Molecular biology and evolution*. **28** (3): 1205-1215.

Lettice, L.A., Heaney, S.J., Purdie, L.A., Li, L., de Beer, P., Oostra, B.A., Goode, D., Elgar, G., Hill, R.E., and E. de Graaff. 2003. A long-range Shh enhancer regulates expression in the developing limb and fin and is associated with preaxial polydactyly. *Hum. Mol. Genet.* **12:** 1725–1735.

Levine, M., and R. Tjian. 2003. Transcription regulation and animal diversity. *Nature* . **424**: 147-151.

Liu, Z., Zhang, J., Sharma, M., Li, M., Chen, S., and T. Wagenknecht. 2001. Three-dimensional reconstruction of the recombinant type 3 ryanodine receptor and localization of its amino terminus. *PNAS.* **98**(11): 6104-6109.

Ludwig, M. 2002. Functional evolution of noncoding DNA. *Current Opinion in Genetics & Development***. 12**:634–639.

Loots, G., and I Ovcharenko. 2004. rVISTA 2.0: evolutionary analysis of transcription factor binding sites. *Nucl. Acids Res*. **32** (suppl 2): W217-W221.

Lynch, M. 2002. Gene duplication and evolution**.** *Science*. *297 (5583): 945-947.*

Lynch, M., and J. S. Conery. 2000. The Evolutionary Fate and Consequences of Duplicate Genes. *Science*. **290** (5494): 1151-1155**.**

Lynch, M., O'Hely, M., Walsh, B., and A. Force. 2001. The Probability of Preservation of a Newly Arisen Gene Duplicate . *Genetics.* 159: 1789-1804.

McCarthy, D. and G. Smyth. 2009. Testing significance relative to a fold-change threshold is a TREAT. *Bioinformatics*. **25**: 765-771.

McEwen, G., Woolfe, A., and D. Goode. 2006. Ancient duplicated conserved noncoding elements in vertebrates: A genomic and functional analysis. *Genome Res.* **16**: 451-465.

McNulty, C., Peres, J., Bardine, N., Akker, W. and A. J. Durston. 2005. Knockdown of the complete Hox paralogous group 1 leads to dramatic hindbrain and neural crest defects. *Development.* **132**: 2861-2871.

Meynert, A. M. 2010. Function and evolution of regulatory elements in vertebrates (PhD thesis). Trinity College. University of Cambridge

Meyer, A., and M. Schartl. 1999. Gene and genome duplications in vertebrates: the one-to-four (-to-eight in fish) rule and the evolution of novel gene functions. *Current Opinion in Cell Biology* . **11**:699–704.

Michael Z Ludwig. 2002. Functional evolution of noncoding DNA. *Current Opinion in Genetics & Development* . **12**:634–639.

Miller, W., Makova, K. D., Nekrutenko, A., R. C. Hardison. 2004. Comparative genomics. *Annual Review of Genomics and Human Genetics.* **5**: 15–56.

Moore, R., and M. D. Purugganan. 2003. The early stages of duplicate gene evolution. *PNAS. **100** (26): 15682-15687.*

Morrissette, J., Xu, L., Nelson, A., Meissner, G. and B. A. Block. 2000. Characterization of RyR-slow, a ryanodine receptor specific to slow-twitch skeletal muscle. *Am J Physiol Regul Integr Comp Physiol.* **279**: R1889-1898.

Murayama, T. and N. Kurebayashi. 2010. Two ryanodine receptor isoforms in nonmammalian vertebrate skeletal muscle: Possible roles in excitation-contraction coupling and other processes. Prog *Biophys Mol Biol*. **105**(3):134-44.

Nabhani, T., Zhu, X., Simeoni, I., Sorrentino, V., Valdivia, H. and J. Garcia. (2002). Imperatoxin A enhances Ca^{2+} release in developing skeletal muscle containing ryanodine receptor type 3. *Biophys J.* **82**, 1319-1328.

Nakashima, Y., Nishimura, S., Maeda, A., Barsoumian, E., Hkamata, Y., Nakai, J., Allen, P., Imoto, K. and T. Kita. 1997. Molecular cloning and characterization of a human brain ryanodine receptor. *FEBS Lett* **3**;417(1):157-62.

Nelson, J.S. 2006. *Fishes of the world*. 4th ed. John Wiley and Sons, Inc. Hoboken, New Jersey, USA.

Nicholas, K.B., Nicholas H.B. Jr., and D. W.Deerfield. 1997. GeneDoc: Analysis and Visualization of Genetic Variation, *Embnew.news.* **4**:14.

Nowak, M., Boerlijst, M., Cooke, J., and J. M. Smith. 1997. Evolution of genetic Redundancy. *Nature*. **388**: **167- 171.**

Ohno, S. 1970. Evolution by gene duplication. Springer**.**

Ono, Y., Kinoshita, S., Ikeda, D., and S. Watabe. 2010. Early Development of Medaka Oryzias latipes Muscles as Revealed by Transgenic Approaches Using Embryonic and Larval Types of Myosin Heavy Chain Genes. *Developmental dynamics*. **239**:1807–1817.

Pennacchio, L.A., E.M. Rubin. 2001. Genomic strategies to identify mammalian regulatory sequences. *Nat Rev Genet*. **2**:100-109.

Perez, C. F., Lo´pez, J. R.,and D. A. Paul. 2004. Expression levels of RyR1 and RyR3 control resting free Ca^{2+} in skeletal muscle. *Am J Physiol Cell Physiol.* **288**: C640–C649.

Primrose, S. B., and R. M. Twyman. 2003. *Genomics: Applications In Human Biology***.** Blackwell Publishing. Oxford, UK.

Protasi, f., Takekura, H., Wang, Y., Chen, S., Meissner, G., Allen, P. and C. Franzini-Armstrong. 2000. RyR1 and RyR3 have different roles in the assembly of calcium release units of skeletal muscle. *Biophysical Journal.* **79**:2494-2508.

Radermacher, M., Rao, V., Grassucci, R., Frank, J., Timerman, AP., Fleischer, S. and T. Wagenknecht . *1994*. Cryo-electron microscopy and three-dimensional reconstruction of the calcium release channel/ryanodine receptor from skeletal muscle. *J Cell Biol. **127**:411–423.*

Rozen, S.and H. J. Skaletsky. 2000. Primer3 on the WWW for general users and for biologist programmers. In: Krawetz S, Misener S (eds) *Bioinformatics Methods and Protocols: Methods in Molecular Biology*. Humana Press, Totowa. NJ. pp 365-386

Rubinstein, A.L. 2003. Zebrafish: from disease modelling to drug discovery. *Current Opinion in Drug Discovery Development* **6**: 218-223.

Samsó, M., Trujillo, R., Gurrola, G., Valdivia, H., and T. Wagenknecht. 1999. Three-dimensional Location of the Imperatoxin A Binding Site on the Ryanodine Receptor. *The Journal of Cell Biology.* **146**(2): 493–499.

Sandelin, A., Bailey, P., Bruce, S., Engstrom, P.G., Klos, J.M., Wasserman, W.W., Ericson, J., and B. Lenhard. 2004. Arrays of ultraconserved noncoding regions span the loci of key developmental genes in vertebrate genomes. *BMC Genomics.* **5:** 99.

Sandow, A. 1952. Excitation-Contraction Coupling in Muscular Response. *Yale J Biol Med* **25** (3): 176–201

Schatz, M., van Heel, M., Chiu, W. and SL .Hamilton. 1999. Structure of the skeletal muscle calcium release channel activated with Ca2+ and AMP-PCP. *Biophys J*. **77:**1936-1944.

Schoenfelder, S., Clay, L. and P. Fraser. 2010. The transcriptional interactome: gene expression in 3D. *Current opinion in genetics development*. **20** (2): 127-133.

Schredelseker, J., Shrivastav, M.,Dayal ,A., and M. Grabner. 2009. Non– Ca^{2+} conducting Ca^{2+} channels in fish skeletal muscle excitation-contraction coupling. *PNAS*. **107**(12): 5658-5663.

Se´mon, M., and K. H. Wolfe. 2007. Rearrangement Rate following the Whole-Genome Duplication in Teleosts. *Mol Biol Evol*. **24** (3): 860-867.

Sorrentino, V., Barone, V. and D. Rossi. 2000. Intracellular Ca^{2+} release channels in evolution. *Curr. Opin. Genetics & Development* **10**, 662-667.

Sharma, M. R. and T. Wagenknecht. 2004. Cryo-electron microscopy and 3D reconstruction of ryanodine receptors and their interactions with E-C coupling proteins. *Basic Appl Myol.* **14**(5): 299-306.

Shultz, E. 2009. Comparative embryology using Japanese medaka fish. Woodrow Wilson Biology Institute.

Siepel, A., Bejerano, G., Pedersen, J. S., Hinrichs, A. S., and M. Hou. 2005. Evolutionarily conserved elements in vertebrate, insect, worm, and yeast genomes. *Genome Res*. **15**: 1034–1050.

Singh, L. N. and S. Hennenhalli. 2010. Correlated changes between regulatory *cis* elements and condition-specific expression in paralogous gene families. *Nucleic Acids Research*. 38 (3):738-749.

Sherwood, L., Klandorf, H. and P.H. Yancey. 2005. Animal Physiology: From Genes to Organisms. *Thompson Brooks/Cole*. pp. 324-430.

Sonnleitner, A., Conti, A., Bertocchini, F., Schindler, H., and V. Sorrentino. 1998. Functional properties of the ryanodine receptor type 3 (RyR3) Ca2F release channel. *The EMBO Journal.* **17** (10):.2790–2798.

Stalker, J., Gibbins, B., Meidl, P., Smith, J., Spooner, W., Hotz, H., and A. V. Cox. 2004. The Ensembl Web Site: Mechanics of a Genome Browser. *Genome Res.* **14**(5):951-955.

Steinke, D., Salzburger, W., Braasch, I., and A. Meyer. 2006. Many genes in fish have species-specific asymmetric rates of molecular evolution. *BMC Genomics*. **7**(1):20.

Storer, N. Y. and L. Zon. 2010. Zebrafish models for p53 function. *Cold Spring Harbor Perspectives in Biology*. **2**: 8.

Summerton, J., and R. D. Welle. 1997. "Morpholino Antisense Oligomers: Design, Preparation and Properties.". *Antisense & Nucleic Acid Drug Development.* **7**(3): 187–95.

Ta, T. and I. N. Pessah. 2007. Ryanodine receptor type 1 (RyR1) possessing malignant hyperthermia mutation R615C exhibits heightened sensitivity to dysregulation by non-coplanar 2,2′,3,5′,6-pentachlorobiphenyl (PCB 95). *Neurotoxicology.* **28**(4): 770–779.

Takeda, H. and A. Shimada. 2010. The art of medaka genetics and genomics: what makes them so unique?. *Annu. Rev. Genet.* **44**: 217-41.

Takeda, H., Naruse, K., and M. Tanaka. 2011. *Medaka: A Model for Organogenesis, Human Disease, and Evolution.* Tokyo,Springer. **7**: 94 – 128**.**

Thompson, D., Gibson, J., Plewniak, F., Jeanmougin, F and D G Higgins. 1997. The CLUSTAL_X windows interface: flexible strategies for multiple sequence alignment aided by quality analysis tool. *Nucl. Acids Res*. **25**:4876-4882.

Urasaki, A., Morvan, G., and K. Kawakami. 2006. Functional Dissection of the Tol2 Transposable Element Identified theMinimal cis-Sequence and a Highly Repetitive Sequence in the Subterminal Region Essential for Transposition. *Genetics*. **174**: 639–649

Vandepoele, K., De Vos, W., Taylor, J. S., Meyer, A., Y. Van de Peer. 2004. Major events in the genome evolution of vertebrates: paranome age and size differ considerably between ray-finned fishes and land vertebrates. *Proc Natl Acad Sci U S A.* **101**: 1638-1643.

Van de Peer, Y., Taylor, J.S., Braasch, I., and A. Meyer. 2001. The ghost of selection past: rates of evolution and functional divergence of anciently duplicated genes. *J. Mol. Evol*. **53**(4-5):436-446.

Vavouri, T., and B. Lehner. 2009. Conserved noncoding elements and the evolution of animal body plans. *BioEssays*. **31**:727–735.

Walsh, J. B. 1995. How often do duplicated genes evolve new function. Genetics**. 139**: 421-428.

Wang, Y., and X. Gu.2000. Evolutionary Patterns of Gene Families Generated in the Early Stage of Vertebrates. *J Mol Evol* . **51**:88–96.

Ward, C. W., Protasi, F., Castillo, D., Wang, Y., Chen, S. R., Pessah, I. N., Allen, P.D., and M. F. Schneider. Type 1 and type 3 ryanodine receptors generate different Ca^{2+} release event activity in both intact and permeabilized myotubes. *Biophys J.* **81**: 3216–3230

Watson, J., Caudy, A., Myers, Ri., and Witkowski, J. 2007. *Recombinant DNA: Genes and Genomes - A Short Course*. Cold Spring Harbor Press. pp. 57–58.

Wilson, C. A., Kreychman, J., and M. Gerstein. 2000. Assessing annotation transfer for genomics: Quantifying the relations between protein sequence, structure and function through traditional and probabilistic scores. *J Mol Biol*. **297**:233–249.

Wittbrodt, J., Shim, A. and M. Schartl.2002. Medaka - A Model organism from the Far East. *Nature Reviews. Genetics*. **3**, 53-64.

Woolfe, A., Goodson, M., Goode, K., Snell, P., McEwen, G.K., Vavouri, T., Smith, S.F., North, P., Callaway, H., K. Kelly. 2005. Highly conserved noncoding sequences are associated with vertebrate development. *PLoS Biol.* **3:** e7.

Wu, H. **2011**. The role of ryanodine receptors in development (PhD thesis). Queen Mary. University of London.

Xie, X., Kamal, M., and E. S. Lander. 2006. A family of conserved noncoding elements derived from an ancient transposable element. *PNAS*. **103**(31): **11659–11664.**

Yoshioka, H. 1963. H. Yoshioka, on the effects of environmental factors upon the reproduction of fishes. 2. Effects of short and long day-lengths on *Oryzias latipes* during spawning season. *Bull. Fac. Fish Hokkaido Univ.*, **14:** 137–151.

Yuan, J., Reed, A., Chen, F. and N. Stewart Jr. 2006. Statistical analysis of real-time PCR data. *BMC Bioinformatics*. **7**: 85.

Zhan, Z and J. Hu. 2006. Development and Validation of Endogenous Reference Genes for Expression Profiling of Medaka (Oryzias latipes) Exposed to Endocrine Disrupting Chemicals by Quantitative Real-Time RT-PCR. *Toxicological Science* **95**(2), 356–368.

Zhang, J. 2003. Evolution by gene duplication: an update. *Trends in Ecology and Evolution*. **18**(6) : 292- 298.

Zhang, J., Rosenbe, H., and M. Nei. 1998. Positive Darwinian selection after gene duplication in primate ribonuclease genes. PNAS. **95**: 3708–3713.

APPENDICES

APPENDIX 1: pGEM® - T Easy Vector Map

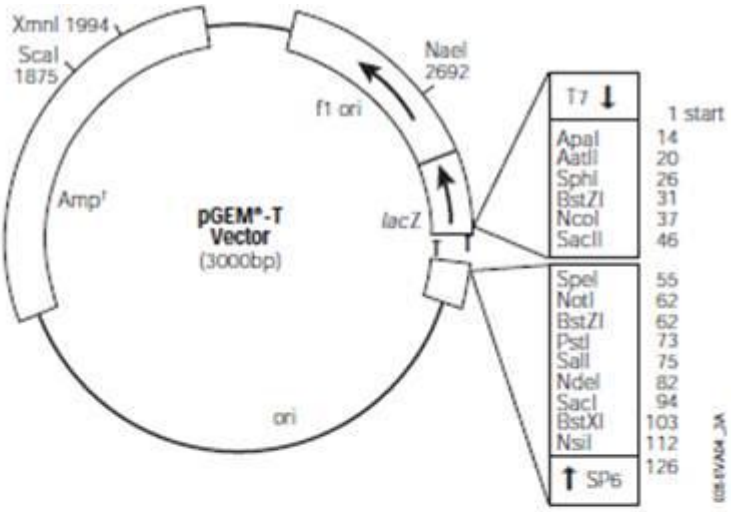

pGEM®-T Vector sequence reference points:

T7 RNA polymerase transcription initiation site	1
multiple cloning region	10–113
SP6 RNA polymerase promoter (–17 to +3)	124–143
SP6 RNA polymerase transcription initiation site	126
pUC/M13 Reverse Sequencing Primer binding site	161–177
lacZ start codon	165
lac operator	185–201
β-lactamase coding region	1322–2182
phage f1 region	2365–2820
lac operon sequences	2821–2981, 151–380
pUC/M13 Forward Sequencing Primer binding site	2941–2957
T7 RNA polymerase promoter (–17 to +3)	2984–3

APPENDIX 2: RyR1a nucleotide sequence alignment with RyR1a sequence obtained from ensemble database.

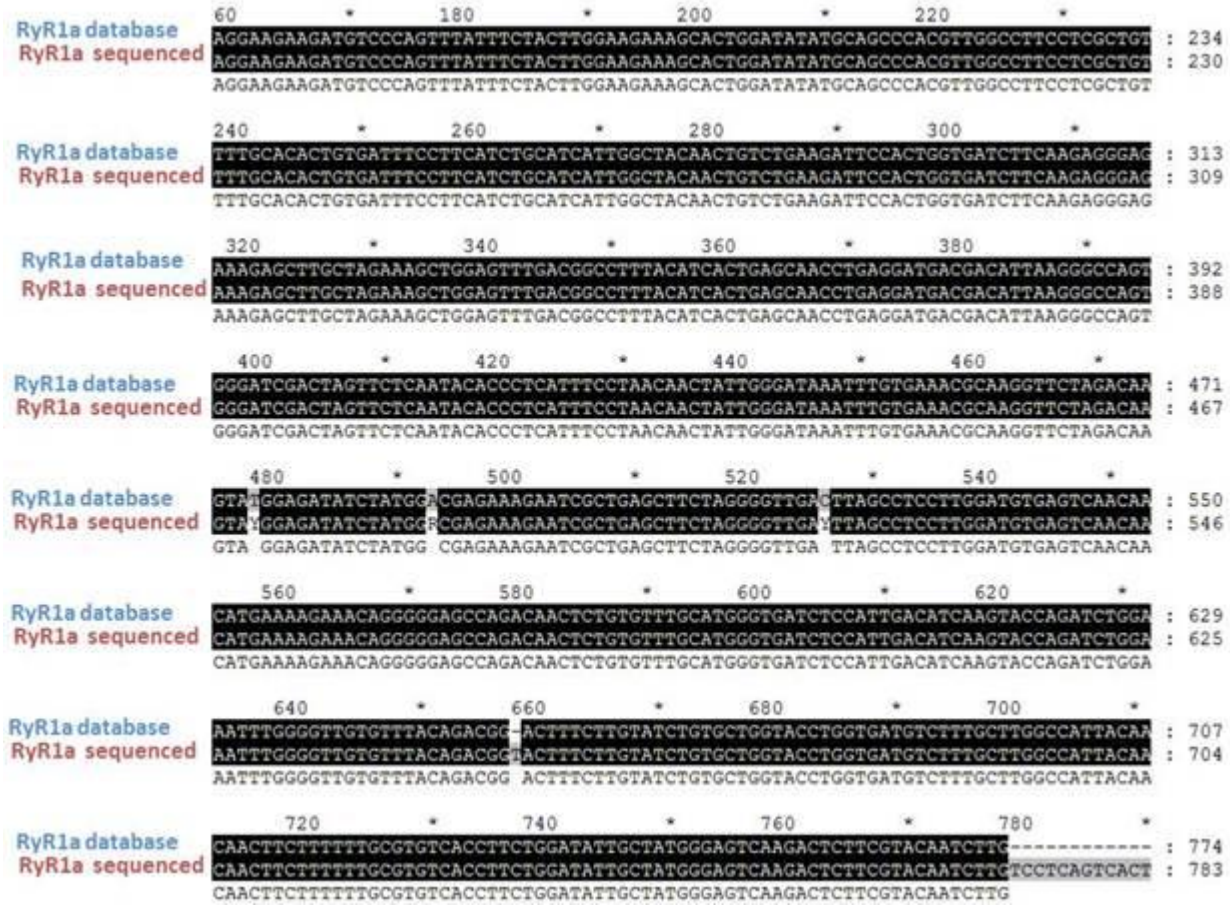

APPENDIX 3: RyR1b nucleotide sequence alignment with RyR1b sequence obtained from ensemble database.

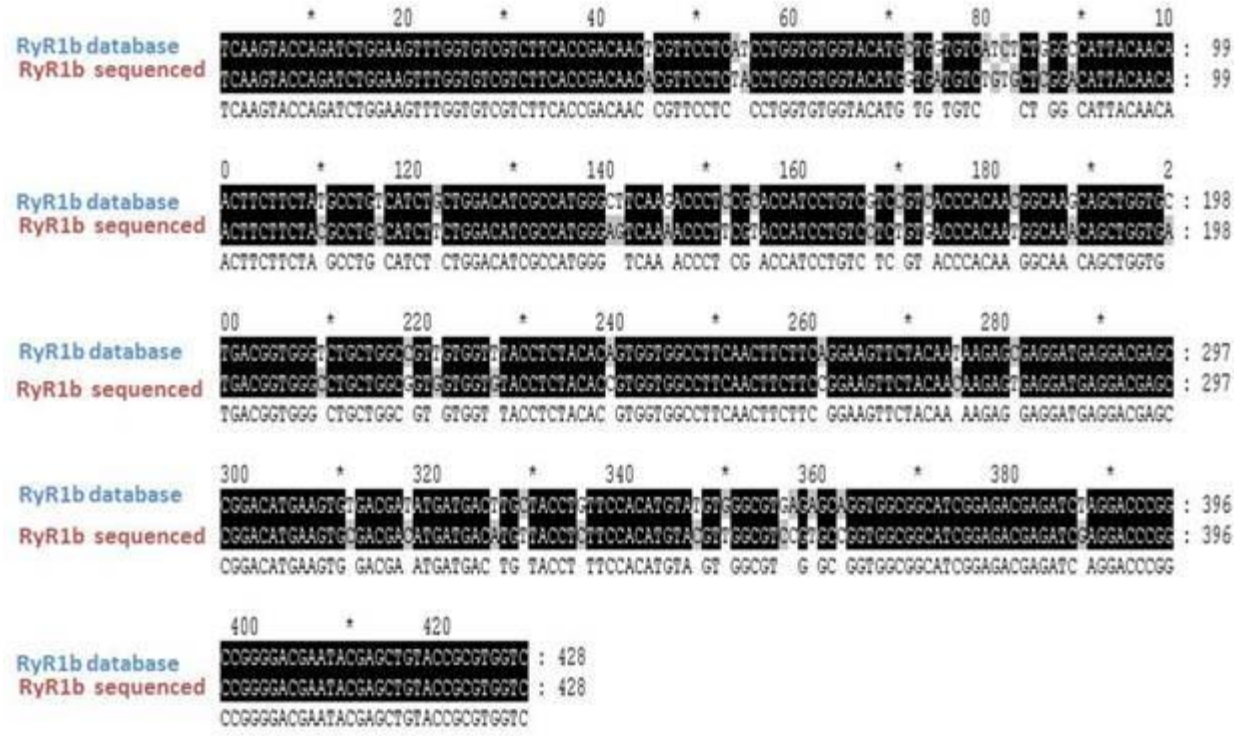

APPENDIX 4: RyR3a nucleotide sequence alignment with RyR1b sequence obtained from ensemble database.

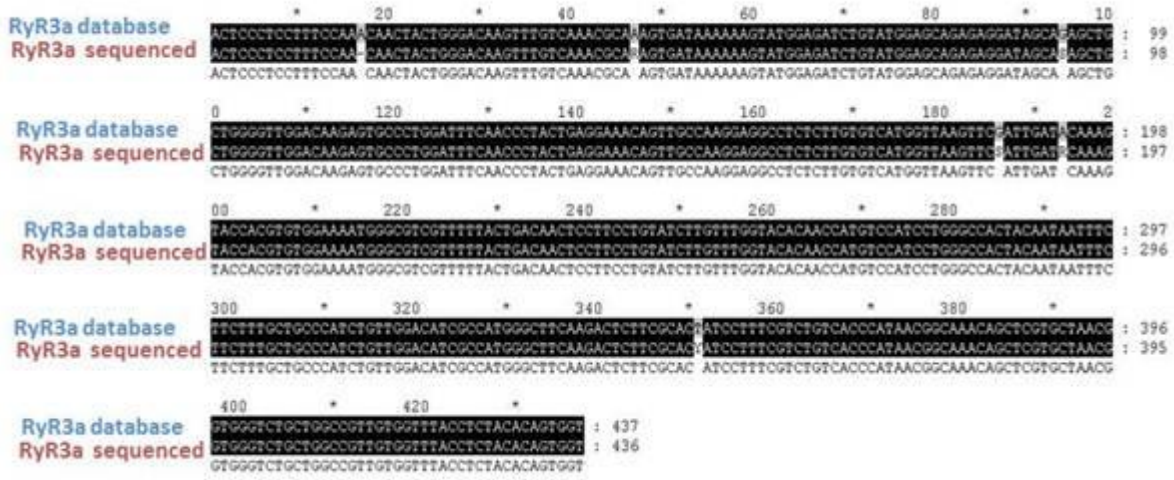

APPENDIX 5: RyR3b nucleotide sequence alignment with RyR1b sequence obtained from ensemble database.

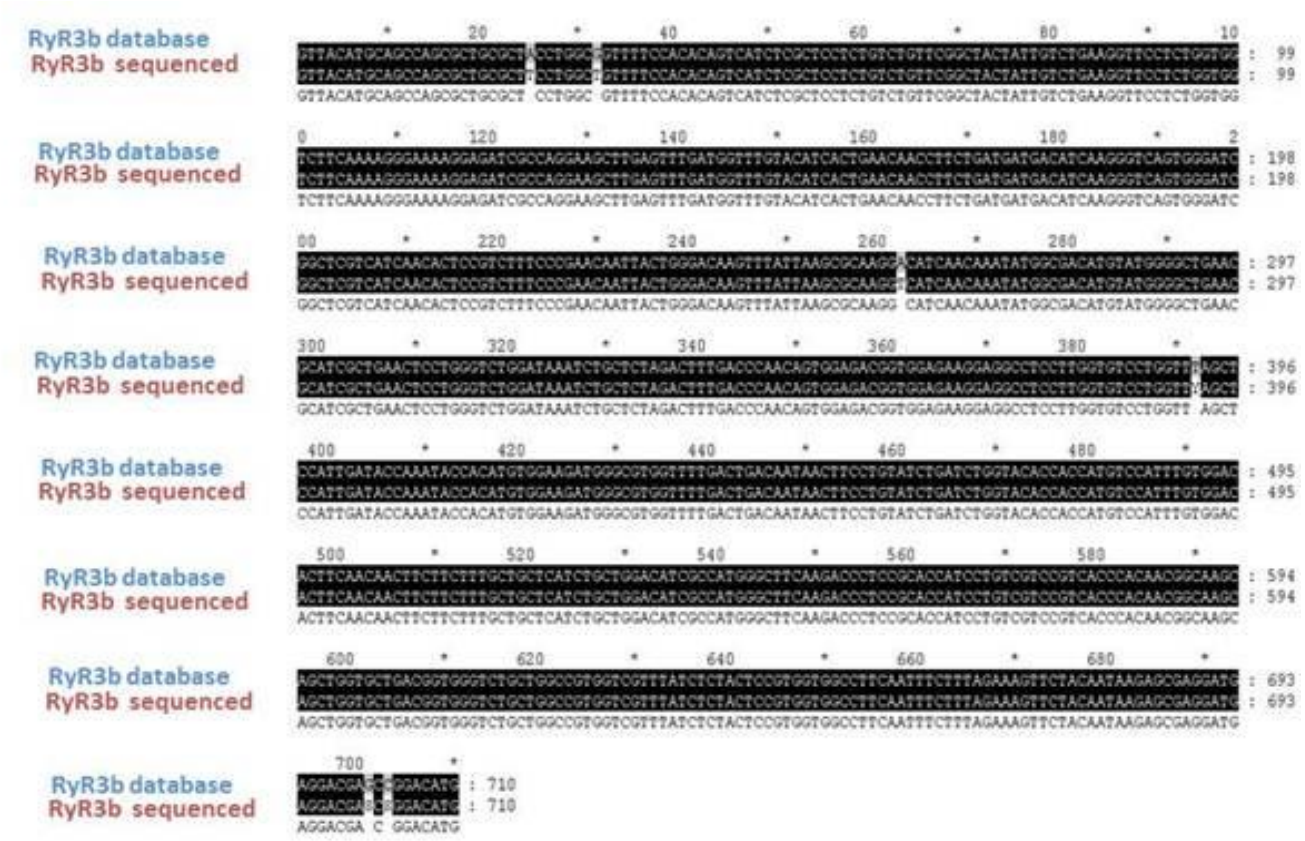

APPENDIX 6: Medaka RyR1a nucleotide sequence conserved more than 70% with fugu RyR1a.

Region1

TAAATTCCTGTAGCTTTCCAGAAAGGGATGTGTGAGCAGCAGGTGCAGGAGCCTGA
AATAGAGAGCAAAGGGGGCGGAGGCTTGGAATGACATAGACAACAAG

Region2

TATTCTCTCTCTGACTGTCCACTGTCTTCTTCTGTTGGGTTGCTGCTGGGTTTCCAGG
GCGGGGACACAGAGGTTAGAATTTGTTTCTGCACGACCGCTGTGCTGATCGCATGG
CACCTC A-
CTTTGGGGGAACTTTTCATCAACCCCCCCAGCACACTGGCACATCTGATCCAAATAT
-ACCCTAATGTATAGACACACAAATATATATA

Region 3

CACAAAGCATCAATGGACAAATGGGGAGGCCAGGTGTATAAGCCAAACCCAGTCC
TGCCAGTGTGTGAGGGGGGGAGTCTGGAGGCGCTTGATGAAAGTACACAGCTGTA
GAGTTGGGCTCATGACACTGAGCTTTACATAAAGCCCAACGTGGCAGTGAGAGCTC
AGTGCCATCATGCTTTCACTGCATTTGCTCTTTTTT-
AATCATAGATGTACAAGTATTTTACTTTGTCTTACTTTTTTTTTTAT

Region 4

TGCCCTTTGAGGTGCGACAGTCAGAACTGGTAATGGGCGGCCAGGGGCAGGGGAC
CAGGAACACAGTGGAGCGGTAGCTCTCGACGCATTGAGTGGCCTCATCATTA---
GAGCCTCACATTCAAACCACATCTCTCC

Region 5

TTGCCATGGAATGTTGTTAATCT CCCC
TCCTCATCTCTTAGTCCTCAACTGTTGTCACCACACTGATCCTTTCTCCTTTCCCCAC
GATCACTGCCACCTCTCCCCTTGTCCCTCCATTTATGGTCCTCAGACTTGAACCTAG
ATCGGGGTAAATCATGTTTCTCTCCA

APPENDIX 7: Medaka RyR1b nucleotide sequence conserved more than 70% with fugu RyR1b.

Region1

AGTGTTTTTCTAACTGTGCTCTCCCCTTTGATCCTGTGTCGGGGTTGGACGCCGGGC
GTCTAGGTCAGATTGGGTTTGTGCACGAGCGCTGTGCTGACCGCATGGCACACTG

Region2

CCACCAGGTGCGACAGACAGAGATGGTATGGGGGGACCA GGGGA-
GGGGACACAGGGGAGCCGGCGAGGACGCAGCTCGCCGCCCCACCGAGTGACCACA
ACGTGACATCACACCCGGCACACCCCCCCCACCCCA----CTCTTTCCA

APPENDIX 8: Medaka RyR3a nucleotide sequence conserved more than 70% with fugu RyR3a.

Region1

ATGAAAATATCCACTTAAATACAAAGTTATAAAAAGA GGTAGAATTTTACTG---
TCAC-AGAAGCCTGTTCATCATCTTGCTTTCTCTTTTATAAT
TTGCTGTTCACAACTAAA---GAGGGTAAGTGACAAGAACACTC--ATTTTTTATGATC-
--AACGGTTTTCATATCACCCATAGAA

Region2

TCTCT--CAGTCCTTTAAGGAAAAGGTAA-----CAATGTGCATGAGCTGT
TTGCTTGCCAGCTTATTGGCTTC-----
TGCTCTTTAGTCAGCAGGCAGAGGAGCCAATAGCTTGTGCT

Region 3

TGTCTAGCCTGCAGCTGTTCCTTGCATACAGCAGTAGTGAAAAATGGACTCTGGCA
ATTTCATGGGCCGTTGCTTCCTTACAGAGTCACAGGAAGTTGGGGTGGAGAGCTAA
AGCAGCGAGGAAAACAATTATAAGGCACAACCTTGGGGTGCCTGTGCTCAATATGG
GCTCACACCATGATTCC

Region 4

CTCTTCAGGCACAAAAATAATAATTACTTCCTGAATATCTACCGACACTTTTGGCTG
GAGGTAATACATGAAAACACCGACTATGACAGTCTGCTCTCAATGCTGACGGTAAC
GT

Region 5

AAACTAACCAGCACCAACCCGCTCTGAAATGAAACCTCTTCCCTCCTTTTGCGCTTC
TCCTCTCTAACCCAGGCTAATCTCCTCTCCCCCACTTCCCAGGTA

Region 6

TAGTG-ACAGTCCTTCTCTGTT--------TTCT
GATTGAATCTAAATGTGTTCTCCTTTGCTTATGTCTGCTTTT-
GTTTTGTTTGTTCCCTT CTGGTCATATTTTT-
ATGTCATCGGTCGCAGTCAACGTGAGTGAGCGGGGTAAATACACG GTTTAGA

APPENDIX 9: Medaka RyR3b nucleotide sequence conserved more than 70% with fugu RyR3b (part 1).

Region1

TTCTTTTTTTTCCCCCCAGGAGAGAACAAGGAGGGCGAGGAGGCCAAAGGAGAAGT
GTTGGCTGTGGCCGGGGAGAAGGAGGAGGTGAGCAAGAACGAGGAGAAGGCTGTG
GAGGCAGGAGAGGAGG

Region2

CTTCTCTTGACTGTGTG-CTGGTGCAAAACCCA--TCACCCTGTCCTTATTGACCCTCT-
CTCTGTGTTGTTTTCTTGCATAACACTT
CCTCAACCCCCCCCAGATACAAAAATAATAATTACTTCCTGAATGGCTATCGGGAG
GTTTGGCTGGAAAGGGCATTCAAAGCCTCCAGCTTTGACCGCCTGTTCTCCCTGCTG
ACGGTAAAGTGACGCCGCAGGGCGTGGCCTTCATCTGTTAAAC-------
CCCGCCCACCA

Region 3

TGACCATTCAGAG GAGCCAGTGGATCCT-
CATTGACCAATCACAACCCCCCCCCTGCCTGAAACGCACCTCCT G-
AACACCTCCCCTTCCCCTGACATTCCTA----------CCTGTTGCCTCCAAA--CT
CACCAGAACACACCCTAATTCCACTGTACCTCCCTCCCAACTACCTCCC----
CCACCTC CCCTTCCC-
AGGTAAGTACTGGGCTCGGCCTGCCTGTGCCCCCCGTGCCCTGTGTTGGCA
CCCCTCTGCCAGTCCTGTTTGCAGAGTGCTTCTTTAGCCCGC------TCGAGCCTTGGG
AG------CAGGCAGGGACC------AAAGCGCCCAGGGGCCCCCGCTATAGGTGCACTA
AACCCCCCAGACAGAGATCCGTCAGGGGTCAGAGGCTGCATGAGCGACTCAGCAG
ACGCC
CGGCGAGCTCCGGCGCCCACAGCTGTAGAAAGGCAGGCTTTGTGGTTGCGGCAGCA
GCGG TAAGGAGGCGCCGCGCTGCAG

Region 4

TTCATCTCTCTTCGTTTGGTAACCGCCTGTCCTCTCTCTTTGCTTGTGTCCTT
GGTGTGTTGTTCGTCTCCTTCCCATCTCTATA-
AAAACCCATCGATGGCAGCCCACACTGGACGGGGTAAATAACAAGTTTAGATCATC
CTGACATGGCTGTGCTTCCTCCCTGAATGCCCCCCTCCATTGTTGTAGTC

APPENDIX 9: Medaka RyR3b nucleotide sequence conserved more than 70% with fugu RyR3b (part 2).

Region 5

TCCTTGTGGGTCT GTCAGTGCCACCGACCCCCCA--------
GGTTTGACTGAAGGTCTGTGGGCTAGTCCAC
AGCTTAAGCAAAGCTTTGTCTTGCTTTGGATTTGGGGCCTTTTTCACAAAGCTGGTT
CC------ACATA-GTTCTAACTTTCACATGGTT

Region 6

AACCTCGCCTATCCGCTGCTTTT CTTAGTGT----------
TGATCAGGCCCAGCGGCGGCCTGCATGTGAAAGTTATCAA
GCTTCCTCCAGCTTATGGAAATGTCCTGGTGT

Region 7

CTTTGGATTCAGTTGTCATTCTGCAATCTAAAGGCTTTGGACTTCA--------
ACAGTGTTTTGAACATGAGACCTGGCCTGC

APPENDIX 10: Medaka RyR1a nucleotide sequence conserved more than 70% with zebrafish RyR1a.

GTCCTGCCAGTGTGTGAGGGGGGGAGTCTG----GAGGCGCTTGATGAAAGT
ACACAGCTGTAGAGTTGGGCTCATGACACT

APPENDIX 11: Medaka RyR1b nucleotide sequence conserved more than 70% with zebrafish RyR1b.

GGATAACCTTTTCATTTTGGTGTGTAACCCTGCTAGATGCTCCCTGATCCAGGACAA
CGAAACGGCGTAA-GATTCT GTGTTTTGCCTCGTTTTAGACCCTTCA----
TGCTTTCATGAAA

APPENDIX 12: Zebrafish RyR3 nucleotide sequence conserved more than 70% with fugu RyR3a.

ACAAAAATAATAATTACTTCCTGAATGGCTATCGGTACGTTTGGCTGGAAAAGGTG
T ACCATACCTCTAGCTTTGACCGTCTGTTCTCCATGCTAACGGTAA

APPENDIX 13: Zebrafish RyR3 nucleotide sequence conserved more than 70% with fugu RyR3b.

CTTCCTCCTCCTAAAGCCTGTCC-CTTTCTGTTGT----CTCCATAACACACT----------
TCAGATACAAAAATAATAATTACTTCCTGAATGGCTATCGGTACGTTTGGCTGGAA
AAGGTGTACCATACCTCTAGCTTTGACCGTCTGTTCTCCATGCTAACGGTAATGTGA

APPENDIX 14: Composition of used reagents

1% Agarose gel

0.5g Agarose, 50ml TAE buffer, and 2.5 UL Ethidum bromides

2% Agarose gel

1g Agarose , 50ml TAE buffer , and 2.5 UL Ethidum bromide

Purification gel

0.5 g low melting point agarose powder, 50 ml TAE buffer, and 2.5 UL Ethidum bromides

1Kb ladder

20 UL of 1kb ladder stock, 10 UL loading dye, and 80 UL ddH2O

dNTP

10 UL of 100 mM dTTP, 10 UL of 100mM dCTP , 10 UL of 100mM dATP, 10 UL of 100 mM dGTP, and 60UL ddH2O

Fresh Oligo

10 UL Oligo dNTP stock in 90 UL ddH2o

Ethanol 75% preparation

79 ml 95% Alcohol in 21 ml ddH2o

1X TAE buffer

50 ml 10X TAE buffer stock in 450 ml ddH2O

50X TAE buffer

121 g Tris, 28.6 ml Glacial acetic acid, and 18.6 g EDTA adjust ddH2O to 500 ml.

Low mass Ladder

4 UL low mass ladder stock, and 1 UL lodind dye

MS-222

300 mg MS-222 in 500 ml ddH2O (adjust PH to 7.0 by adding NaOH)